2022

# Toxin Production and Growth Responses of Freshwater Cyanobacterium Microcoleus anatoxicus to Salinity

Simone Henry

# Toxin Production and Growth Responses of Freshwater Cyanobacterium *Microcoleus anatoxicus* to Salinity

A Thesis Presented

by

Simone Henry

To the Keck Science Department

of Claremont McKenna, Pitzer, and Scripps Colleges

In partial fulfillment of

The degree of Bachelor of Arts

Senior Thesis in Organismal Biology

December 13, 2021

## ACKNOWLEDGEMENTS

I would like to thank Dr. Rosalina Stancheva Hristova, head of the California Primary Algae Laboratory at California State University San Marcos (CSUSM) for being my mentor for this summer and first reader for this thesis, and for their incredible knowledge and tremendous support. I would like to thank Dr. Betsy Read, Professor of Biological Sciences at CSUSM for mentoring me on all molecular aspects of the following study and for their continual support. Thank you to Briana Vega, my lab partner throughout this summer who helped with all data set up and collection, for their unending positivity. Thank you to Nate Kristan, the lab technician at the Primary Algae Lab who design some of the culturing treatments and for welcoming me to the lab. Thank you to Pete Chandrangsu, Assistant Professor of Biology at W. M. Keck Science Department and my second reader, for their generous time and help. Finally, thank you to the National Science Foundation (NSF) and CSUSM for the Research Experience for Undergraduates (REU). Thank you to W. M. Keck Science Department for the education to prepare me for this experience.

Field image of *Microcoleus anatoxicus*. Credit: Rich Fadness.

# TABLE OF CONTENTS

## ABSTRACT

*Microcoleus* is an anatoxin-producing genus of cyanobacteria found globally. Anatoxin (ATX) is a high potency neuromuscular toxin. Fatalities caused by ingesting ATX-contaminated water, or the ATX-producing algae, have been recorded since the 18th century, but have more recently increased in magnitude and frequency. This experiment is intended as a pilot study to explore how future conditions of the Russian River under increased agricultural and industrial pollution, and climate change might affect the growth and toxin production of *M. anatoxicus*. *M. anatoxicus* underwent 12 treatments made up of 3 treatment groups targeting increased salinity and nutrient gradients. The only significant correlation found was a negative relationship between intracellular ATX concentrations and phosphates. Tendencies however showed that ATX production increased at high salinity levels despite the reduced biomass. Biomass was greater with increases in nutrients, however toxin concentrations decreased with increased nutrients. This study has suggestive potential towards more accurately predicting how human activities affect future freshwater ecosystems.


---

## INTRODUCTION

Cyanobacteria are a diverse group of aquatic prokaryotes and, as the oldest autotrophic organisms on Earth, are responsible for the formation of the oxygenated atmosphere. Their fossil record, known as stromatolites, were formed over 2 billion years ago. Since then, cyanobacteria have achieved global distribution, diversified into about 2,700 known species and an estimated 4,000 species yet to be identified (Nabout et al., 2013). They are found from geothermal vents, to caves, to oceans, and to freshwater streams (Whitton, 2012). These algae take on planktonic and filamentous forms, and species can be free-floating in the water column, metaphytic, epiphytic, or epilithic (benthic) (Quiblier et al., 2013).

Today, climate change and anthropogenic pollutants are likely responsible for disproportionate cyanobacterial proliferations that have had devastating effects on ecosystems (Bouma-Gregson et al., 2019; Burford et al., 2020). Insight into their phylogenetic history, ecological range, and morphology may illustrate the factors influencing the formation of blooms and the consequences of proliferations.

Planktonic cyanobacteria specifically have garnered special attention because of the increasing frequency and intensity of blooms which have had detrimental effects on marine ecosystems (Quiblier et al., 2013). Freshwater benthic cyanobacteria are somewhat less well studied than their planktonic counterparts in terms of species interactions and toxin-production capabilities (Quiblier et al., 2013; S. A. Wood et al., 2020). Many marine and freshwater cyanobacteria produce cyanotoxins. Cyanotoxins are some of the most potent natural aquatic toxins, having often fatal effects on animals (R. Wood, 2016). Cyanotoxins in bodies of freshwater, as compared to in the ocean, are of particular of concern because the toxins are more concentrated in the smaller water volumes. In North America, there are five primary cyanotoxins seen in freshwater: microcystins, nodularins, anatoxins (ATX), saxitoxins, and cylindrosperopsin (Figure 1) (Svirčev et al., 2019).

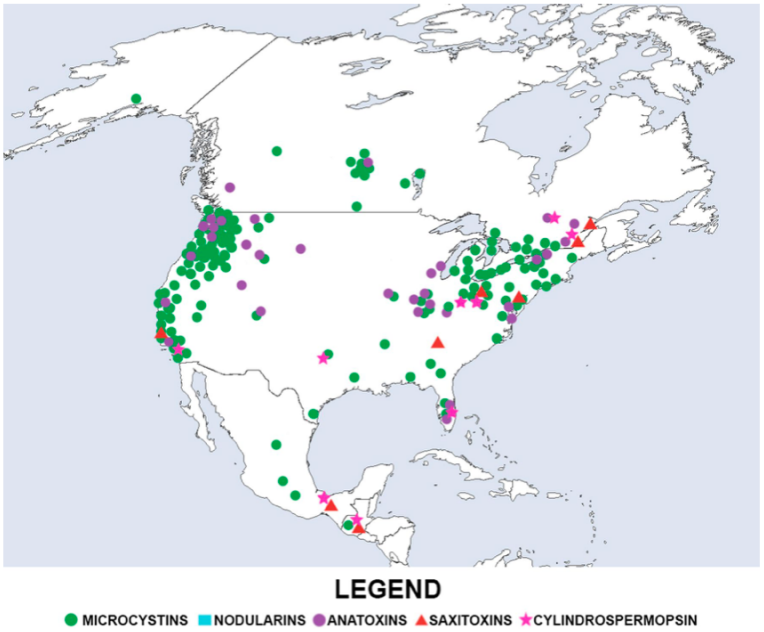


**Figure 1.** Distribution of most commonly reported cyanotoxins in North America (Svirčev et al., 2019).

Due to the increasing frequency of harmful blooms, and their effects on public health, livestock, and pets, studies of toxin-producing cyanobacteria are especially critical (Backer et

al., 2013; Biré et al., 2020; Svirčev et al., 2019). Records of dog poisonings and deaths after the ingestion of algae predate the 1920s and reported annual dog poisonings have steadily increased. This may be due to increased awareness, along with increases in number of harmful algae bloom events (Backer et al., 2013). Other organisms, humans included, are at increasing risk of encountering cyanotoxins due to changing environments (Svirčev et al., 2019).

### Introduction to cyanobacterium *Microcoleus*

The cyanobacterium of interest for this study is the freshwater, benthic, filamentous genus *Microcoleus.* Like many cyanobacteria, *Microcoleus* has a wide geographic range and is a burgeoning area of research. *Microcoleus* is the main producer of ATX in streams, lakes, and ponds worldwide, including in northern California (Conklin et al., 2020). ATX are strongly associated with local dog poisonings in California. Outbreaks of freshwater harmful algal blooms in North America were first reported in 2002 in the Eel River in northern California where 3 dogs died in an hour after 5 minutes of exposure in a pond (Puschner et al., 2008). In response to the dangers, and increasing frequency of toxic algae, the California Water Board created non-regulatory recreational cyanotoxin advisory levels. For ATX, any level of detection is considered unsafe. 20 µg/L is considered to be at warning level, and 90 µg/L is considered dangerous (Joab & Chetelat, 2019). Recent studies identified several toxigenic *Microcoleus* genotypes in rivers in northern California (Bouma-Gregson et al., 2019). A novel ATX-producing species *Microcoleus anatoxicus,* Stancheva & Conklin 2020, isolated from Russian River (Figure 2), has been described and its genome completely sequenced, and is the sample of interest for the following study (Conklin et al., 2020).


**Figure 2.** Map of Russian River ("Russian River (California)," 2021). The purple square provides an approximation of where PTRS1 was collected.

On a molecular scale, ATX are strong neuromuscular blockers with four structural variations, two of which are found in *M. anatoxicus*: anatoxin-a (ATX) (Figure 3), dihydroanatoxin-a (dhATX) (Conklin et al., 2020; Svirčev et al., 2019). At first, dhATX was speculated to be a less toxic, degredation product of ATX. Often dhATX is found extracellularly whereas ATX is usually found in higher concentrations intracellularly. However, recent studies provided evidence that dhATX may be biosynthesized, at least in part, independently from ATX (Colas et al., 2021; Conklin et al., 2020; Méjean et al., 2016).

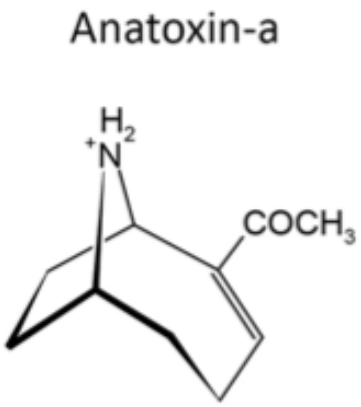


**Figure 3.** Molecular structure of anatoxin-a (Svirčev et al., 2019).

**Morphological Characteristics of *Microcoleus anatoxicus***

*Microcoleus* begins its growth in bodies of freshwater by attaching single filaments to rocks, which multiply quickly and consolidate into dense mat. The mats often can detach from the rock due to trapped oxygen and may float on the water surface (S. A. Wood et al., 2020). *Microcoleus* mats are made up of hundreds of filaments consisting of trichomes, defined as small appendages, covered by a colorless mucilaginous sheath (Figure 4 and 5A). The filaments are unbranched, and, depending on the species, single or multiple trichomes will develop inside the sheath. Development of the sheath depends on the environment. Sheath may sometimes be missing or miscolored. Cells of the trichome store nutrients in granules on either side of the cross walls (Figure 6A). The only differentiated cell is the apical cell, which are the rounded, thicker, terminal ends of the filament (Figure 7). Filaments reproduce by fragmentation or short segments of cells developing into a hormogonium.

Unhealthy, starving, or damaged *Microcoleus* filaments can be morphologically characterized in several ways. When nutrients are limiting, cells relyon internal stores housed

in granules, which subsequently degrade and become reddish in color or disappear (Figure 6B). In addition, the sheath surrounding the filaments becomes thickened and multilayered.

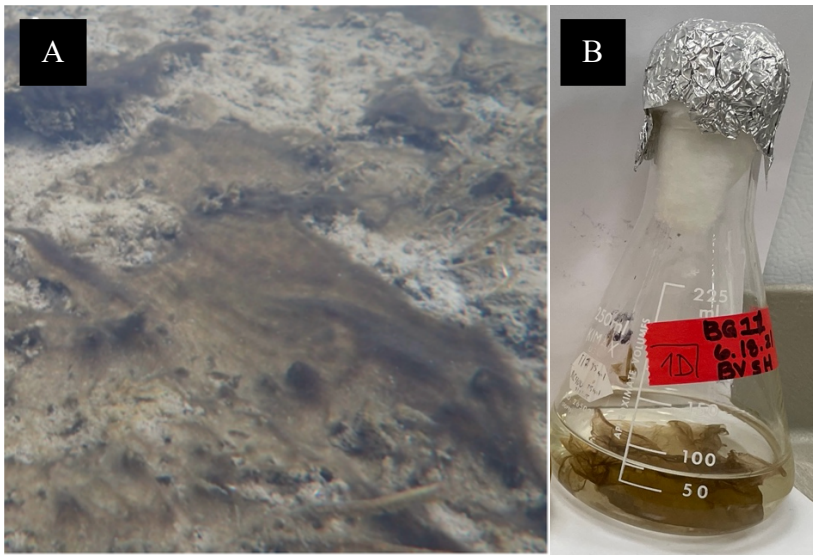


**Figure 4.** Macroscopic field view of *M. anatoxicus* (A) (Conklin et al., 2020) and macroscopic view of *M. anatoxicus* in BG11 growth medium (B).

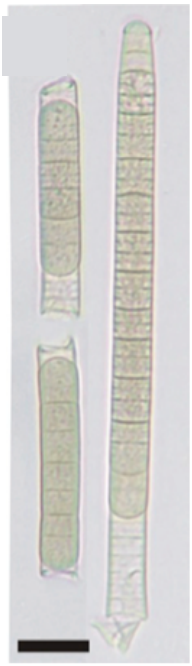

**Figure 5.** Microscopic view of a healthy sheath around *M. anatoxicus*. Scale bar: 10 µm (Conklin et al., 2020).

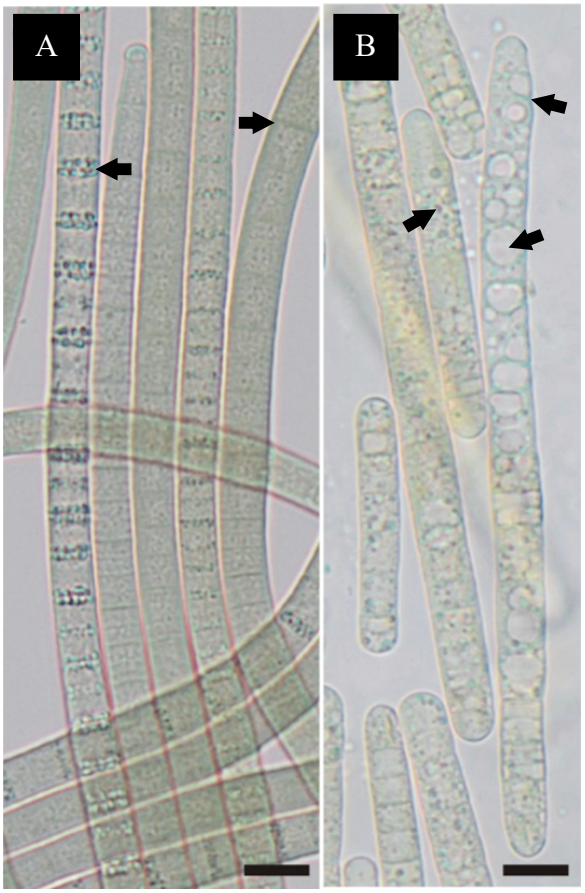


**Figure 6.** Microscopic view of *M. anatoxicus* showing healthy cells with arrows denoting crosswalls and granules (A) and unhealthy filaments with arrows denoting vacuoles and crosswall constriction (B). Scale bar: 10 µm (Conklin et al., 2020).

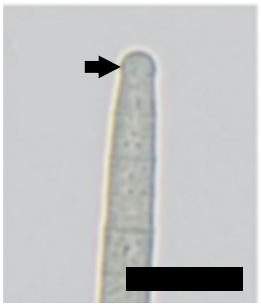

**Figure 7.** Microscopic view of example apical cells of *M. anatoxicus* in BG11. Scale bar: 10 µm (Conklin et al., 2020).

**Molecular Characteristics of *Microcoleus***

Historically, cyanobacteria taxa are identified and classified morphologically. As genetic technologies have advanced and become more accessible, species are being

reidentified, reclassified, and described in greater detail. The genus *Microcoleus* was reclassified by Strunecký et al. (2011), and many species previously belonging to the genus *Phormidium* were transferred to *Microcoleus* based on molecular evidence. Speciation of cyanobacteria can occur without any morphological changes, complicating taxonomic endeavors (Dvořák et al., 2012). In part of a study to further describe the molecular characteristics of *M. anatoxicus*, Conklin et al. (2020) investigated the genes and pathways for toxin production. The complete anatoxin-a gene cassette was recovered from one *M. anatoxicus* strain (PTRS1) from the Russian River and showed homology to two other strains collected at nearby locations. The full cassette was about 23.2 kb consisting of genes *anaABCDEFGIJK* (Figure 8) (Conklin et al., 2020).


**Figure 8.** Anatoxin-a gene cassette of Microcoleus sp. PTSR1 (Conklin et al., 2020).

Unique to this cassette is that *anaG* has no methyltransferase domain, as compared to other cyanobacteria, and possesses *anaK* genes, unlike other *Microcoleus* sequences from a nearby locale, the Eel River (Conklin et al., 2020). Conklin et al. (2020) hypothesize that *anaG* is responsible for the synthesis of anatoxin-a or homoanatoxin-a, and that *anaK* catalyzes the process of converting ATX to dhATX.

### Global Studies on Anatoxin-A production and *Microcoleus*

The genus *Microcoleus* has been recorded and studied globally, in areas including in New Zealand, Europe, and North America (B. Anderson et al., 2018; Harland et al., 2013; Quiblier et al., 2013; S. A. Wood et al., 2020). Strains in New Zealand tend to produce large amounts dhATX or homo-anatoxins over anatoxins, whereas strains across Asia, Europe, and the Americas tend to be predominantly ATX-producing, although there remains a lot of

variation (Colas et al., 2021; S. A. Wood et al., 2018). However, in the initial toxin testing of *M. anatoxicus* PTRS1, after culturing in BG11, ATX concentrations were <14 µg/L, and dhATX concentrations were at 14,714 µg/L.

The functional role of anatoxins are not completely clear but researchers hypothesize an adaptive ecological function of competitive and defensive benefits of ATX synthesis (B. Anderson et al., 2018; Holland & Kinnear, 2013). These strategies include decreasing motility on green algae, and the poisoning of macroinvertebrates and aquatic plants (B. Anderson et al., 2018; Kearns & Hunter, 2000, 2001). Kearns & Hunter (2001) found ATX (produced by the cyanobacterial genus *Anabaena*) severely decreased motility of a co-occurring planktonic algae after 3 days and caused complete paralysis after 12 days. This finding provides support for a competitive function of toxin production. A local study by Anderson et al. (2018), found toxins produced by *M. anatoxicus* (previously morphologically identified as *Phormidum*), primarily dhATX, but other chemical compounds as well, to be especially toxic to three macroinvertebrates (*Hyalella Azteca, Chironomus dilutus,* and *Ceriodaphnia dubia*), providing support for defensive functions. The macroinvertebrates were grown in filtered *M. anatoxicus* culturing medium, which contained known and unknown cyanotoxins, but not cyanobacterial cells. As additional support for a defensive function, a New Zealand strain of *Microcoleus* increased toxin concentrations during periods of growth, which suggest perhaps a protective function (Harland et al., 2013).

Despite these possible functions, the toxicity of a mat or the future toxicity of blooms is unpredictable (Heath et al., 2010). Mats are made of heterogeneous genotypes of toxic and non-toxic filaments, therefore determining the toxicity of a field sample may rely on the abundance of toxic filaments within the entire colony (Heath et al., 2010). The function of

the toxins, and the triggers for their production, remain unclear. Additional research is needed to answer these questions. Benthic cyanobacterial blooms producing potent toxins are increasing globally, scientific support is needed for more efficient and effective mitigation efforts (Fetscher et al., 2015; Quiblier et al., 2013; R. Wood, 2016).

### Anthropogenic Impacts, Climate Change and Cyanobacteria Growth

The downstream effects of human activity has directly and indirectly resulted in coastal acidification, salinization, deoxygenation, increased trace metals and nutrient concentrations (Sutula et al., 2021). Particularly the eutrophication of freshwater may trigger cyanobacterial blooms (Cañedo-Argüelles et al., 2013; Herbert et al., 2015; Smith et al., 1999; Sutula et al., 2021). Industries such as agriculture, or mining, as well as larger processes such as sea-level rise or climatic temperature increases, cause an influx of nutrients and salts into freshwater bodies (Cañedo-Argüelles et al., 2013). Sea-level rise pushes saline sea water further up streams that open into the ocean. The rise in water level is also expected to increase erosion that releases trapped particles in the ground out into the water. Temperature increases are also expected. Temperature increases can cause evaporation and that can cause an increase in the concentration particles in a body of freshwater (Herbert et al., 2015; IPCC, 2021). Herbert et al. (2015) further explains another direct anthropogenic cause of salinization: mining. Mining industries bring deeply buried brine water up to the surface to be deposited as wastewater. This discharge contaminates surrounding aquatic systems, increasing salinity (Herbert et al., 2015). Cyanobacteria tend to have some better resistance to salinity than other species, as described by Kurobe et al. (2018) which found a shift toward cyanobacterial community dominance in brackish water around San Francisco

(Kurobe et al., 2018). As freshwater streams salinize, cyanobacterial species may be less susceptible and thus be able to outcompete other species to some extent.

While agriculture salinizes freshwater to a lesser degree, it is a main source of anthropogenic eutrophication of freshwater systems (Herbert et al., 2015; Smith et al., 1999). Nitrogen and phosphorus are often the limiting nutrients, so fertilizers tend to have high levels of both to maximize growth. But not all of the fertilizer is taken up by the intended crops. The nutrients leak into the groundwater or run into streams and, just as crops use the nutrients for growth, so do aquatic plants and algae (Smith et al., 1999). Favorable factors that cause the cyanobacteria blooms additionally include higher temperature and low water flow, both of which have also been progressed by anthropogenic waste and climate change (Svirčev et al., 2019). Nitrogen is extremely important for algae growth and its availability has doubled in parts of ocean off the California coast due to polluted run offs, especially that from agricultural areas (Quiblier et al., 2013; Sutula et al., 2021; S. A. Wood et al., 2020).

These, now salinized and nutrient-rich freshwater streams, act as drains carrying particularly high concentrations of particles out into the ocean. Oceans are relatively low in nutrients and high in salts, but polluted freshwater streams are a main cause of coastal eutrophication (Smith et al., 1999; Sutula et al., 2021).

Industrial and mining waste, while high in salts as described earlier, tend to contain high concentrations in metals which are flushed into streams and rivers. These metals are potentially toxic and stressors for *Microcoleus* (Harland et al., 2013). Increased copper stress has been implicated in the New Zealand study which found that iron and copper exposures had a negative impact on growth, but no significant impact on ATX production (Harland et al., 2013).

Some pollutants appear to have positive effects on growth. For example, the heavy use of fertilizer in agriculture increases the influx of nutrients like nitrogen and phosphate. *Microcoleus* does not have the ability to fix nitrogen, thus it uses uptake strategies to harvest nitrogen from the environment (S. A. Wood et al., 2020). The new abundance of nitrogen is speculated to have caused and continue to cause *Microcoleus* blooms. Similarly, the phosphates needed for proliferation are leeched from the water by *Microcoleus* in combination with products of mutualistic proteobacteria (S. A. Wood et al., 2020). Like nitrogen, the introduction of more phosphorus into freshwater streams can intensify the growth of these cyanobacteria. Conversely, Subbiah et al. (2019) found field water samples of ATX to have negative relationships with ions including chlorides, nitrogen ($NO_3$ and $NH_4$), and sulfates, but positive relationships with phosphorus and measurements such as pH. Variation in the relationships between water quality parameters and toxin concentrations or cyanobacterial growth can be attributed to local conditions, and differences in experimental media or *Microcoleus* strains. This only emphasizes the complexity of these relationships and the importance of further studies.

Temperature is predicted to continue to increase and water flow is expected to diverge such that current low flows are expected to slow and high flows are excepted to increase (Schneider, 2015). The total dissolved solids (TDS) have generally increased in California groundwater compared to measurements from 1910 to a period between 1993 and 2015. (Hansen et al., 2018). Because of agriculture waste products, nutrient availability is also expected to increase. As described above, benthic algal growth is determined, abiotically, by water quality factors such as particle concentration, nutrient levels, pH, water dynamics, and temperature (Schneider, 2015). How these factors will change under future

climate and even more so, how climate change will then affect benthic algal toxin production is especially difficult to predict due to unknown adaptation abilities, and complex interspecific and abiotic interactions (Schneider, 2015).

### The Experiment, the Purpose, and Goals

This experiment was intended to test how possible future drouth influenced by anthropogenic climate change in the Russian River may affect the growth and toxin production of *Microcoleus* in a controlled, laboratory setting. Increased temperature leads to water evaporation and higher concentration of ions and salts, therefore we exposed *M. anatoxicus* to increased salinity stress hypothesizing that it would cause increased toxin production as a defensive mechanism and decrease in growth of this freshwater species. We also predicted that with increased nutrient concentrations growth would increase, and with increased stress, ATX production would increase.

## METHODS

### Sampling Site and Collection

The sample of *M. anatoxicus* used in this study was collected in 2015 from a benthic mat from State Site Camp Rose (#114RR3119, 38.613618, -122.831158) in the Russian River. The sample transported in an insulated cooler for isolation by Dr. Rosalina Stancheva Hristova at the California Primary Algae Laboratory at California State University, San Marcos (CSUSM).

### Isolation, Culturing, and Initial Morphological Identification

Free-floating trichomes of the non-axenic sample were transferred, along with a few drops of liquid BG11, using a Pasteur pipette, into a petri dish with solid BG11 (1% agar).

Strains were grown at 20-23 C°, with irradiance of 80 mmol photons $m^{-2}s^{-1}$ and a 12:12-h light:dark cycle. Every 2 weeks strains were transferred to a fresh agar medium until a monoculture was obtained. This took approximately 3 months. Under the same conditions, single filaments were cultured in 125-mL Erlenmeyer flasks containing 60 mL of liquid BG11 medium. Both field samples and cultures were observed and recorded with an Olympus SZ-40 stereo microscope and Olympus microscope BX41 with an attached Olympus SC30 digital camera (Olympus Imaging America). Morphological identification used characteristics such as cell width, length, color, granulation, extracellular mucilage, and motility as guided by Komárek & Anagnostidis (2005) and the sample had a minimum of 40 cells measured from 20 trichomes.

**Treatments Set Up**

*Microcoleus anatoxicus* strain PTRS1 was cultured in twelve liquid media representing different combinations of freshwater with natural or artificial sea water under the same culturing conditions described above. The intended control media was treatment 1 (T1), liquid BG11 (Sigma-Aldrich, St. Louis, MO). BG11 is the most commonly used growth medium for freshwater cyanobacteria (Allen & Stanier, 1968) in which the nitrate and phosphate levels are exceptionally high (R. Anderson, 2005). The second treatment (T2) was BG11 diluted to 50% with deionized water (DIW). Treatment 3, 4, and 5 (T3, T4, and T5) were 10%, 20%, and 25% dilutions (respectively) in concentrations of artificially enriched filtered sea water (eFSW). eFSW was created using filtered sea water (FSW) collected from the Pacific Ocean at the Scripps Institution of Oceanography Pier and kept in stock at CSUSM. For the eFSW treatments, the FSW was enriched with major elements of 7.5% $NaNO_3$, 0.5% $NaH_2PO_4$, and a “Trace Elements cocktail” (consisting of 2.2% $ZnSO_4$, 1%

$Cocl_2$, 18% $MnCl_2$, 0.63% $NaMoO_4$, $FeCl_3$, and $Na_2EDTA$), and a Vitamin cocktail (0.01% Biotin, 0.1% $B_{12}$, and Thiamine HCL) (Soto et al., 2006). Treatment 6 (T6) consists of addition of 0.25 g/L NaCl in BG11. Treatments 7 through 10 (T7, T8, T9, and T10) were artificial sea salt (SS) solutions consisting of mimics of 10%, 20%, 25%, and 30% of salts found in the ocean (Supplemental Table 1). Treatment 11 (T11) uses plain filtered sea water (pFSW) diluted to 25% with DIW. Treatment 12 (T12) uses pFSW diluted to 25% with BG11.

The stressors induced in T2, T11 and T12 were intended to be significantly reduced nutrients in combination with variably increased salinity. Stressors in T3 - T5, and T7 - T10 were intended to be steady increased salts gradients, and decreased nitrogen (N) and phosphorus (P). T6 was intended to have just increased salinity. The treatments were grouped into three content gradients: BG11 treatment group (T1, T2, T6), FSW (T3, T4, T5, T11, T12) and SS (T7, T8, T9, T10).

For each medium we inoculated four flasks on June 18, 2021, each containing 400 mL of each medium (Supplemental Table 2) and a small clump of *Microcoleus* filaments. Three of the flasks (A, B, and C) were used for toxin analysis and RNA extraction, and the remaining flask (D) was used for morphological observations. *Microcoleus* treatments were incubated at 20 C° to 22 C°, with an irradiance of 80 mmol photons $m^{-2}$ $s^{-1}$ and a 12:12-h light:dark cycle.

The allowed growth period across all treatments ranged from 26 to 31 days, then cells and liquid were taken for toxin measurements and RNA extraction for gene expression quantification. Best growing cultures, as determined by sight, were extracted first, and least successful growth was extracted last. After 26 days of growth, all treatments in the BG11

group were extracted (T1, T2, and T6) (July 15). After 27 days of growth, T3, T4, and T5 from the FSW treatment group were extracted (July 16). After 30 days, most of the SS and another set of flasks from the FSW group were extracted (T7, T8, T9, and T12) (July 19). T10 and T11, which showed the poorest growth of all the treatments, were extracted after 31 days (July 20).

**Chemistry Composition of Media**

One additional flask of each media was sent to Dr. Ramesh Goel at the University of Utah. Nutrient concentrations ($NO_2$-N, $NO_3$-N, $PO_4$-P, and $NH_4$-N), Cl, $SO_4$ were analyzed through chromatography. Conductivity, pH, total dissolved solids (TDS), and salinity of each media was measured with Oakton portable meters.

**Cyanotoxins Analyses**

From each flask a subsample was collected for toxin analysis. First, *Microcoleus* filaments were removed very carefully from the sides and bottom of the flasks and gently homogenized. Approximately 15 ml of representative biomass and culturing liquid from flasks A, B, and C of each media was collected in plastic 15 ml tube. The fresh samples were shipped on overnight on ice to Dr. Gregory Boyer at the State University of New York. Next day, the whole samples were first filtered to differentiate between the toxins in the filaments (intracellular) and in the culturing liquid (extracellular). Then the filaments were lyophilized until dry and dry weight mass was determined. We used the dry weight mass as proxy of filament growth. Using ultrasound, powder was extracted in 5 ml of 50% methanol and centrifuged to clarify. The toxins were measured both in the filtered liquid (extracellular) and in the lyophilized filaments (intracellular). Toxin measurements of ATX, dhATX, homo-anatoxin-a and dihydro-homo-anatoxin-a were determined by liquid chromatography and

mass spectrometry methods (LC-MS/MS) with a US-EPA method 545 modification. Limits of toxin measurements ("non-detect") depended on the amount extracted per sample. The experimental strain PTRS1 was tested for toxins before the experiment (on April 30, 2021) to confirm the toxin production, considering that the strain is maintained in the lab since 2015. However, in the pre-treatment sample, the toxins were measured as a whole, without distinguishing between intra-, and extracellular concentrations as they were for this experiment when they were measured at the end of July.

For this experiment, toxin measurements were received in two main parts: toxin measurements from the dry weight and toxin measurements from the filtrate. Toxins from the dry weight were assumed to have been stored within the cell and will be referred to as intracellular. Toxins measured from the liquid were assumed to have existed extracellularly.

### Morphological Methods at End of Treatments

The morphology of the filaments from each treatment was analyzed from fresh material on the date of extractions. The samples were observed and documented with an Olympus microscope BX41 with an attached Olympus SC30 digital camera (Olympus Imaging America). Morphological features, such as cell width and length, color, granulation, extracellular mucilage, and motility were characterized (Komárek & Anagnostidis, 2005).

### Methods for Gene Expression Quantification

Analysis of gene expression followed four steps: (1) RNA extraction, (2) cDNA synthesis, (3) Real-Time PCR, (4) statistical analysis. The harshness of some media resulted in the slowed growth of cells. Given that and time restrictions, RNA extractions were performed after 26 to 31 days (see Experimental Set-Up for further details). Cells were harvested by filtration. The filtrate was retained and disposed using safety precautions. The

biomass of *Microcoleus* mat captured on the filter was ground to a powder with liquid nitrogen. Growth for flasks 10A, B, C, and 11A, B, and C were particularly low. Because of this, flasks 10A, B, and C were combined into a single extraction for treatment 10. Flasks 11A, B, and C were combined into a single extraction for treatment 11. RNA was isolated using the Guanidium isothyiocyante method. The amount and purity of the RNA extracted was assessed using Thermo Scientific Nanodrop 2000 (Supplemental Table 3) by measuring the $A_{260}$, $A_{260/280}$, and the $A_{260/230}$. RNA extractions were performed in groups of 4 flasks (eg. 1A, 1B, 1C, and 2A were extracted in one batch, then 2B, 2C, 3A, and 3C in a second batch, and so on). because the purity of extracted RNA was low, several samples underwent 1 to 2 QIAGEN RNeasy RNA Clean Ups. It was determined that too much RNA was lost during clean ups, so they were not performed on all samples. Based on nanodrop results and visual assessment, a second chloroform wash was performed on 6B, 6C, 7A and 7B in attempt to celan up the RNA. Remaining samples had no clean ups (Supplemental Table 3). Flask 1B and 9C were determined to have the best quality RNA (Table 4).

**Table 4.** RNA extraction quality results of a BG11 and 25% SS treatment flask using Nanodrop.

| **Treatment and Flask ID** | **Media** | **Concentration (ng/ul)** | **A260/A280** | **A260/A230** |
|---|---|---|---|---|
| 1B | BG11 | 175.5 | 2.13 | 1.54 |
| 9C | 25% SS | 1485.4 | 1.70 | 1.16 |

These two RNA samples from treatment 1 and 9 were converted into cDNA and then gene expression was quantified using a RT PCR. QIAGEN Omniscript Reverse Transcriptase procedure was used for cDNA Synthesis. QuantStudio RT PCR machine was used, with three technical replicates performed using three independent cDNA syntheses (no experimental replicates, same sample was used to synthesize new cDNA each time). Gene expression levels for every gene within the operon, except anaD, were quantified. In the

absence of a defined housekeeping gene, relative levels of gene expression were compared between the 25% SS treatment and the BG11 treatment (intended control) (Supplemental Figure 11). Because no experimental replicates were performed, and replicates were only independent at the level of cDNA synthesis, gene expression was quantified in relation to total RNA amount.

**Statistical Analyses**

Results were analyzed in Excel and Rstudio. Excel was used to collect and organize the data. R was used to run all statistical tests, covariance tests, and create all graphs. Initial covariances were tested using the `pairs.panels` function from the `psych` package in R. Graphs were created using the `ggplot2` package in R. Treatment groups could not be assessed for normality because sample sizes ranged from 3 to 5. Simple linear regressions were performed to gain a general understanding of the relationship between variables. The equation (given in $y = mx + b$), adjusted $R^2$ (R), and the p-value ($p_R$) will be presented to gain an idea of the tendencies of the relationships between variables. The more rigorous, non-parametric Spearman's Rank-Order Correlation test was performed to gain a more realistic idea of the strength of relationships between variables. The Spearman test ranks the relationship between the variables and assessed its fit against a monotonic function. For the Spearman test, the "$r_S$" value (also called "rho") denotes how perfectly the association of ranks fits against the monotonic function. "$p_S$" will signify the significant between the variables as determined by the Spearman test. Output from the simple linear regressions and Spearman's Rank-Order Correlation will be presented in conjunction with each other to provide a holistic interpretation. For both tests, $p < 0.05$ will be considered significant.

# RESULTS

## Media Chemistry

The data are analyzed as whole, evaluating the observations and measurements from all 12 treatments, and in their treatment groups, which show gradients in media chemistry. Media groupings are supported as follows:

1. **BG11 group**. This groups includes BG11-based media in aim to create nutrient gradients. The BG11 group consists of pure BG11 (T1), 50% DI diluted BG11 (T2), and BG11 with addition of NaCl (T6). BG11 group has lowest chloride concentrations (20.4 - 213.5 mg/L) and is indicated with green color in the figures.
2. **FSW group**. This group which includes FSW-based media proportionally mixed with BG11 consists of 10% eFSW (T3), 20% eFSW (T4), 25% eFSW (T5), T11 and T12, which consist of 25% pFSW in DIW and BG11, respectively. FSW group has high chloride concentrations (1810.8 - 4558.9 mg/L) and is indicated with cyan color in the figures.
3. **SS group**. This groups incudes artificial sea salt mixture (SS) proportionally mixed with BG11 consisting of the treatments 10% SS (T7), 20% SS (T8), 25%SS (T9), 30% (T10). SS group has highest chloride concentrations (1999.7 - 5230.1 mg/L) and is indicated with yellow color in the figures.

This experiment was intended as a pilot experiment to test the effect of different chemical combinations of *M. anatoxicus,* so the gradient treatments were very limited. Concentrations for all nutrients between all treatments are shown below in Figures 10 – 14.

The biggest difference between the treatment groups were chloride and sulfate concentrations. The BG11 treatment groups had, by a large margin, the lowest chloride and

sulfate concentrations. The SS and FSW groups had similar chloride, and less so of sulfate concentrations. All treatments had relatively similar nitrate and phosphate levels. However, in the FSW and SS groups, the increased salinity gradient was loosely reversely related to nutrient gradients. Generally, treatments are heterogeneous, but T7 - T10 and T3 - T5 successfully showed salinity gradients.

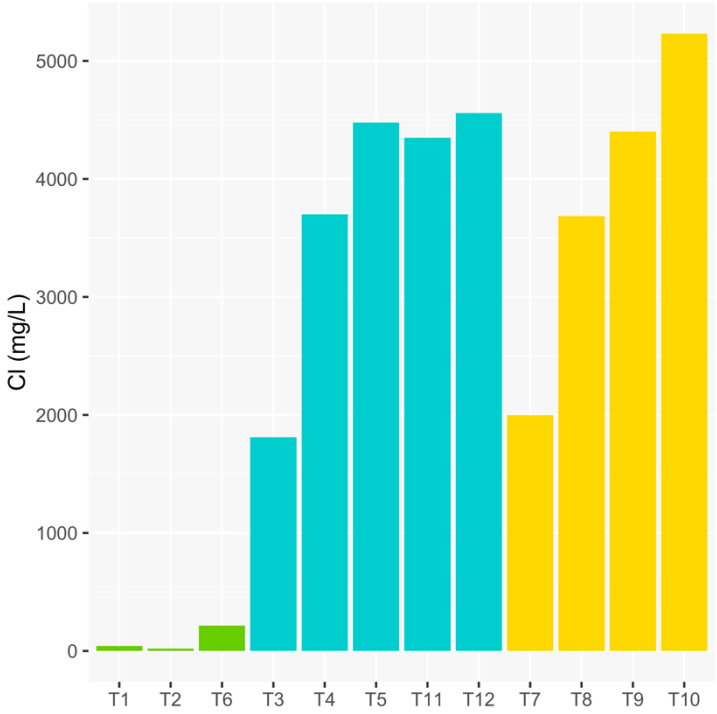


**Figure 10.** Chloride concentrations for all culturing treatments (T1 – T12). Bar color corresponds to the grouping for statistical analysis (BG11 group = green, FSW group = cyan, SS group = yellow).

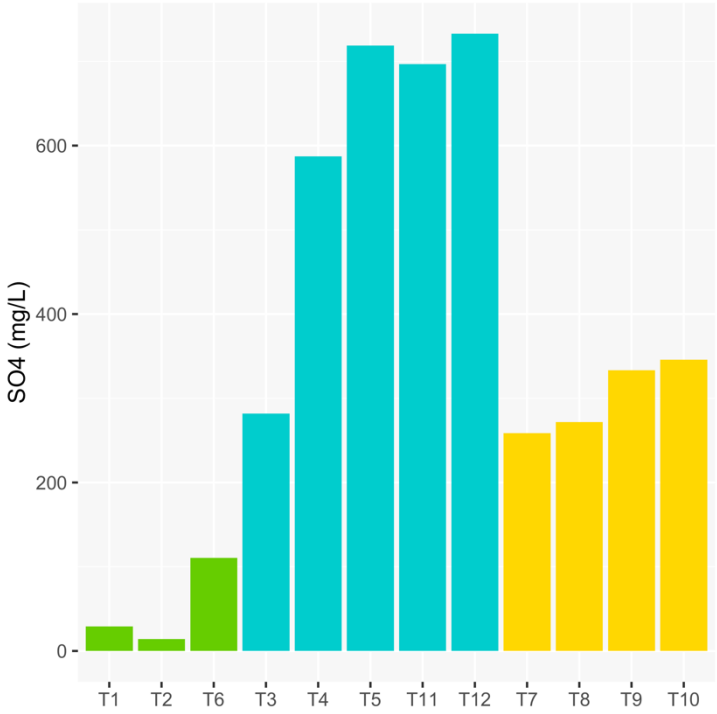


**Figure 11.** Sulfate concentrations for all culturing treatments (T1 – T12). Bar color corresponds to the grouping for statistical analysis (BG11 group = green, FSW group = cyan, SS group = yellow).

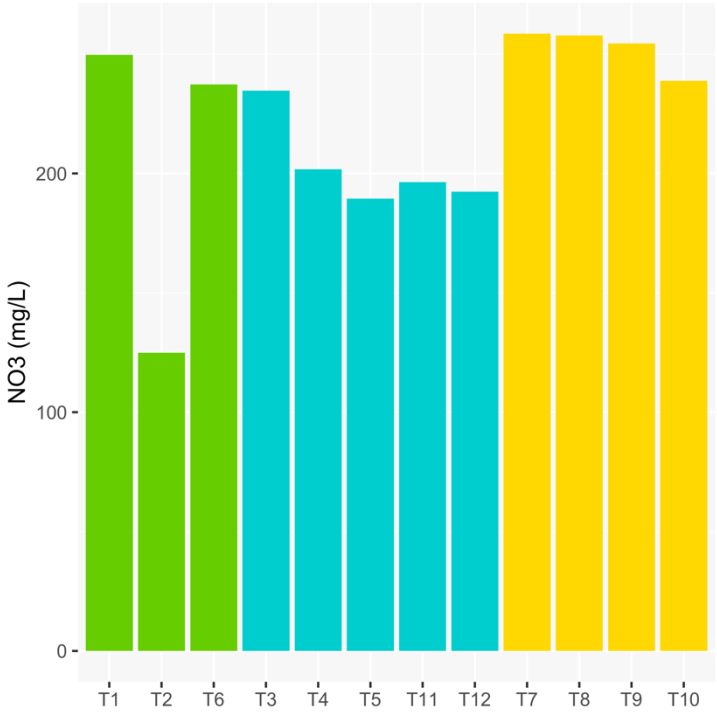


**Figure 12.** Nitrate concentrations for all culturing treatments (T1 – T12). Bar color corresponds to the grouping for

statistical analysis (BG11 group = green, FSW group = cyan, SS group = yellow).

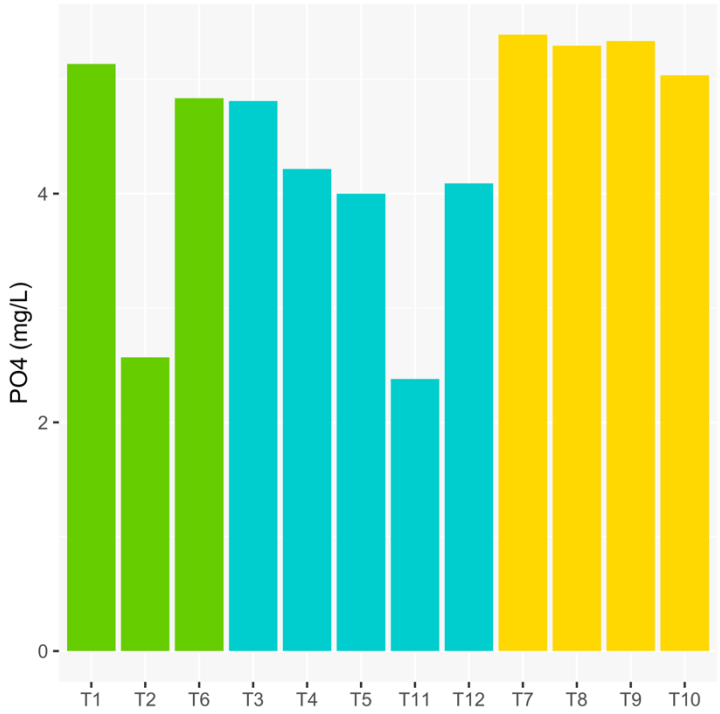


**Figure 13.** Phosphate concentrations for all culturing treatments (T1 – T12). Bar color corresponds to the grouping for statistical analysis (BG11 group = green, FSW group = cyan, SS group = yellow).

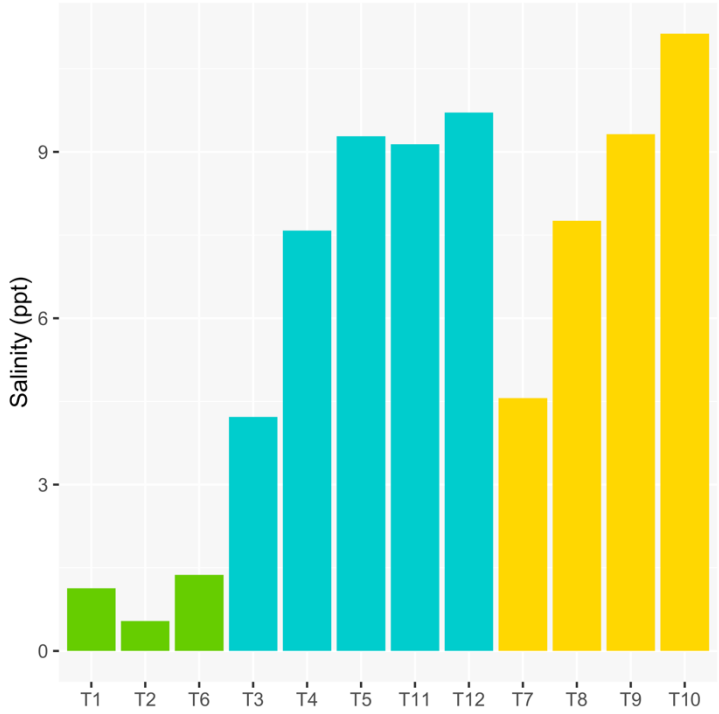


**Figure 14.** Salinity concentrations for all culturing treatments (T1 – T12). Bar color corresponds to the grouping for statistical analysis (BG11 group = green, FSW group = cyan, SS group = yellow).

**Covariance within Chemistry**

Across each treatment groups, strong covariance (above 0.7) and moderate covariance (0.5 to 0.7) was found between some independent variables (Supplemental Figures 15 – 17). Cl, $SO_4$, conductivity, TDS, and salinity strongly covary across all groups. Salinity will be used as the independent variable of interest for Cl, conductivity, and TDS. $SO_4$ had the weakest covariance and will still be separately analyzed (Figure 18).

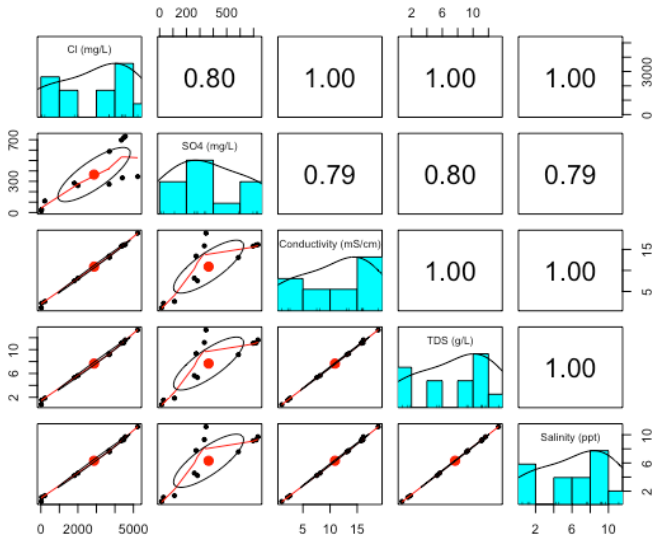


**Figure 18.** Covariance between chlorides, sulfates, conductivity, TDS, and salinity across all treatment groups (T1 – T12).

### Media Growth and Toxin Production

*Microcoleus* growth was intense in most of the treatments, except for SS groups (T9, T10) and FSW group treatment T11, where only small filament accumulations with reddish color or nearly colorless were observed at the time of extraction (Supplemental Figures 19 - 30). In the remaining flasks, filaments formed dense olive-brownish to reddish mats on the walls of the flasks, and some mats were detached and free-floating. T3 (10% FSW and 90% BG11) had exceptionally higher growth. T3 toxin measurements were among the lowest. On the other hand, T10 (30% SS and 70% BG11) had the lowest dry weight, but the highest ATX. T10 dhATX concentrations were still low. Figures 31 – 34 describe these observations.

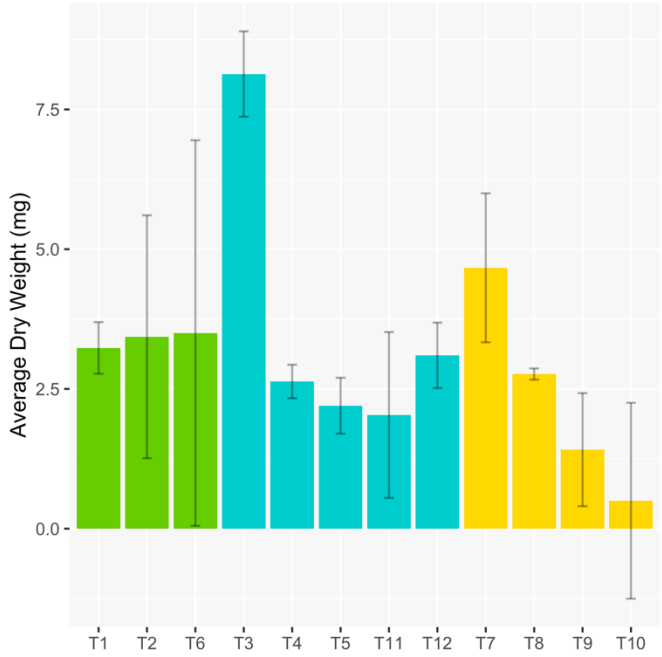


**Figure 31:** *M. anatoxicus* average dry weight mass and standard error (n=3 per treatment) in all culturing treatments (T1 – T12). Bar color corresponds to the grouping for statistical analysis (BG11 group = green, FSW group = cyan, SS group = yellow).

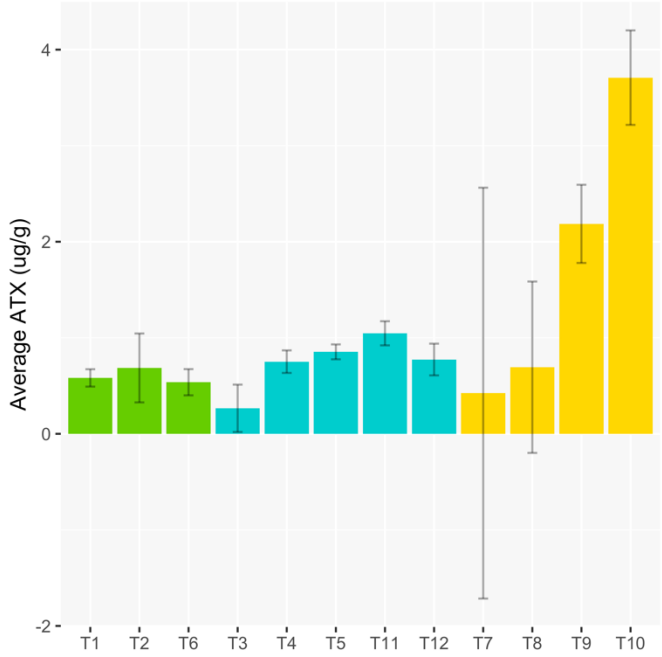


**Figure 32:** *M. anatoxicus* average intracellular ATX and standard error (n=3 per treatment) in all culturing treatments (T1 – T12). Bar color corresponds to the grouping for statistical analysis (BG11 group = green, FSW group = cyan, SS group = yellow).

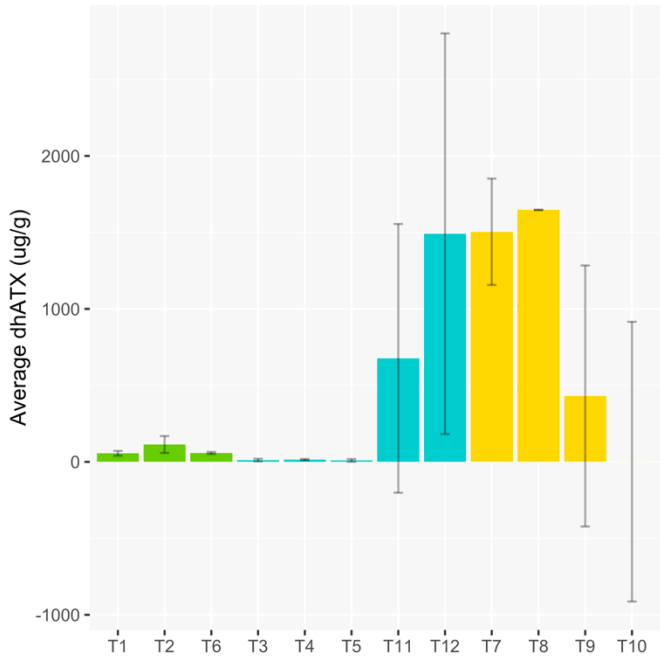


**Figure 33:** *M. anatoxicus* average intracellular dhATX and standard error (n=3 per treatment) in all culturing treatments (T1 – T12). Bar color corresponds to the grouping for statistical analysis (BG11 group = green, FSW group = cyan, SS group = yellow).

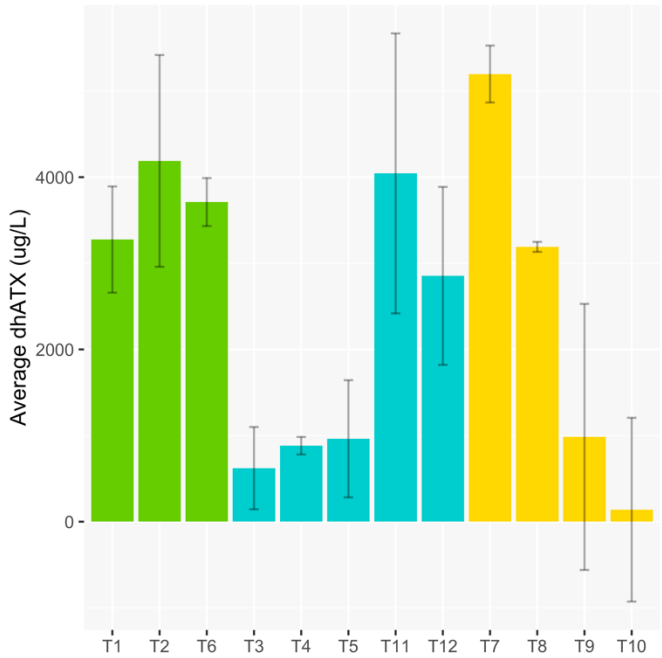


**Figure 34:** *M. anatoxicus* average extracellular dhATX and standard error (n=3 per treatment) in all culturing treatments (T1 – T12). Bar color corresponds to the grouping for

statistical analysis (BG11 group = green, FSW group = cyan, SS group = yellow).

The initial toxin testing of *Microcoleus* strain PTRS1 prior to experiment grown in BG11 showed ATX <14 µg/L and dhATX 14714 µg/L. Note that prior and experimental measurements of toxins are not directly comparable because methodology used in prior assessments differed from that used in this experiment. However, during the experiment the average ATX and dhATX in the freshwater BG11 control (T1) were 0.58 and 55.93 µg/g, and in 50% diluted BG11 (T2) were 0.68 and 113.34 µg/g, respectively. In all treatments with increased salinity, combined FSW and SS, the ranges of ATX and dhATX were 0.26 - 3.71 µg/g, and 1.06-1646.95 µg/g respectively. *M. anatoxicus* produces much more dhATX than ATX but there is a possibility that dhATX may be at least partially a biodegradation product of ATX. ATX may be a more stable indicator of toxin production, but dhATX correlations are still explored. Within the data, it is unclear how the production of these toxins (or degradation) relates, and therefore it is still important to analyze all three toxin fractions against the environmental variables.

Across all treatments, toxins showed no, or very low covariance between each other (Figure 30). However, moderate to strong covariance were found between all toxins in the BG11 group and in the SS treatment group (|0.7| to |0.97| covariance) (Figures 35-38). The main difference between these two groups is that for the BG11 treatments, all toxins were positively correlated with each other, whereas in the SS treatments, both internal and external dhATX decreased with increase in ATX production. As for the FSW treatment group, only low to moderate covariances were found. In contrast to SS, moderate positive covariances were found in FSW between ATX and extracellular dhATX (0.68). Intracellular ATX and dhATX in the FSW group showed no covariance (0.34). Consistent across all treatments was

that extracellular dhATX showed positive covariance with intracellular dhATX (0.9 in BG11 and SS, and 0.74 in FSW) (Figures 35-38).

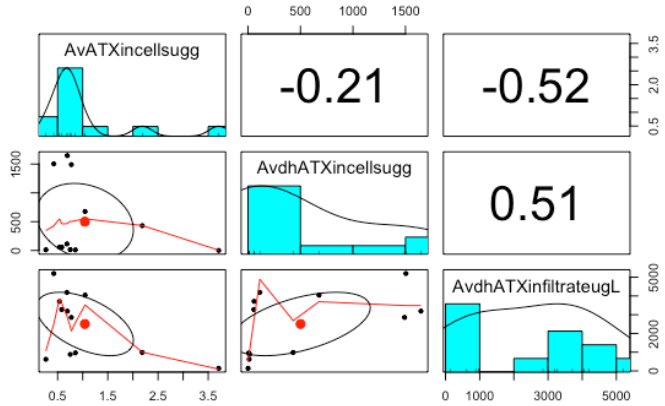


**Figure 35:** Covariance of intracellular ATX, dhATX, and extracellular dhATX across all treatments (T1 – T12).

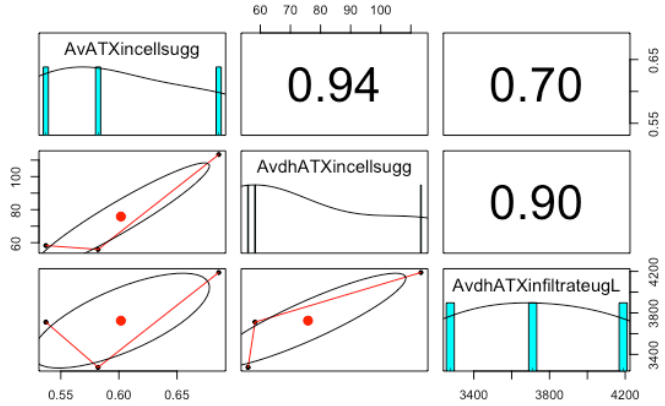


**Figure 36:** Covariance of intracellular ATX, dhATX, and extracellular dhATX across the BG11 treatments (T1, T2, and T6).

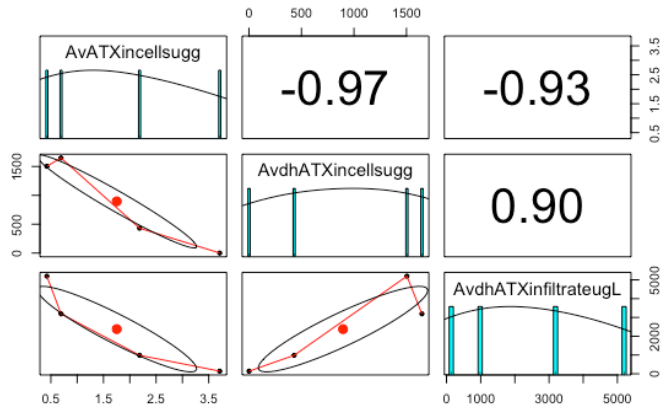


**Figure 37:** Covariance of intracellular ATX, dhATX, and extracellular dhATX across the SS treatments (T7 – T10).

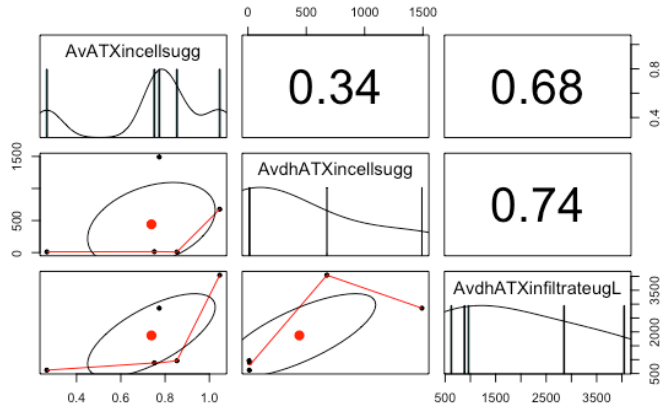


**Figure 38:** Covariance of intracellular ATX, dhATX, and extracellular dhATX across the FSW treatments (T3 - T5, T11, and T12).

**Morphological Results**

At the end of treatments, morphology of the filaments contrasted that of the control, BG11 (T1) (Figure 39). Figure 39A shows a typical morphology of *M. anatoxicus* grown in optimal control conditions (BG11). Filaments had unconstructed cells with granulated content. The apical cells had thickened cell wall called calyptra. The trichomes were single enclosed in a colorless individual mucilaginous sheath. Increased salinity leads to intense production of extracellular polysaccharide mucilage. In 20% and 25% FSW treatment (T4 & T5) often several trichomes are formed inside a common wide sheath (Figure 39B) by

breaking up trichomes apart and forming apical cell with additional mucilaginous material on the top of the calyptra (Figure 39C). Similar enlarged calyptras and multiple trichomes in a common sheath were observed in 25% SS treatment (T9), but this treatment also caused cell constrictions (Figure 39D), and keratomization of the cells (Figure 39E). The cell protoplast looks “net-like”, or like having “vacuoles”, because the thylakoids are widened. This is an indication of stress conditions, such as increased amount of salts in medium 9 (Figure 39E), or nutrient starvation in medium 11 (Figure 39F). Cyanophycin granules store polyphosphates and carotenoids when nutrients are in excess. Note that the granules in the control are scattered through the cell (Figure 39A), while in media with increased salinity they are larger and along either side of the cross wall (Figure 39B - D), slightly decreasing in size and number in Figure 39E. The presence of granules indicated plenty of nutrients in the media. The lack of cyanophycin granules in medium 11 (Figure 39F) indicates nutrient starvation. The strains under salinity and nutrient stress produced odor volatile compounds, in contrast to the control, grown in optimal conditions.

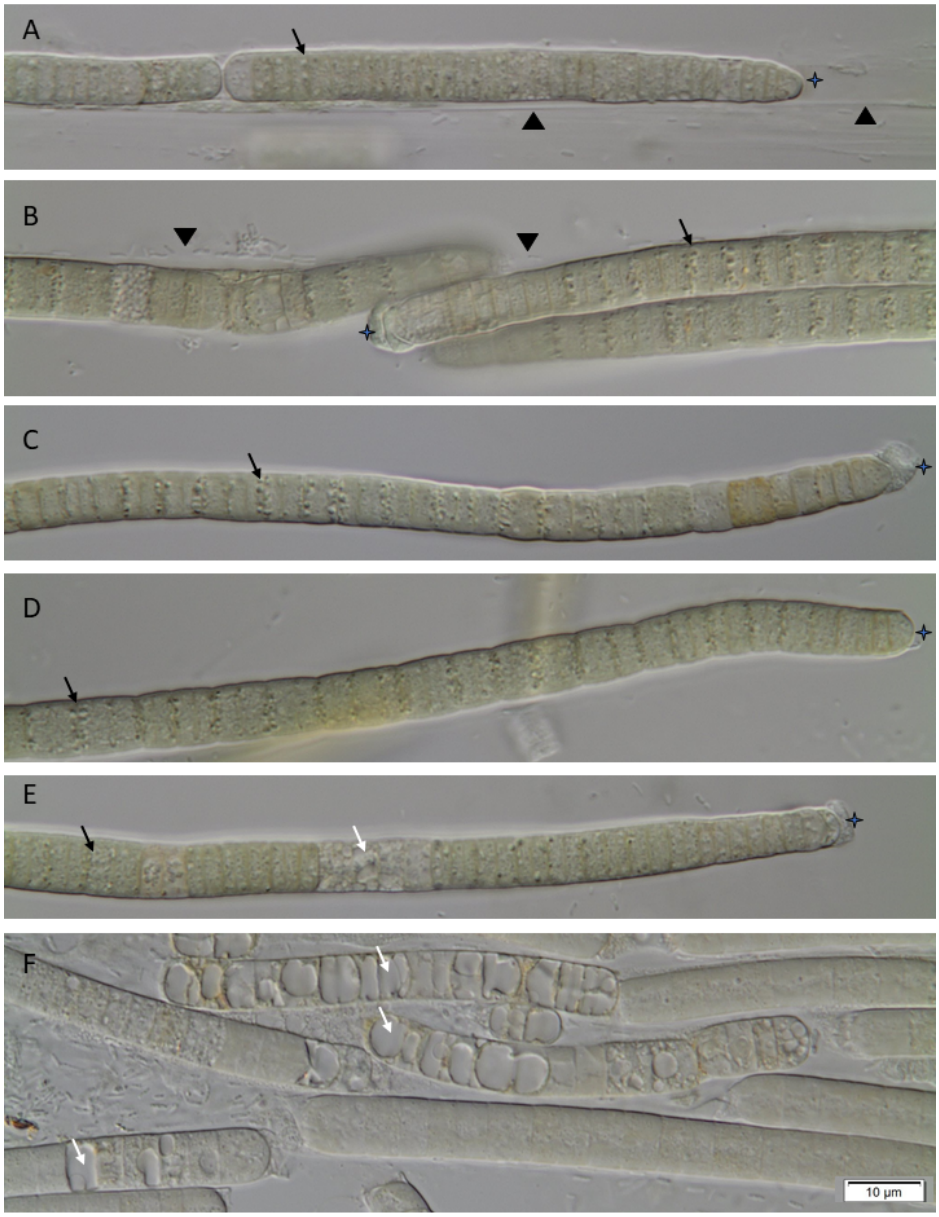


**Figure 39A-F.** *M. anatoxicus* morphology in different salinity treatments. Figure A. T1 (BG11, control). Figure B. T4 (20% eFSW). Figure C. T5 (25% eFSW). Figures D, E. T9 (25% SS). Figure F. T11 (25% pFSW). Legend: cyanophycin granules (black arrows), kerotomized cells (white arrows), mucilaginous sheath (triangles), kalyptra (stars).

**Effect of Water Chemistry on *Microcoleus* biomass**

The water chemistry parameters analyzed in this section include nutrient concentrations ($NO_3$ and $PO_4$), $SO_4$, and salinity. Salinity was the main aspect aimed to be varied. There were no significant correlations between salinity and dry weight mass in any of the treatment groups, however *Microcoleus* biomass decreased with increasing salinity in both SS and FSW treatment groups (Figures 40 & 41, Supplemental Tables 5 – 7).

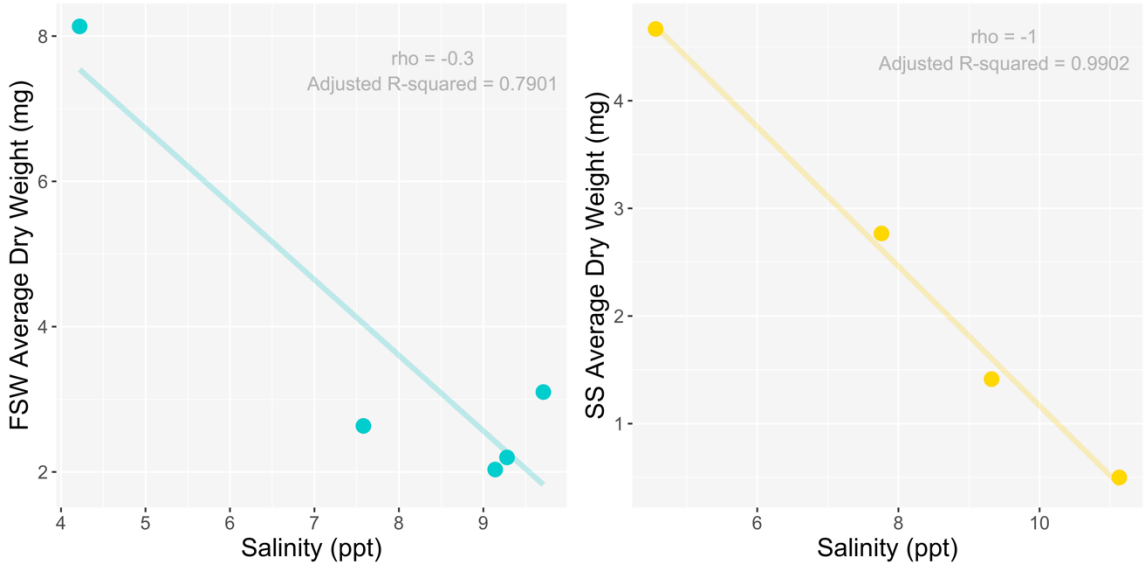


**Figure 40 & 41.** Relationship between *M. anatoxicus* average dry weight mass and salinity for the FSW (left) and SS treatment (right) groups (n=5 and 4) (Supplemental Table 6 & 7).

There were no significant correlations between dry weight mass and nitrates, phosphates, or sulfates, but there was a positive relationship between $NO_3$ and the dry weight, and a vague negative correlation between $SO_4$ and dry weight in the FSW group (Figures 41 & 42, Supplemental Tables 8 – 16). While nitrogen is an important growth factor, the inhibitory effect of salinity may have outweighed any benefit of the nutrient, causing tentative but not significant relationships. The negative pattern observed with sulfates fits this negative pattern with salinity.

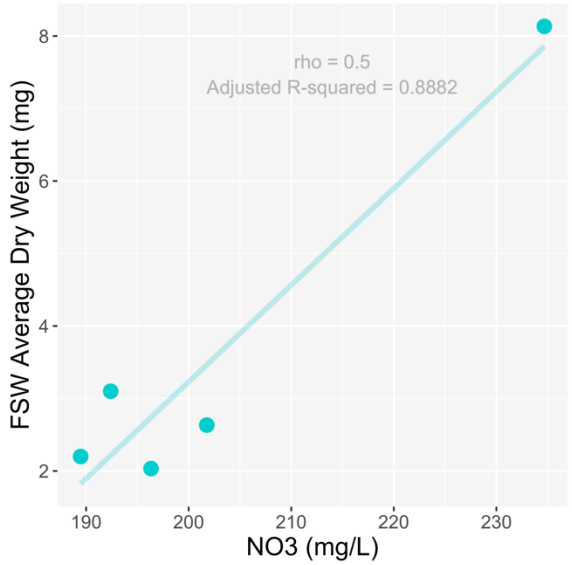


**Figure 41.** Relationship between *M. anatoxicus* average dry weight mass and nitrates for the FSW treatment group (n=5) (Supplemental Table 10).

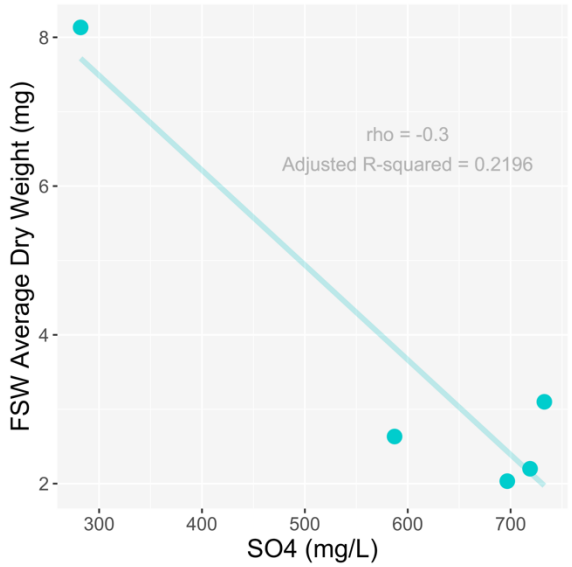


**Figure 42.** Relationship between *M. anatoxicus* average dry weight mass and sulfates for the FSW treatment group (n=5) (Supplemental Table 16).

### Effect of Water Chemistry on Intra- and Extracellular Toxin Concentrations

The only correlation that passed Spearman's Ranked Correlation test was the negative relationship between intracellular ATX and phosphate concentration in the FSW treatments (Figure 43, Supplemental Table 19). Only one other toxin showed a tendency with $PO_4$ was

intracellular dhATX in the BG11 group which also decreased with increased phosphates (Figure 44, Supplemental Table 20) (Supplemental Tables 17 – 25).

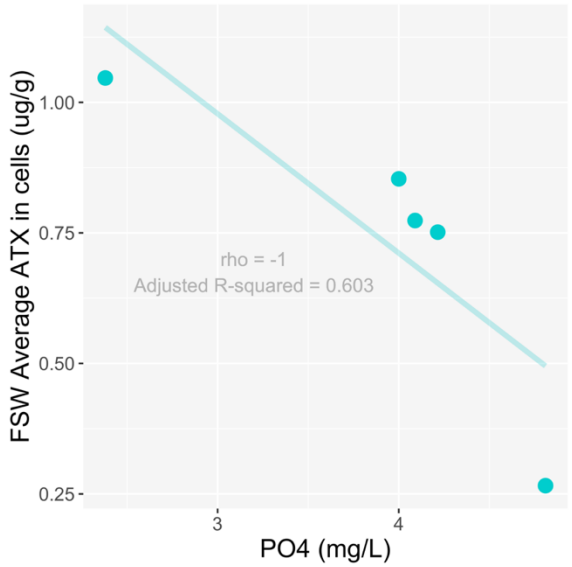


**Figure 43.** Negative relationship between *M. anatoxicus* average intracellular ATX and phosphates in the FSW treatment group (S = 40, $\mathbf{p_S = 0.01667}$, $r_S$ = -1, n=5) (Supplemental Table 19).

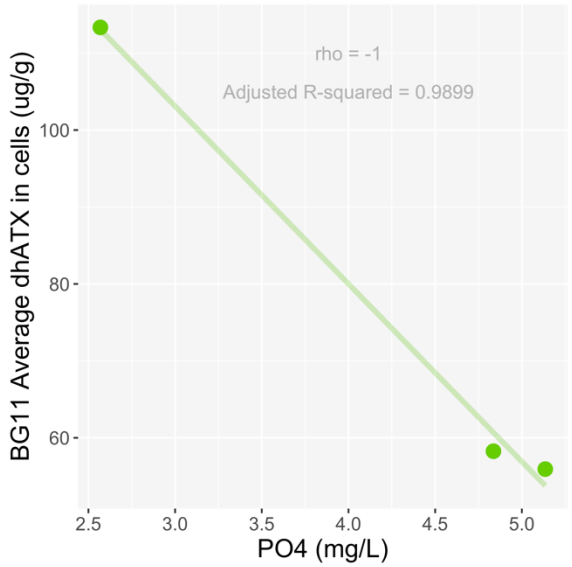


**Figure 44.** Negative relationship between *M. anatoxicus* average intracellular dhATX and phosphates in the BG11 treatment group (Supplemental Table 20).

Similarly, toxin production decreased with increasing nitrogen concentration, but these relationships were only found for intracellular ATX in the FSW group (Figure 45) and for intracellular dhATX in the BG11 group (Figure 46). None of these passed the more rigorous Spearman test (Supplemental Tables 26 – 34).

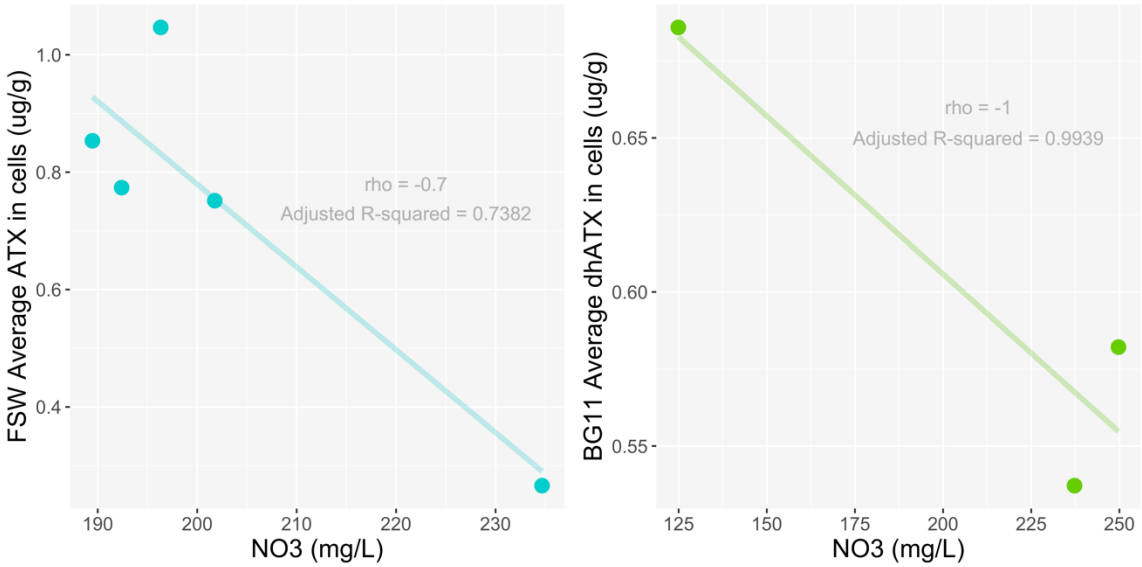


**Figure 45 & 46.** (Left) Relationship between *M. anatoxicus* average intracellular ATX and nitrates in the FSW treatment group (n=5) (Supplemental Table 26). (Right) Relationship between *M. anatoxicus* average intracellular dhATX and nitrates in the BG11 treatment group (n=3) (Supplemental Table 27).

Increased sulfates caused some weak increases in intracellular ATX in the SS and FSW, but both intra- and extracellular dhATX were negatively affected by sulfates (Figures 47 – 50) (Supplemental Tables 35 – 42).

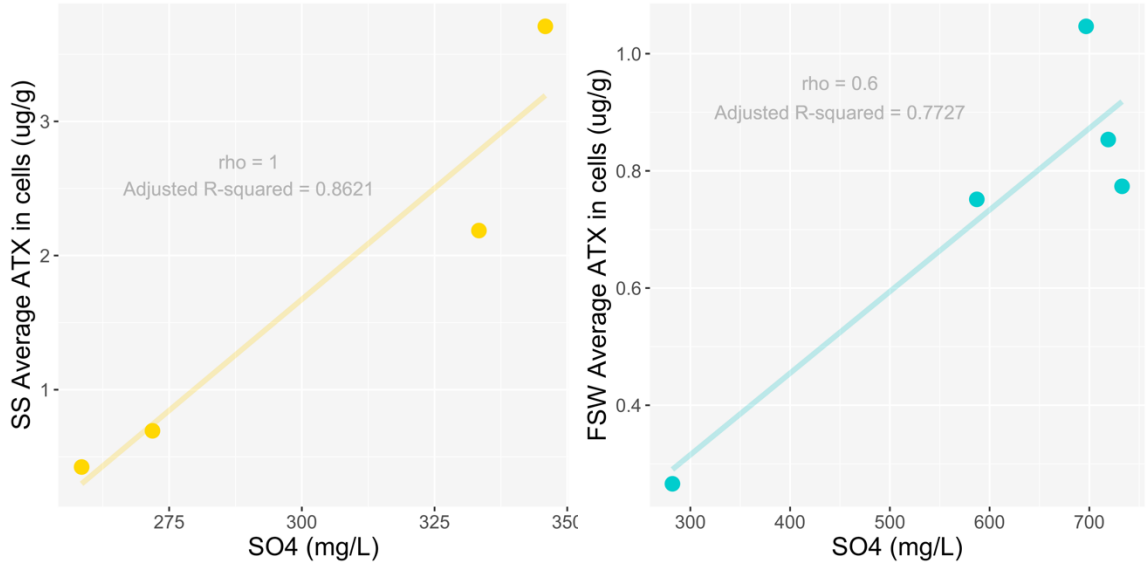


**Figure 47 & 48.** (Left) Relationship between *M. anatoxicus* average intracellular ATX and sulfates in the SS treatment group (n=4) (Supplemental Table 35). (Right) Relationship between *M. anatoxicus* average intracellular ATX and sulfates in the FSW treatment group (n=5) (Supplemental Table 36).

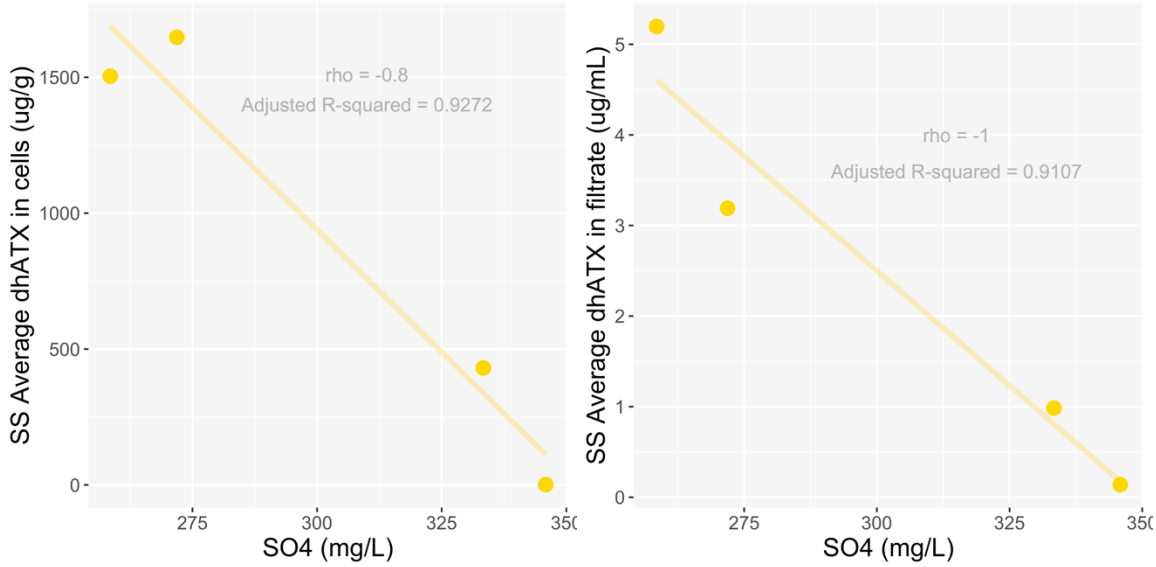


**Figure 49 & 50.** (Left) Relationship between *M. anatoxicus* average intracellular dhATX and sulfates in the SS treatment group (n=4) (Supplemental Table 38). (Right) Relationship between *M. anatoxicus* average extracellular dhATX and sulfates in the SS treatment group (n=4) (Supplemental Table 41).

Generally, it seems that both intra- and extracellular dhATX production may be negatively affected by nutrient concentrations and $SO_4$, but ATX production, also the more reliable measurement of synthesis, may be positively affected by salinity and $SO_4$, and negatively affected by nutrients. There was a negative relationship between intracellular ATX and salinity in the BG11 group, but it was positive in the FSW group (Figure 51 & 52). While almost no relationships were found between dhATX and salinity, there was some negative relationship in the SS group for extracellular dhATX and salinity (Figure 53) (Supplemental Tables 43 – 51).

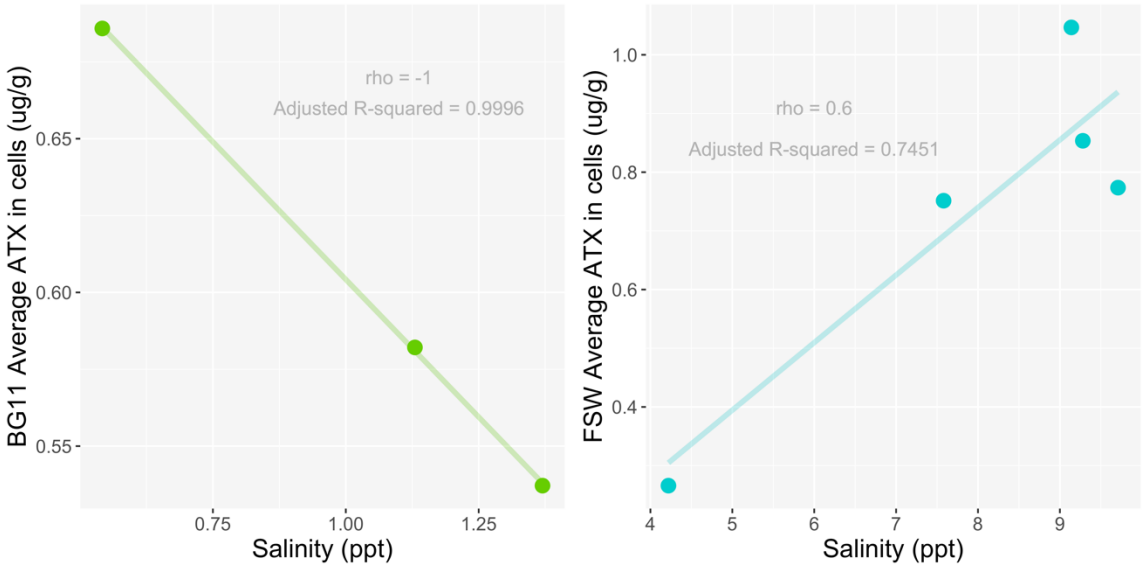


**Figure 51 & 52.** Relationship between *M. anatoxicus* average intracellular ATX and salinity in the BG11 (left) and FSW (right) treatment groups (Supplemental Tables 43 & 45).

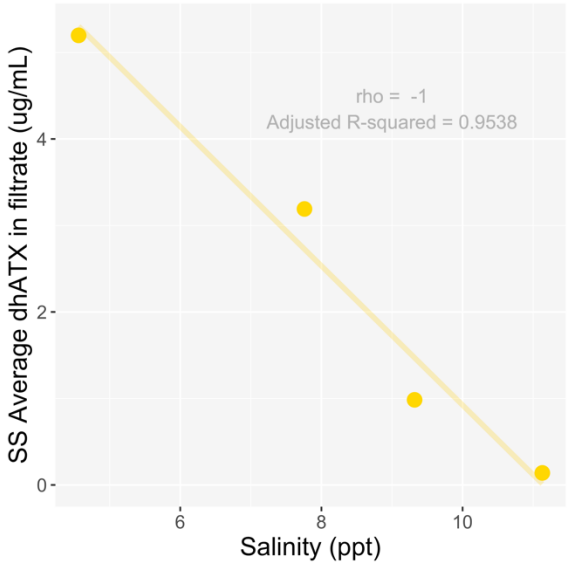


**Figure 53.** Relationship between *M. anatoxicus* average extracellular dhATX and salinity in the SS treatment group (Supplemental Table 50).

### Effect of Biomass on Toxin Production

In this experiment, toxin production seemed relatively unconnected directly to growth. Previous literature supported a positive relationship between growth parameters and toxin production, but we only observed an decreases in ATX (FSW) and extracellular dhATX (SS) with increased dry weight (Harland et al., 2013). (Figure 54 & 55, Supplemental Table 54 & 59). Intracellular dhATX showed no relationship in any treatment (Supplemental Tables 52 – 60).

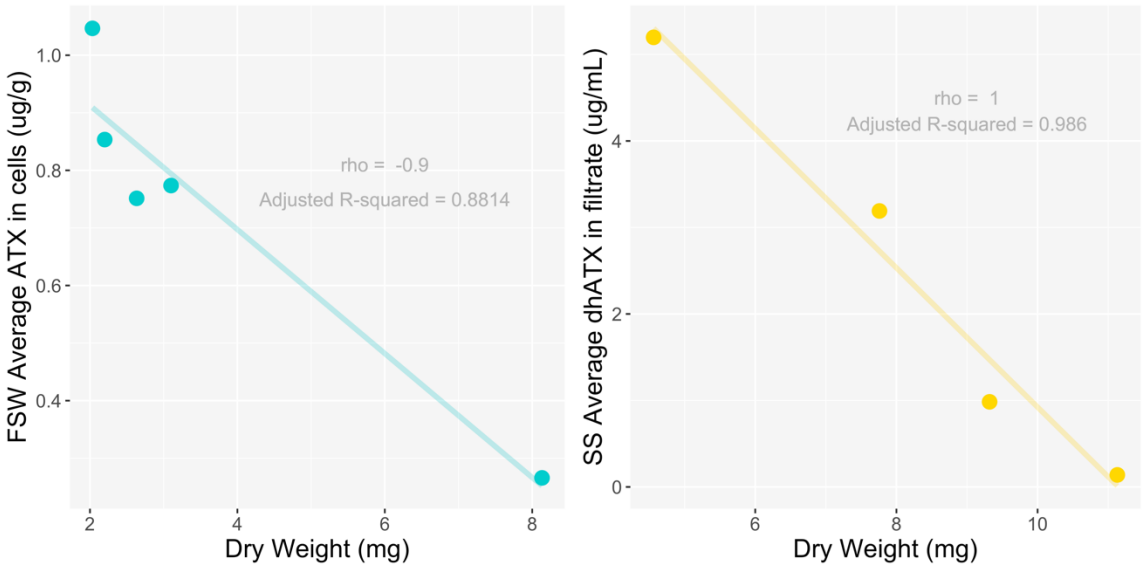


**Figure 54 & 55.** (Left) Relationship between *M. anatoxicus* average dry weight mass and average intracellular ATX in the FSW treatment group (n=5) (Supplemental Table 54). (Right) Relationship between *M. anatoxicus* average dry weight and average extracellular dhATX in the SS treatment group (n=4) (Supplemental Table 59).

Below, Table 61, provides a summary of the direction of all relationships found in the different treatment groups in this study between media chemistry and response variables.

**Table 61.** Summary of Media Chemistry Results.

| **Controlled Variables** | **Response Variables** | | | |
|---|---|---|---|---|
| | **Dry Weight Mass** | **Intracellular ATX** | **Intracellular dhATX** | **Extracellular dhATX** |
| **Salinity** | - FSW / -SS | - BG11 / + FSW | None | - SS |
| **Sulfates** | - FSW | + FSW / + SS | - SS | - SS |
| **Nitrogen** | + FSW | - FSW | - BG11 | None |
| **Phosphates** | None | - FSW | - BG11 | None |
| **Response Variable** | | | | |
| **Dry weight** | N/A | None | - FSW | - SS |

**ATX Gene Regulation Quantification**

ATX gene expression was compared between the intended control, BG11 (T1) and 25% SS (T9). No housekeeping gene was used, instead, the average of three technical replicates of T9 was compared to T1. Nearly all of the genes in the anatoxin-a operon are expressed at a higher level when cells are grown in 25% SS compared to BG11 controls (Figure 56).

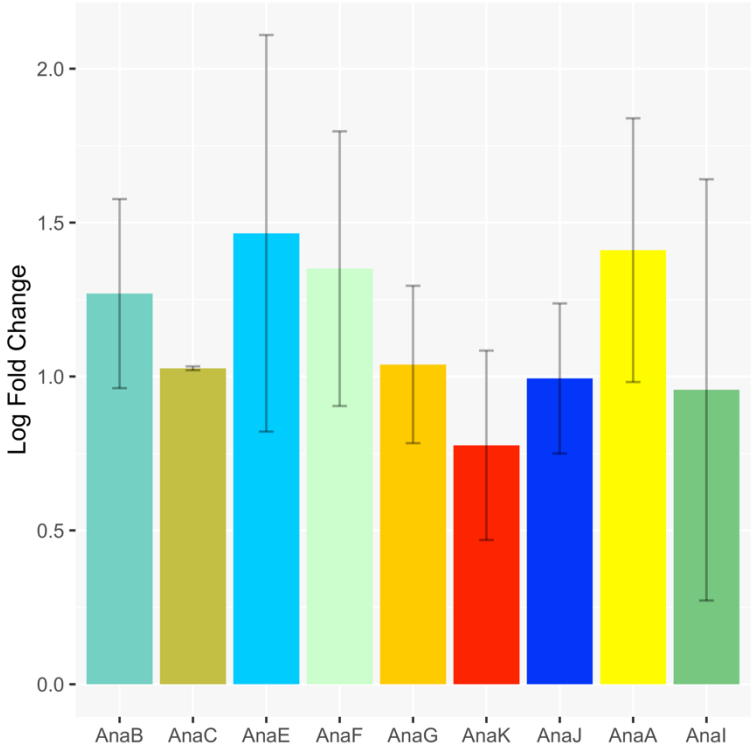


**Figure 56.** Log of the fold change of genes within the Anatoxin-a cassette of T9 (25% SS) compared to T1 (control, 100% BG11) (colors correspond to colors in Figure 9) (Table 62).

**Table 62.** Real-time PCR Gene Amplification Data (Refers to data presented in Figure 56).

| | Fold Change | SD (+/-) | BG11 Theoretical Melt Temp | BG11 Expected Melt Temp | 25% SS Theoretical Melt Temp | 25% SS Expected Melt Temp |
|---|---|---|---|---|---|---|
| **AnaB** | 3.558 | 1.360 | 82.333 | 82.214 | 79.325 | 78.978 |
| **AnaC** | 2.792 | 0.994 | 84.779 | 84.626 | 82.635 | 81.991 |
| **AnaE** | 4.329 | 1.905 | 84.762 | 84.644 | 77.240 | 74.732 |
| **AnaF** | 3.859 | 1.562 | 85.511 | 85.358 | 77.873 | 78.351 |
| **AnaG** | 2.826 | 1.291 | 84.916 | 84.272 | 78.696 | 77.710 |
| **AnaK** | 2.174 | 0.735 | 82.249 | 82.874 | 78.298 | 75.451 |
| **AnaJ** | 2.701 | 0.784 | 83.776 | 82.539 | 73.367 | 72.250 |
| **AnaA** | 4.098 | 1.535 | 82.227 | 82.844 | 77.495 | 78.316 |
| **AnaI** | 2.603 | 1.982 | 79.292 | 79.458 | 70.513 | 68.622 |

The detected anatoxin gene upregulation agreed with measured toxin concentrations inside the cell; compared to BG11, the *M. anatoxicus* cultures in 25% SS at the end of treatment showed higher concentrations of intracellular ATX or dhATX (µg/g) (Figures 57 & 58) (Supplemental Tables 61 & 62) but the difference was not statistically significant. The insignificance may be a result of low sample size, but it may suggest that regulation of anatoxin production may not be determined at the gene level, but instead governed post-transcriptionally at the level of protein translation or activity. In contrast to intracellular measurements, extracellular dhATX concentrations were significantly lower in SS treatment ($F_{1,4} = 32.18$, $p = 0.004764$) (Figure 59) (Supplemental Table 63). The dry weight mass of *Microcoleus* was nearly twice less in 25% SS treatment compared to BG11 control, but the cells produced much more anatoxins as indicated by both intracellular toxin measurements and gene upregulation (Figure 60, Supplemental Table 64). The decrease in extracellular dhATX in 25% SS treatment (T9) may be an indication of better cellular retention of the toxins, possibly due to morphological modifications, such as wider layered sheaths enclosing

multiple trichomes observed in this culturing treatment (T9) and lacking in the control conditions (T1).

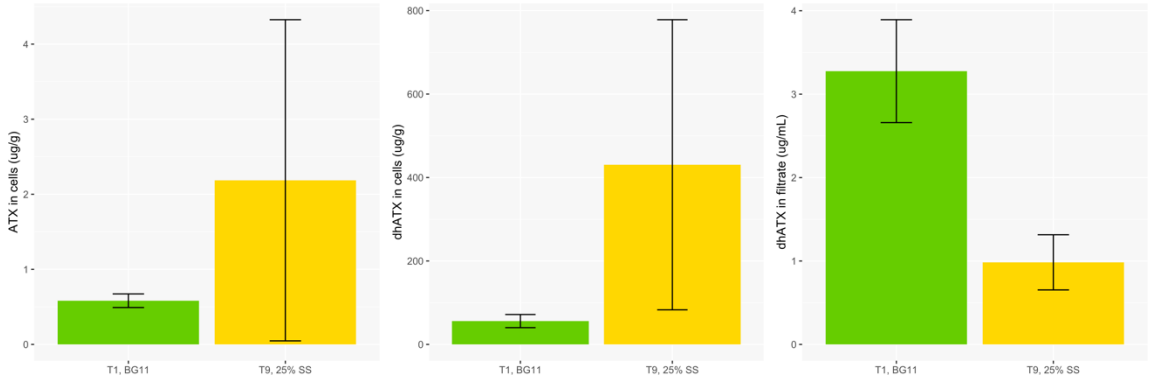


**Figure 57 - 59.** (Left, Figure 60) Intracellular ATX in *M. anatoxicus* cultures in BG11 compared to 25% SS (Supplemental Table 63). (Middle, Figure 61) Intracellular dhATX in *M. anatoxicus* cultures in BG11 compared to 25% SS (Supplemental Table 64). (Right, Figure 62) Extracellular dhATX in *M. anatoxicus* cultures in BG11 compared to 25% SS ($F_{1,4} = 32.18$, **p = 0.00477**) (Supplemental Table 65) (T1 = green, T9 = yellow).

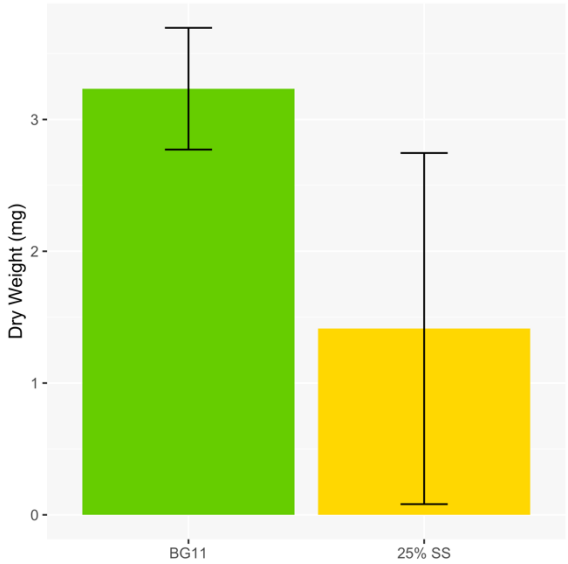


**Figure 60.** Average dry weight mass of *M. anatoxicus* in BG11 compared to 25% SS medium (Supplemental Table 66) (T1 = green, T9 = yellow).

## DISCUSSION

This set of experiments is intended as a pilot test to examine how variable conditions relevant to anthropogenic climate change might affect the growth and toxicity of *Microcoleus anatoxicus.* We analyzed the salinization and influx of nutrients as it affects a single species, which can further be applied to changes in its surrounding freshwater ecosystem. It is important to rapidly improve our knowledge of conditions that worsen blooms to better advise future mitigation and prevention. The purpose of this study is to provide initial guidance concerning those conditions for future investigation.

We predicted that exposure to increased salinity would increase *M. anatoxicus* toxin production, and that biomass, as an indicator of growth, would decrease under these conditions. SS treatment group had the most pronounced salinity gradient, closely followed by FSW, both providing useful data about the effect of salts on *Microcoleus* growth and toxin production. However, it is important to notice that the salinity in these treatments was 4- to 10-fold higher that in the freshwater control medium, and the chloride concentrations were up to 100-fold higher. Furthermore, FSW had higher sulfate concentrations, nearly double, that of SS. Decreases in dry weight mass in response to increased salinity and sulfates was consistent across these two treatment groups. In the very high saline and sulfate gradient groups of FSW and SS, ATX production increased. Intra- and extracellular dhATX decreased in the SS group. This may provide further evidence in support of the finding by Méjean et al. (2016) that dhATX is likely biosynthesized. In addition, our morphological observations showed that wide layered sheaths with multiple trichomes were developed in SS treatments, possibly protecting the cells from extremely high ambient salinity and retaining the toxins in the cells. If dhATX is strictly a degradation product of ATX, then both should positively covary, however dhATX decreased despite increasing ATX in FSW and SS.

We also predicted that increased nutrients, suggested by the BG11 treatment group (although FSW and SS showed high nitrate and phosphate concentrations), would cause increased growth as measured by dry weight. While increased nitrogen did increase dry weight mass in the FSW group, phosphate had no correlations. While this may be due to a lack of other factors required for growth, or small sample size, it supports the prediction by S. A. Wood et al. (2020) that high nitrogen abundance is the primary cause of *Microcoleus* blooms. We also found that every measure of toxins decreased in response to increased nutrients. The only relationship that showed significance against the Spearman's Rank-Order Correlation was a negative trend in ATX in response to increasing phosphate. Perhaps this is reflective of energy tradeoffs towards growth under nutrient access, switching to toxin production under nutrient constraint as possible protective, defensive, or competitive measures. This hypothesis is further supported by our finding that intracellular ATX and extracellular dhATX both tended to decrease with increased biomass; this opposes Harland et al., (2013) which suggested a protective function in the New Zealand strain as toxins increased during growth periods.

The second purpose of this study was to describe toxin dynamics at the genetic level. This proved less productive, as multiple challenges arose in efforts to quantify gene expression that we learned require more sensitive and resilient techniques to define molecular changes more accurately in *M. anatoxicus* ATX production. In this experiment, the RNA extractions from only one flask of T9 and one flask of T1 produced good quality RNA. Gene expression of 25% SS + 75% BG11 (T9) was compared against 100% BG11 (T1). All genes tested showed similar upregulation. This makes sense because all genes are on the same operon. AnaG, hypothesized to be responsible specifically for ATX synthesis, was

upregulated to a similar range of other genes on the operon. What is more ambiguous is that the actual measured ATX concentration in the two samples were not significantly different, although T9 produced somewhat more than T1. Although three technical replicates of cDNA were made, experimental replicates as well as successful RNA extractions from other SS treatments would allow a more definitive understanding of these results. In any case, these results appear contrary to our prediction that the extreme increase of salts would cause a decrease in toxins. ATX production was upregulated, which agreed with our measurements of higher intracellular toxin concentrations in T9 versus T1. This may support the finding of increases of toxin production under stress.

It is evident from the variation in the trends identified that an improved study would include a larger sample size, smaller chemistry increments and a more rigorous control model to limit confounding variables and to better reflect freshwater conditions. However, this set of pilot experiments produced informative tendencies that suggest design options for future tests, and future conditions and biological pathways worth further study.

**Environmental Relevance**

Future freshwater streams are predicted to be deoxygenated and have increased salinity, in addition to higher levels of nutrients due to agricultural and industrial pollution. The salinity of the Russian River ranges from about 0.1 to 0.16 ppt which is typical freshwater environment. However the intended freshwater control media, BG11, has much higher salinity and falls under Oligohaline with respect to salinity (Figure 61) ("Chapter 14: Salinity," 2006). In addition to a much higher salinity, the nutrient concentrations were far higher than the current levels found in the Russian River (Supplemental Table 67), suggesting that *M. anatoxicus* is an euryhaline species which could grow well in both

eutrophic and brackish conditions. Predicted impacts of pollution in freshwater streams suggest an increase in salinity and nutrient concentrations (Herbert et al., 2015). BG11 media may somewhat replicate possible water quality of an extremely polluted stream, but the application of each of the 12 treatments to realistic projected conditions remains unclear. The gap between current Russian River conditions and the salinity treatments used in this experiment needs to be filled by future studies.

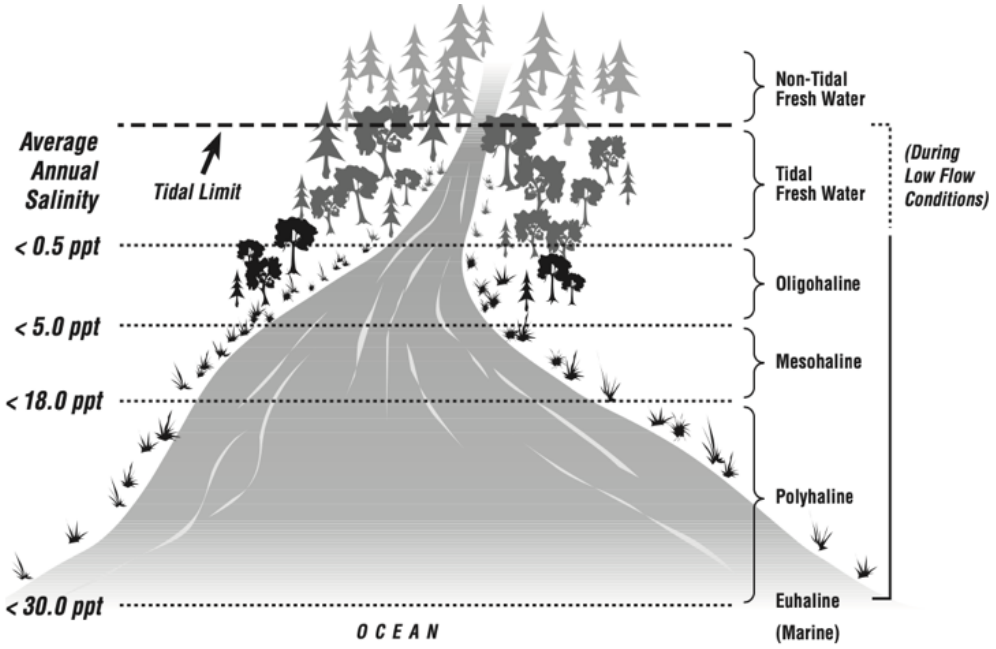


**Figure 61.** Approximate salinity gradient from total freshwater to marine ("Chapter 14: Salinity," 2006)

**Future Studies**

There are three main suggestions for future studies that focus on this species and a similar model. No statistically significant relationships were found in this study due to the low sample size and presence of confounding variables; however it gives insight to possible patterns of growth and toxin production of *M. anatoxicus*. The main findings of this experiment were that increased salinity coupled with decreased nitrates and phosphates have

negative effect on *M. anatoxicus* growth but increased the cellular production of anatoxins. Formal replications of some treatments, especially such that specific nutrient levels can be better controlled, would help to limit some of the unintended variation in concentrations seen in our treatments. While the direct impact of sulfates has been less studied than other dissolved compounds, they affected all response variables in this study, unlike nitrates or phosphates.

Secondly, a better biomass measurement method was needed in this study. The dry weight mass used was only that of the representative amount sent for toxin analysis. That representative amount was determined by appearance, not by a fraction of total biomass. While cell count was considered, it proved impractical.

Finally, perfecting an RNA extraction procedure capable of dealing with degrading cells that produce increased proteins and polysaccharides in the sample without compromising the quality or concentration would allow for a more holistic approach to the molecular portion of this study.

In terms of our direct findings, this pilot study offers many potential endeavors for scientific progress. One possible future study would explore the relationship between phosphates and intracellular ATX. This was the only significance relationship found, and the small sample sizes suggest additional efforts in this direction. The negative correlation may be interesting in studying how both abundance of nutrients and starvation affect toxin production and lead to further tests of a preservative or defensive role of toxins. Interestingly, only phosphates showed this concrete relationship. Nitrogen only possessed negative tendencies which was insignificant under Spearman's Rank-Order Correlation. A study on a larger scale may have different results.

Future studies inspired by previous literature in conjunction with this study include exploring functions of toxins, mutualistic bacteria, and of multiple trichome growth in a single sheath. An interesting morphological aspect of this experiment was that some treatments grew multiple trichomes in a single sheath under increased salinity (T4, T5, T9, T12). While this phenomenon is rarely seen in the field, it is difficult to replicate in lab conditions. Future research, guided in part by these treatments, may shed light on what kind of conditions lead filaments in the natural world to grow in this way and how this morphological modification is related cell protection and toxin intracellular retention,

*Microcoleus* cultures used in this study were non-axenic, and its mutualistic bacteria were not accounted for in this study, which adds other potential confounding variables that may or may not influence toxin production (and vice versa). Mutualistic bacteria may have thrived or failed under the conditions implemented in this experiment. This may have affected the response variables in ways we were not able to measure. The synergistic potential of this mutualism on toxin production or growth may be important to examine.

Finally, the function of cyanotoxins could be of interest as well. If nutrients or environmental stressors are not strongly correlated with toxins, the next steps may be to investigate the competitive or defensive interspecific functions of intra- and extracellular toxins.

# REFERENCES


Allen, M. M., & Stanier, R. Y. (1968). Selective Isolation of Blue-green Algae from Water and Soil. *Journal of General Microbiology*, *51*(2), 203–209. https://doi.org/10.1099/00221287-51-2-203

Anderson, B., Voorhees, J., Phillips, B., Fadness, R., Stancheva, R., Nichols, J., Orr, D., & Wood, S. A. (2018). Extracts from benthic anatoxin-producing *Phormidium* are toxic to 3 macroinvertebrate taxa at environmentally relevant concentrations: Cyanobacteria toxicity to 3 invertebrates. *Environmental Toxicology and Chemistry*, *37*(11), 2851–2859. https://doi.org/10.1002/etc.4243

Anderson, R. (2005). *Algal Culturing Techniques* (1st ed.). Elsevier.

Backer, L., Landsberg, J., Miller, M., Keel, K., & Taylor, T. (2013). Canine Cyanotoxin Poisonings in the United States (1920s–2012): Review of Suspected and Confirmed Cases from Three Data Sources. *Toxins*, *5*(9), 1597–1628. https://doi.org/10.3390/toxins5091597

Biré, R., Bertin, T., Dom, I., Hort, V., Schmitt, C., Diogène, J., Lemée, R., De Haro, L., & Nicolas, M. (2020). First Evidence of the Presence of Anatoxin-A in Sea Figs Associated with Human Food Poisonings in France. *Marine Drugs*, *18*(6), 285. https://doi.org/10.3390/md18060285

Bouma-Gregson, K., Olm, M. R., Probst, A. J., Anantharaman, K., Power, M. E., & Banfield, J. F. (2019). Impacts of microbial assemblage and environmental conditions on the distribution of anatoxin-a producing cyanobacteria within a river network. *The ISME Journal*, *13*(6), 1618–1634. https://doi.org/10.1038/s41396-019-0374-3

Burford, M. A., Carey, C. C., Hamilton, D. P., Huisman, J., Paerl, H. W., Wood, S. A., & Wulff, A. (2020). Perspective: Advancing the research agenda for improving understanding of cyanobacteria in a future of global change. *Harmful Algae*, *91*, 101601. https://doi.org/10.1016/j.hal.2019.04.004

Cañedo-Argüelles, M., Kefford, B. J., Piscart, C., Prat, N., Schäfer, R. B., & Schulz, C.-J. (2013). Salinisation of rivers: An urgent ecological issue. *Environmental Pollution*, *173*, 157–167. https://doi.org/10.1016/j.envpol.2012.10.011

Chapter 14: Salinity. (2006). In *Voluntary Estuary Monitoring Manual*. U.S. Environmental Protection Agency.

Colas, S., Marie, B., Lance, E., Quiblier, C., Tricoire-Leignel, H., & Mattei, C. (2021). Anatoxin-a: Overview on a harmful cyanobacterial neurotoxin from the environmental scale to the molecular target. *Environmental Research*, *193*, 110590. https://doi.org/10.1016/j.envres.2020.110590

Conklin, K. Y., Stancheva, R., Otten, T. G., Fadness, R., Boyer, G. L., Read, B., Zhang, X., & Sheath, R. G. (2020). Molecular and morphological characterization of a novel dihydroanatoxin-a producing Microcoleus species (cyanobacteria) from the Russian River, California, USA. *Harmful Algae*, *93*, 101767. https://doi.org/10.1016/j.hal.2020.101767

Dvořák, P., Hašler, P., & Poulíčková, A. (2012). Phylogeography of the Microcoleus vaginatus (Cyanobacteria) from Three Continents – A Spatial and Temporal Characterization. *PLoS ONE*, *7*(6), e40153. https://doi.org/10.1371/journal.pone.0040153

Fetscher, A. E., Howard, M. D. A., Stancheva, R., Kudela, R. M., Stein, E. D., Sutula, M. A., Busse, L. B., & Sheath, R. G. (2015). Wadeable streams as widespread sources of benthic cyanotoxins in California, USA. *Harmful Algae*, *49*, 105–116. https://doi.org/10.1016/j.hal.2015.09.002

Hansen, J. A., Jurgens, B. C., & Fram, M. S. (2018). Quantifying anthropogenic contributions to century-scale groundwater salinity changes, San Joaquin Valley, California, USA. *Science of The Total Environment*, *642*, 125–136. https://doi.org/10.1016/j.scitotenv.2018.05.333

Harland, F., Wood, S., Moltchanova, E., Williamson, W., & Gaw, S. (2013). Phormidium autumnale Growth and Anatoxin-a Production under Iron and Copper Stress. *Toxins*, *5*(12), 2504–2521. https://doi.org/10.3390/toxins5122504

Heath, M. W., Wood, S. A., & Ryan, K. G. (2010). Polyphasic assessment of fresh-water benthic mat-forming cyanobacteria isolated from New Zealand: Benthic cyanobacteria in NZ. *FEMS Microbiology Ecology*, no-no. https://doi.org/10.1111/j.1574-6941.2010.00867.x

Herbert, E. R., Boon, P., Burgin, A. J., Neubauer, S. C., Franklin, R. B., Ardón, M., Hopfensperger, K. N., Lamers, L. P. M., & Gell, P. (2015). A global perspective on wetland salinization: Ecological consequences of a growing threat to freshwater wetlands. *Ecosphere*, *6*(10), art206. https://doi.org/10.1890/ES14-00534.1

Holland, A., & Kinnear, S. (2013). Interpreting the Possible Ecological Role(s) of Cyanotoxins: Compounds for Competitive Advantage and/or Physiological Aide? *Marine Drugs*, *11*(7), 2239–2258. https://doi.org/10.3390/md11072239

IPCC. (2021). *IPCC - Regional fact sheet – North and Central America*. IPCC.

Joab, C., & Chetelat, G. (2019). Harmful Algal Bloom Primer. *REGIONAL WATER QUALITY CONTROL BOARD CENTRAL VALLEY REGION*, 28.

Kearns, K. D., & Hunter, M. D. (2000). Green algal extracellular products regulate antialgal toxin production in a cyanobacterium. *Environmental Microbiology*, *2*(3), 291–297. https://doi.org/10.1046/j.1462-2920.2000.00104.x

Kearns, K. D., & Hunter, M. D. (2001). Toxin-producing Anabaena flos-aquae induces settling of Chlamydomonas reinhardtii, a competing motile alga. *Microbial Ecology*, *42*(1), 80–86. https://doi.org/10.1007/s002480000086

Komárek, J., & Anagnostidis, K. (2005). Cyanoprokaryota. 2. Oscillatoriales. *Süsswasserflora von Mitteleuropa*, *19*(2), 729.

Kurobe, T., Lehman, P. W., Hammock, B. G., Bolotaolo, M. B., Lesmeister, S., & Teh, S. J. (2018). Biodiversity of cyanobacteria and other aquatic microorganisms across a freshwater to brackish water gradient determined by shotgun metagenomic sequencing analysis in the San Francisco Estuary, USA. *PLOS ONE*, *13*(9), e0203953. https://doi.org/10.1371/journal.pone.0203953

Méjean, A., Dalle, K., Paci, G., Bouchonnet, S., Mann, S., Pichon, V., & Ploux, O. (2016). Dihydroanatoxin-a Is Biosynthesized from Proline in *Cylindrospermum stagnale* PCC 7417: Isotopic Incorporation Experiments and Mass Spectrometry Analysis. *Journal of Natural Products*, *79*(7), 1775–1782. https://doi.org/10.1021/acs.jnatprod.6b00189

Nabout, J. C., da Silva Rocha, B., Carneiro, F. M., & Sant'Anna, C. L. (2013). How many species of Cyanobacteria are there? Using a discovery curve to predict the species number. *Biodiversity and Conservation*, *22*(12), 2907–2918. https://doi.org/10.1007/s10531-013-0561-x

Puschner, B., Hoff, B., & Tor, E. R. (2008). Diagnosis of Anatoxin-a Poisoning in Dogs from North America. *Journal of Veterinary Diagnostic Investigation*, *20*(1), 89–92. https://doi.org/10.1177/104063870802000119

Quiblier, C., Wood, S., Echenique-Subiabre, I., Heath, M., Villeneuve, A., & Humbert, J.-F. (2013). A review of current knowledge on toxic benthic freshwater cyanobacteria – Ecology, toxin production and risk management. *Water Research*, *47*(15), 5464–5479. https://doi.org/10.1016/j.watres.2013.06.042

Russian River (California). (2021). In *Wikipedia*. https://en.wikipedia.org/w/index.php?title=Russian_River_(California)&oldid=1051004030

Schneider, S. C. (2015). Greener rivers in a changing climate?—Effects of climate and hydrological regime on benthic algal assemblages in pristine streams. *Limnologica*, *55*, 21–32. https://doi.org/10.1016/j.limno.2015.10.004

Smith, V. H., Tilman, G. D., & Nekola, J. C. (1999). Eutrophication: Impacts of excess nutrient inputs on freshwater, marine, and terrestrial ecosystems. *Environmental Pollution*, *100*(1–3), 179–196. https://doi.org/10.1016/S0269-7491(99)00091-3

Soto, A. R., Zheng, H., Shoemaker, D., Rodriguez, J., Read, B. A., & Wahlund, T. M. (2006). Identification and Preliminary Characterization of Two cDNAs Encoding Unique Carbonic Anhydrases from the Marine Alga *Emiliania huxleyi*. *Applied and Environmental Microbiology*, *72*(8), 5500–5511. https://doi.org/10.1128/AEM.00237-06

Strunecký, O., Elster, J., & Komárek, J. (2011). Taxonomic revision of the freshwater cyanobacterium “Phormidium” murrayi = Wilmottia murrayi. *Fottea*, *11*(1), 57–71. https://doi.org/10.5507/fot.2011.007

Sutula, M., Ho, M., Sengupta, A., Kessouri, F., McLaughlin, K., McCune, K., & Bianchi, D. (2021). A baseline of terrestrial freshwater and nitrogen fluxes to the Southern California Bight, USA. *Marine Pollution Bulletin*, *170*, 112669. https://doi.org/10.1016/j.marpolbul.2021.112669

Svirčev, Z., Lalić, D., Bojadžija Savić, G., Tokodi, N., Drobac Backović, D., Chen, L., Meriluoto, J., & Codd, G. A. (2019). Global geographical and historical overview of cyanotoxin distribution and cyanobacterial poisonings. *Archives of Toxicology*, *93*(9), 2429–2481. https://doi.org/10.1007/s00204-019-02524-4

Whitton, B. A. (Ed.). (2012). *Ecology of Cyanobacteria II*. Springer Netherlands. https://doi.org/10.1007/978-94-007-3855-3

Wood, R. (2016). Acute animal and human poisonings from cyanotoxin exposure—A review of the literature. *Environment International*, *91*, 276–282. https://doi.org/10.1016/j.envint.2016.02.026

Wood, S. A., Biessy, L., & Puddick, J. (2018). Anatoxins are consistently released into the water of streams with Microcoleus autumnalis-dominated (cyanobacteria) proliferations. *Harmful Algae*, *80*, 88–95. https://doi.org/10.1016/j.hal.2018.10.001

Wood, S. A., Kelly, L. T., Bouma-Gregson, K., Humbert, J., Laughinghouse, H. D., Lazorchak, J., McAllister, T. G., McQueen, A., Pokrzywinski, K., Puddick, J., Quiblier, C., Reitz, L. A., Ryan, K. G., Vadeboncoeur, Y., Zastepa, A., & Davis, T. W. (2020). Toxic benthic freshwater cyanobacterial proliferations: Challenges and solutions for enhancing knowledge and improving monitoring and mitigation. *Freshwater Biology*, *65*(10), 1824–1842. https://doi.org/10.1111/fwb.13532

## SUPPLEMENTAL FIGURES AND TABLES

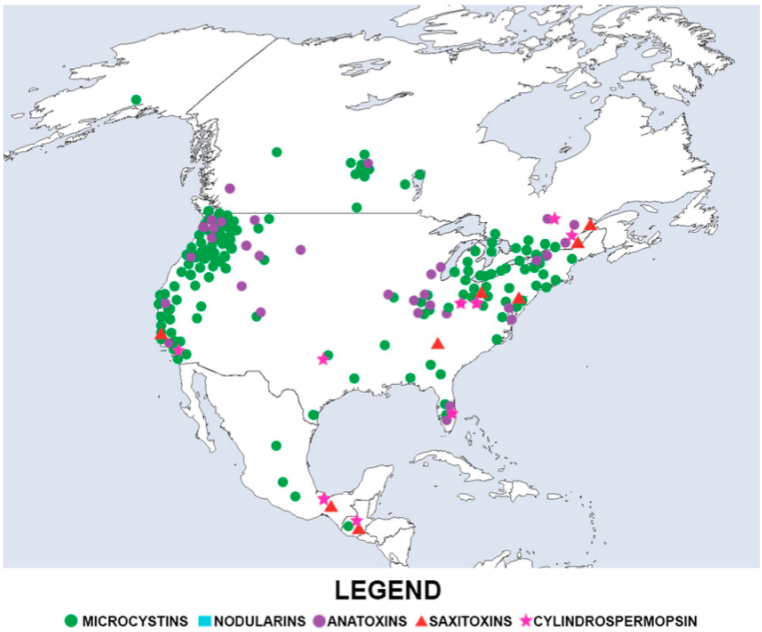


**Figure 1.** Distribution of most commonly reported cyanotoxins in North America (Svirčev et al., 2019).


**Figure 2.** Map of Russian River ("Russian River (California)," 2021). The purple square provides an approximation of where PTRS1 was collected.

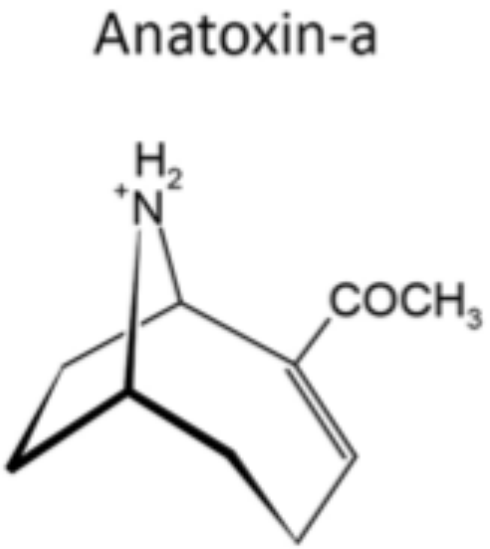


**Figure 3.** Molecular structure of anatoxin-a (Svirčev et al., 2019).

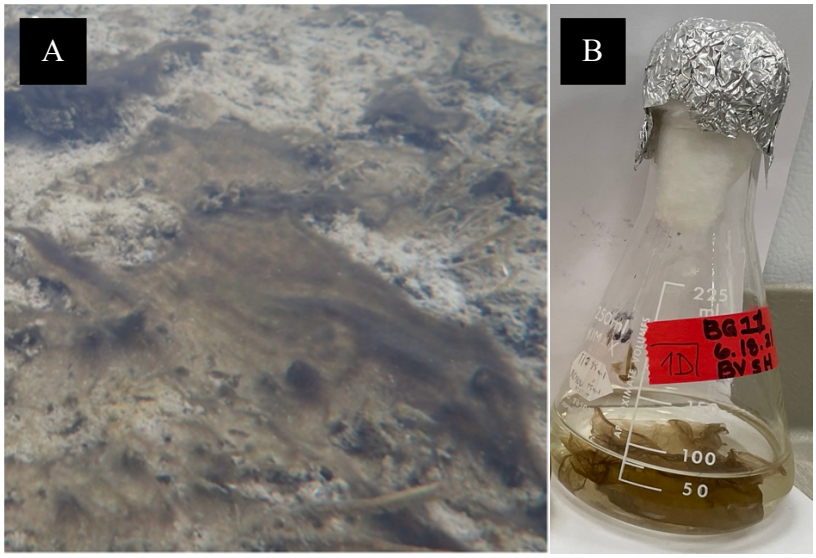


**Figure 4.** Macroscopic field view of *Microcoleus* (A) (Conklin et al., 2020) and macroscopic view of *Microcoleus* in BG11 growth medium (B).

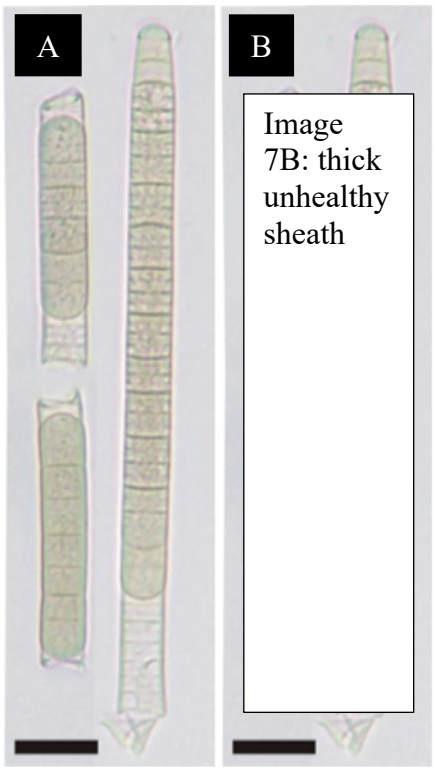


**Figure 5.** Microscopic view of a healthy sheath around *Microcoleus* (A) and of a thickened sheath (B). Scale bar: 10 µm (Conklin et al., 2020).

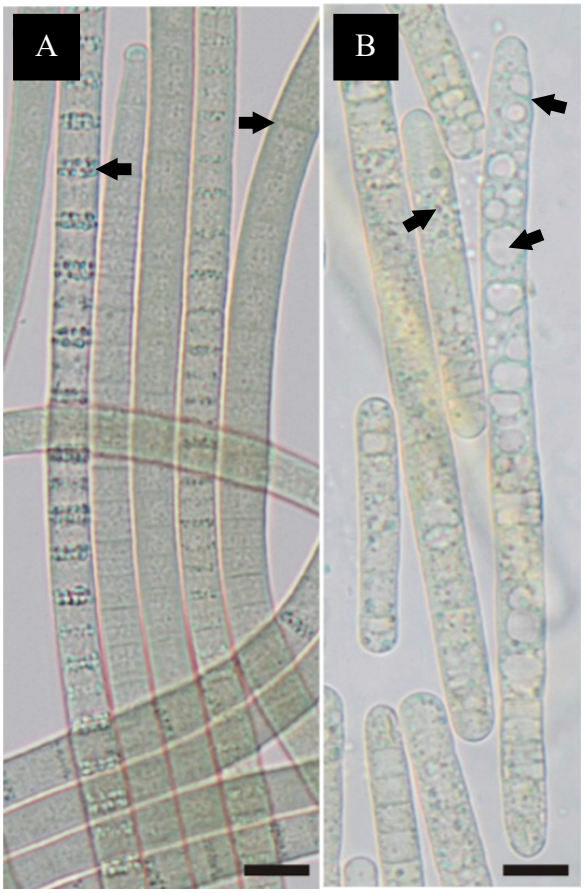


**Figure 6.** Microscopic view of *Microcoleus* showing healthy cells with arrows denoting crosswalls and granules (A) and unhealthy filaments with arrows denoting vacuoles and crosswall constriction (B). Scale bar: 10 µm (Conklin et al., 2020).

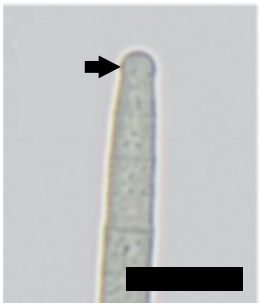

**Figure 7.** Microscopic view of example apical cells of Microcoleus PTRS1 in BG11. Scale bar: 10 µm (Conklin et al., 2020).

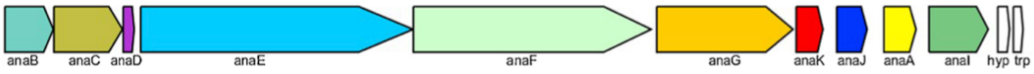


**Figure 8.** Anatoxin-a gene cassette of Microcoleus sp. PTSR3 (Conklin et al., 2020).

**Table 1.** Salts used to mimic the concentration of sea salts. Amounts above are given per liter of DIW. The 100% sea water was not made.

| **Salts** | **100% Sea Water** | **10% Sea Water** | **20% Sea Water** | **25% Sea Water** | **30% Sea Water** |
|---|---|---|---|---|---|
| **Sodium Chloride (NaCl)** | 26.88 grams / 1 L water | 2.688 grams / 1 L water | 5.376 grams / 1 L water | 6.720 grams / 1 L water | 8.064 grams / 1 L water |
| **Magnesium Chloride ($MgCl_2$)** | 4.09 grams / 1 L water | 0.409 grams / 1 L water | 0.818 grams / 1 L water | 1.023 grams / 1 L water | 1.227 grams / 1 L water |
| **Calcium Chloride ($CaCl_2$)** | 1.11 grams / 1 L water | 0.111 grams / 1 L water | 0.222 grams / 1 L water | 0.278 grams / 1 L | 0.333 grams / 1 L water |
| **Magnesium Sulfate ($MgSO_4$)** | 1.08 grams / 1 L water | 0.108 grams / 1 L water | 0.216 grams / 1 L water | 0.270 grams / 1 L water | 0.324 grams / 1 L water |
| **Potassium Sulfate ($K2SO_4$)** | 0.85 grams / 1 L water | 0.085 grams / 1 L water | 0.170 grams / 1 L water | 0.213 grams / 1 L water | 0.255 grams / 1 L water |

**Table 2.** Description of the 12 treatments.

| **ID No.** | **1** | **2** | **3** | **4** | **5** |
|---|---|---|---|---|---|
| **Contents** | 100% BG11 | 50% BG11 + 50% DIW | 10% eFSW + 90% BG11 | 20% eFSW + 90% BG11 | 25% eFSW + 90% BG11 |
| **Intended Stressors** | None | Reduced nutrients | Increased salts | Reduced pH, Increased salts | Reduced pH, Increased salts |

| | | |
|---|---|---|
| **6** | BG11 + NaCl | Increased NaCl |
| **7** | 10% SS + 90% BG11 | Reduced pH, Increased salts |
| **8** | 20% SS + 90% BG11 | Reduced pH, Increased salts |
| **9** | 25% SS + 90% BG11 | Reduced pH, Increased salts |
| **10** | 30% SS + 90% BG11 | Reduced pH, Increased salts |
| **11** | 25% pFSW + 75% DIW | Reduced pH, and nutrients, Increased salts |
| **12** | 25% pFSW + 75% BG11 | Reduced pH, and nutrients, Increased salts |

**Table 3.** Nanodrop results and extraction notes of each extraction. Shading on table represents the batches in which the RNA was extracted. 2C, 3A, and 3B were not tested after their second clean up because the nanodrop results from 2B, the other flask in the batch of extractions and clean ups, was extremely poor quality. 6C results were lost.

| **Sample and Flask ID** | **Media** | **Concentration (ng/uL)** | **A260** | **A280** | **260/280** | **260/230** | **Extraction Notes** | **Final State** |
|---|---|---|---|---|---|---|---|---|
| **1A** | BG11 | 240.1 | 6.002 | 2.751 | 2.18 | 1.12 | none | 1 clean up |
| **1B** | BG11 | 175.5 | 4.388 | 2.056 | 2.13 | 1.54 | none | 1 clean up |
| **1C** | BG11 | 91.1 | 2.277 | 1.036 | 2.2 | 1.18 | none | 1 clean up |
| **2A** | 50% BG11: DI | 86.3 | 2.158 | 0.981 | 2.2 | 1.07 | none | 1 clean up |
| **2B** | 50% BG11: DI | 10.2 | 0.255 | 0.102 | 2.51 | 0.05 | none | 2 clean ups |

| | | | | | | | | |
|---|---|---|---|---|---|---|---|---|
| **2C** | 50% BG11: DI | NA | NA | NA | NA | NA | Not tested because 2B was so low | 2 clean ups |
| **3A** | 10% eFSW: BG11 | NA | NA | NA | NA | NA | Not tested because 2B was so low | 2 clean ups |
| **3B** | 10% eFSW: BG11 | NA | NA | NA | NA | NA | Not tested because 2B was so low | 2 clean ups |
| **3C** | 10% eFSW: BG11 | 631.4 | 15.786 | 9.011 | 1.75 | 0.48 | none | No clean up |
| **4A** | 20% eFSW: BG11 | 490.1 | 12.252 | 6.716 | 1.82 | 0.69 | none | No clean up |
| **4B** | 20% eFSW: BG11 | 50.6 | 1.266 | 0.739 | 1.71 | 0.19 | none | No clean up |
| **4C** | 20% eFSW: BG11 | 186.3 | 4.657 | 2.586 | 1.8 | 0.51 | none | No clean up |
| **5A** | 25% eFSW: BG11 | 5.9 | 0.147 | 0.077 | 1.91 | 1.1 | Went through a lot of temperature changes | 1 clean up after heated to attempt to resuspend in 38 C water bath and then in 50 C water bath |
| **5B** | 25% eFSW: BG11 | 3.0 | 0.076 | 0.046 | 1.66 | 0.83 | Went through a lot of temperature changes | 1 clean up after heated to attempt to resuspend in 38 C water bath and then in 50 C water bath |
| **5C** | 25% eFSW: BG11 | 24.5 | 0.613 | 0.366 | 1.68 | 0.1 | Pellet dislodged from wall of tube and fell out, | 1 clean up after heated to attempt to resuspend |

| | | | | | | | | |
|---|---|---|---|---|---|---|---|---|
| | | | | | | | majority of RNA lost | in 38 C water bath and then in 50 C water bath |
| **6A** | NaCl with BG11 | 112.8 | 2.819 | 1.72 | 1.64 | 0.54 | Went through a lot of temperature changes | 1 clean up after heated to attempt to resuspend in 38 C water bath and then in 50 C water bath |
| **6B** | NaCl with BG11 | 776.1 | 19401 | 10.255 | 1.89 | 1.35 | Performed second chloroform wash | Suspended in LiCl and 100% Ethanol |
| **6C** | NaCl with BG11 | NA | NA | NA | NA | NA | Performed second chloroform wash | Suspended in LiCl and 100% Ethanol |
| **7A** | 10% SS: BG11 | 338 | 8.451 | 4.112 | 2.06 | 3.31 | Performed second chloroform wash | Suspended in LiCl and 100% Ethanol |
| **7B** | 10% SS: BG11 | 199.9 | 4.998 | 4.175 | 1.20 | 0.60 | Performed second chloroform wash | Suspended in LiCl and 100% Ethanol |
| **7C** | 10% SS: BG11 | 320.5 | 8.013 | 6.411 | 1.25 | 0.86 | None | No clean up |
| **8A** | 20% SS: BG11 | 344.8 | 8.619 | 7.002 | 1.23 | 0.92 | None | No clean up |
| **8B** | 20% SS: BG11 | 1760.6 | 44.014 | 24.661 | 1.78 | 0.86 | None | No clean up |
| **8C** | 20% SS: BG11 | 640.7 | 16.018 | 9.585 | 1.67 | 0.99 | None | No clean up |
| **9A** | 25% SS: BG11 | 156.5 | 3.912 | 2.304 | 1.7 | 0.3 | None | No clean up |

| | | | | | | | | |
|---|---|---|---|---|---|---|---|---|
| **9B** | 25% SS: BG11 | 145.6 | 3.639 | 2.088 | 1.74 | 0.31 | None | No clean up |
| **9C** | 25% SS: BG11 | 961.8 | 24.046 | 13.776 | 1.81 | 1.09 | None | No clean up |
| **10** | 30% SS: BG11 | 162 | 4.051 | 2.23 | 1.82 | 0.31 | Growth was extremely low, 10A, 10B, and 10C were combined into one extraction | No clean up |
| **11** | 25% pFSW: DI | 342.9 | 8.573 | 4.636 | 1.85 | 0.71 | Growth was extremely low, 11A, 11B, and 11C were combined into one extraction | No clean up |
| **12A** | 25% pFSW: BG11 | 16.35 | 0.4095 | 0.25 | 1.7 | 0.3 | None | No clean up |
| **12B** | 25% pFSW: BG11 | 216.65 | 5.417 | 2.7555 | 1.965 | 0.95 | None | No clean up |
| **12C** | 25% pFSW: BG11 | 19.7 | 0.493 | 0.2795 | 1..76 | 0.33 | None | No clean up |

**Table 4.** RNA extraction quality results of a BG11 and 25% SS treatment flask using Nanodrop.

| **Treatment and Flask ID** | **Media** | **Concentration (ng/ul)** | **A260/A280** | **A260/A230** |
|---|---|---|---|---|
| 1B | BG11 | 175.5 | 2.13 | 1.54 |
| 9C | 25% SS | 1485.4 | 1.70 | 1.16 |

| | 1 | 2 | 3 | 4 | 5 | 6 | 7 | 8 | 9 | 10 | 11 | 12 |
|---|---|---|---|---|---|---|---|---|---|---|---|---|
| A | | | | Ana A 1B CONTROL | Ana A 1B CONTROL | Ana A 1B CONTROL | Ana A 9C 25% SS | Ana A 9C 25% SS | Ana A 9C 25% SS | Ana K 1B CONTROL | Ana K 1B CONTROL | Ana K 1B CONTROL |
| B | | | | Ana B 1B CONTROL | Ana B 1B CONTROL | Ana B 1B CONTROL | Ana B 9C 25% SS | Ana B 9C 25% SS | Ana B 9C 25% SS | Ana K 9C 25% SS | Ana K 9C 25% SS | Ana K 9C 25% SS |
| C | | | Ana I NO TEMPLATE | Ana C 1B CONTROL | Ana C 1B CONTROL | Ana C 1B CONTROL | Ana C 9C 25% SS | Ana C 9C 25% SS | Ana C 9C 25% SS | Ana A NO TEMPLATE | Ana A NO TEMPLATE | Ana A NO TEMPLATE |
| D | | | Ana I NO TEMPLATE | Ana E 1B CONTROL | Ana E 1B CONTROL | Ana E 1B CONTROL | Ana E 9C 25% SS | Ana E 9C 25% SS | Ana E 9C 25% SS | Ana B NO TEMPLATE | Ana B NO TEMPLATE | Ana B NO TEMPLATE |
| E | | | Ana J NO TEMPLATE | Ana F 1B CONTROL | Ana F 1B CONTROL | Ana F 1B CONTROL | Ana F 9C 25% SS | Ana F 9C 25% SS | Ana F 9C 25% SS | Ana C NO TEMPLATE | Ana C NO TEMPLATE | Ana C NO TEMPLATE |
| F | | | Ana J NO TEMPLATE | Ana G 1B CONTROL | Ana G 1B CONTROL | Ana G 1B CONTROL | Ana G 9C 25% SS | Ana G 9C 25% SS | Ana G 9C 25% SS | Ana E NO TEMPLATE | Ana E NO TEMPLATE | |
| G | | | | Ana I 1B CONTROL | Ana I 1B CONTROL | Ana I 1B CONTROL | Ana I 9C 25% SS | Ana I 9C 25% SS | Ana I 9C 25% SS | Ana F NO TEMPLATE | Ana F NO TEMPLATE | Ana K NO TEMPLATE |
| H | | | | Ana J 1B CONTROL | Ana J 1B CONTROL | Ana J 1B CONTROL | Ana J 9C 25% SS | Ana J 9C 25% SS | Ana J 9C 25% SS | Ana G NO TEMPLATE | Ana G NO TEMPLATE | Ana K NO TEMPLATE |

**Figure 9.** 96-well RT PCR plate set up. Color coded by gene. "CONTROL" is the BG11 treatment. "25% SS" is the 25% sea salt treatment. "NO TEMPLATE" is the no template control in which only the gene was loaded. "1B" and "9C" refer to the flask and treatment IDs.

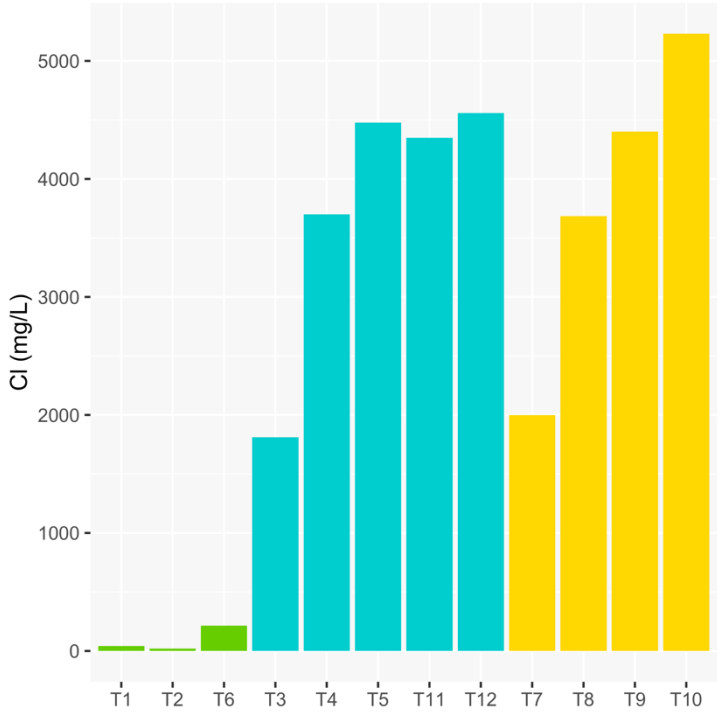

**Figure 10.** Chloride concentrations (mg/L) for all culturing treatments (T1 – T12). Bar color corresponds to the grouping for statistical analysis (BG11 group = green, FSW group = cyan, SS group = yellow).

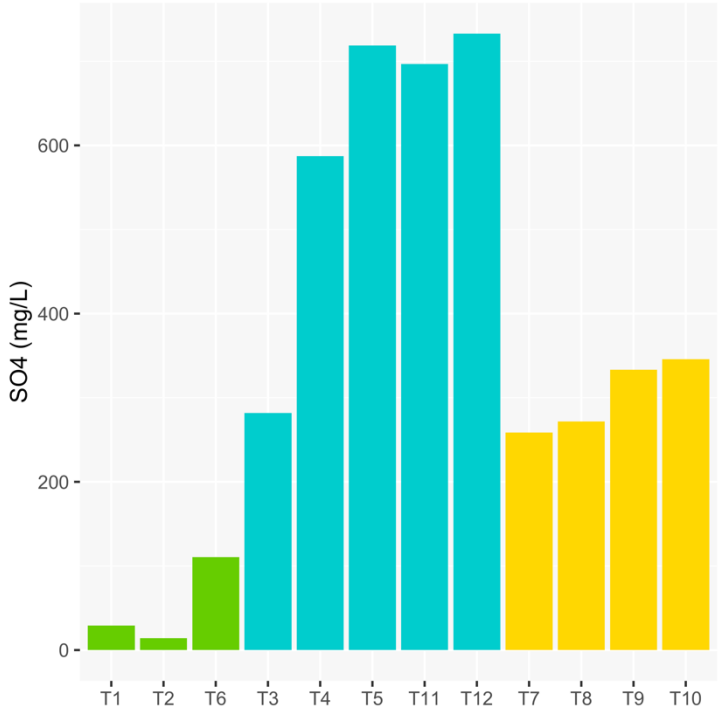


**Figure 11.** Sulfate concentrations (mg/L) for all culturing treatments (T1 – T12). Bar color corresponds to the grouping for statistical analysis (BG11 group = green, FSW group = cyan, SS group = yellow).

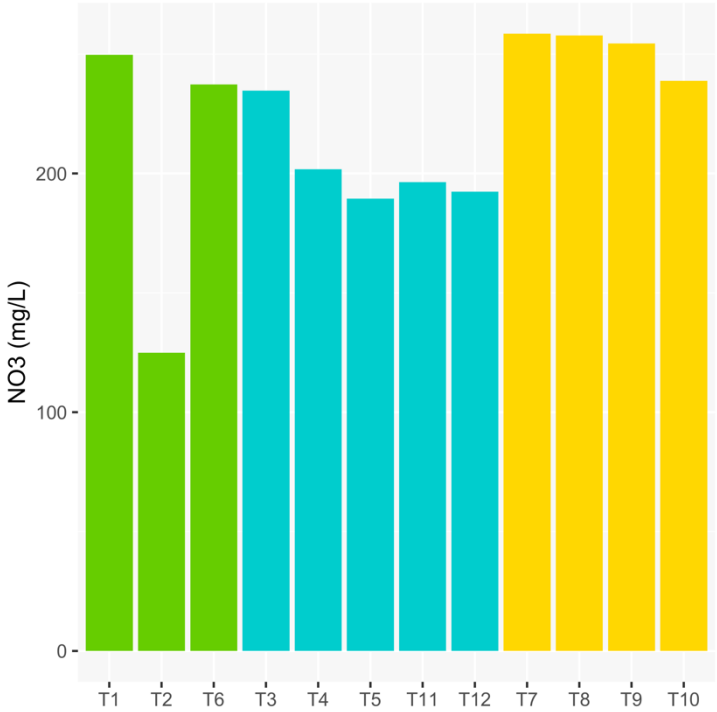


**Figure 12.** Nitrate concentrations (mg/L) for all culturing treatments (T1 – T12). Bar color corresponds to the grouping for statistical analysis (BG11 group = green, FSW group = cyan, SS group = yellow).

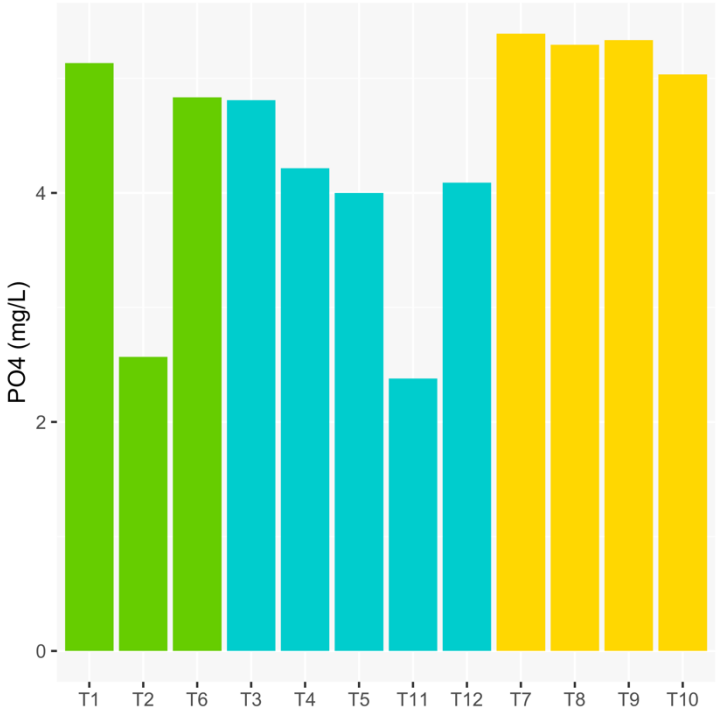


**Figure 13.** Phosphate concentrations (mg/L) for all culturing treatments (T1 – T12). Bar color corresponds to the grouping

for statistical analysis (BG11 group = green, FSW group = cyan, SS group = yellow).

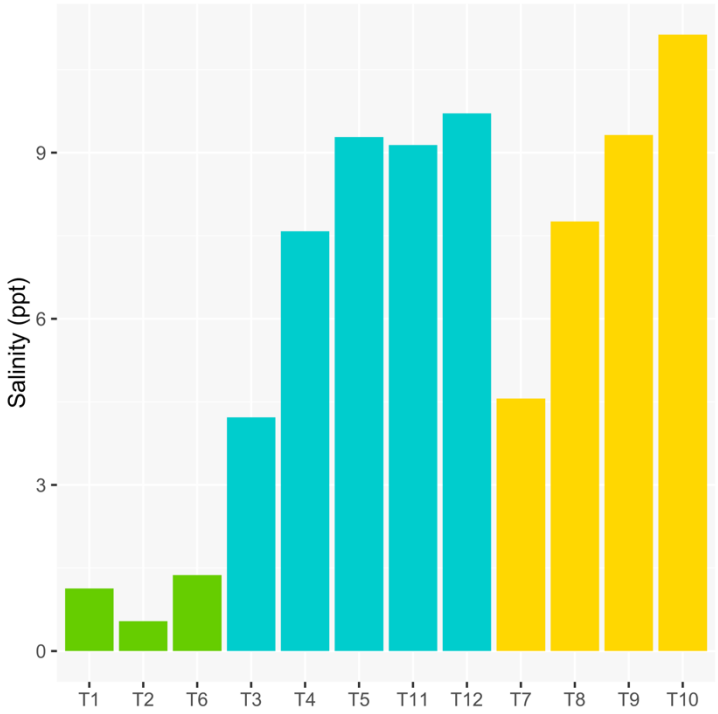


**Figure 14.** Salinity concentrations (ppt) for all culturing treatments (T1 – T12). Bar color corresponds to the grouping for statistical analysis (BG11 group = green, FSW group = cyan, SS group = yellow).

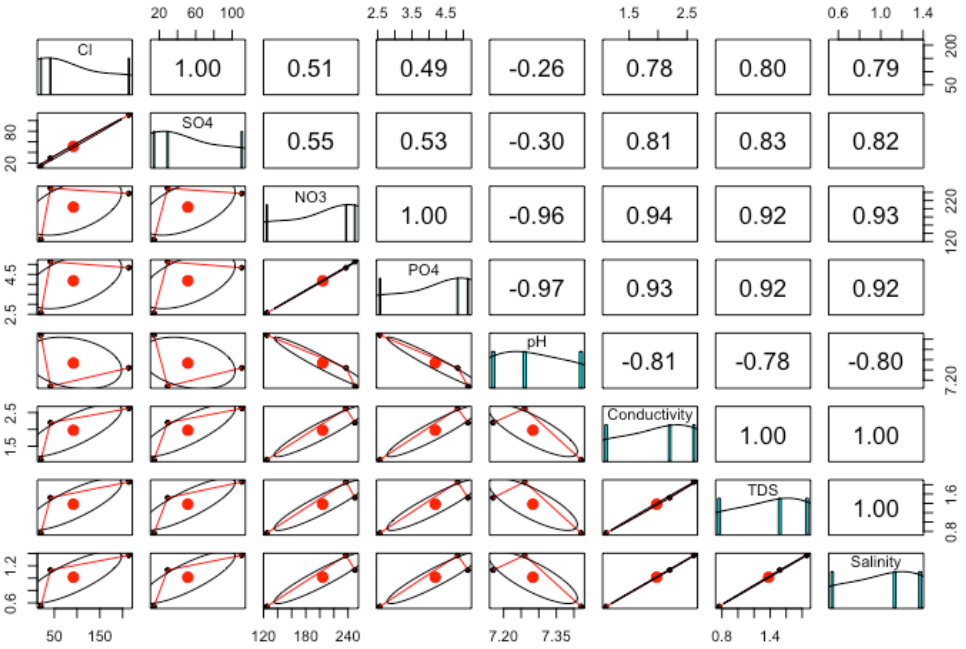

**Figure 15.** Covariance between the independent variables with correlation coefficients for the BG11 treatment group.

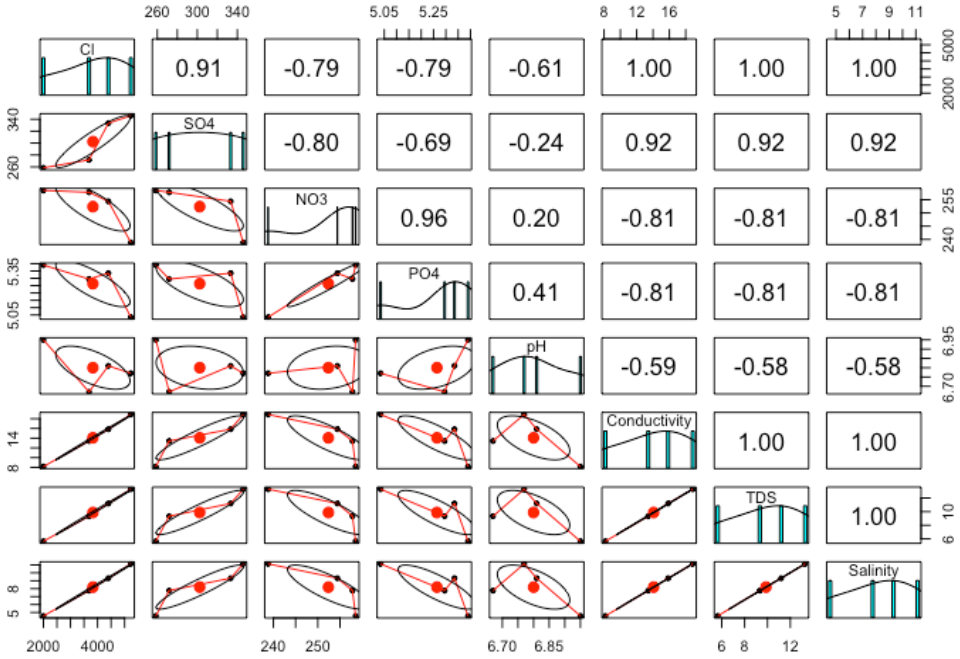


**Figure 16.** Covariance between the independent variables with correlation coefficients for the BG11 treatment group.

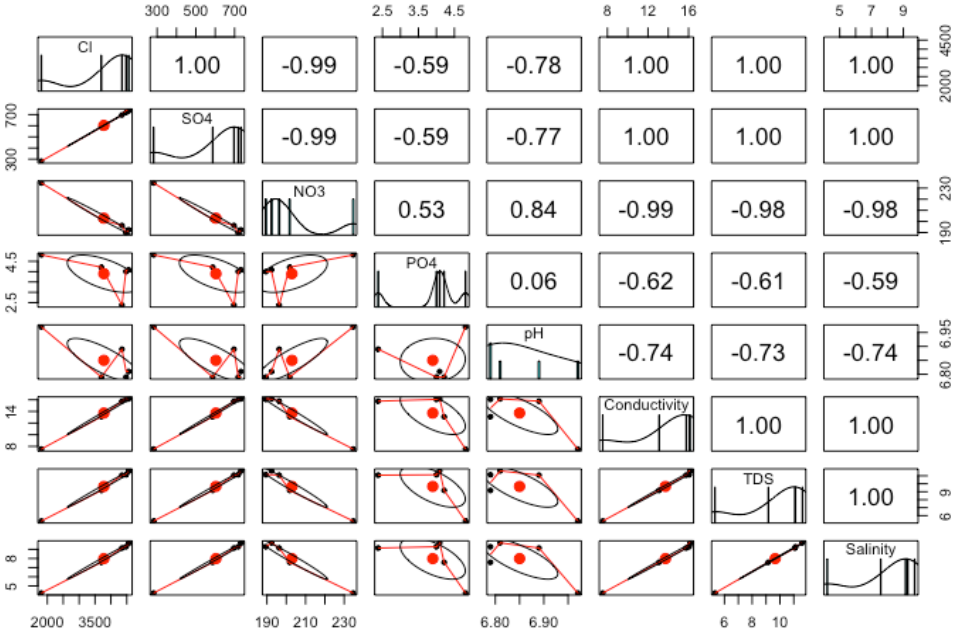


**Figure 17.** Covariance between the independent variables with correlation coefficients for the BG11 treatment group.

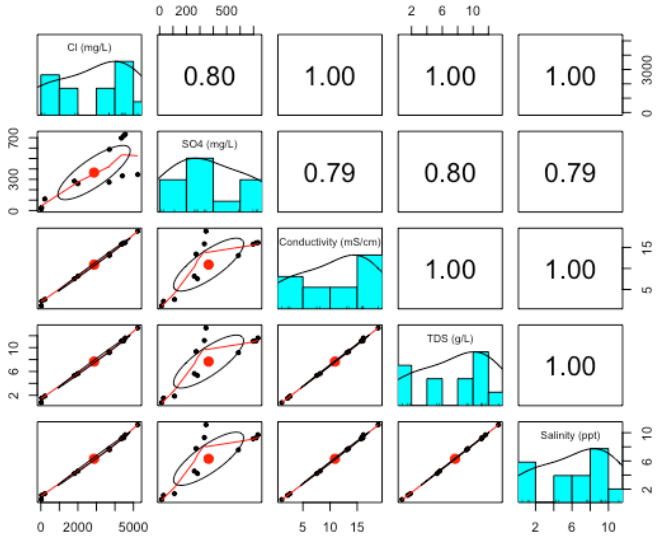


**Figure 18.** Covariance between chlorides, sulfates, conductivity, TDS, and salinity across all treatment groups (T1 – T12).


**Figure 19.** Image of T1, BG11, taken before RNA extraction.


**Figure 20.** Image of T2, 50% BG11:50% DIW, taken before RNA extraction.

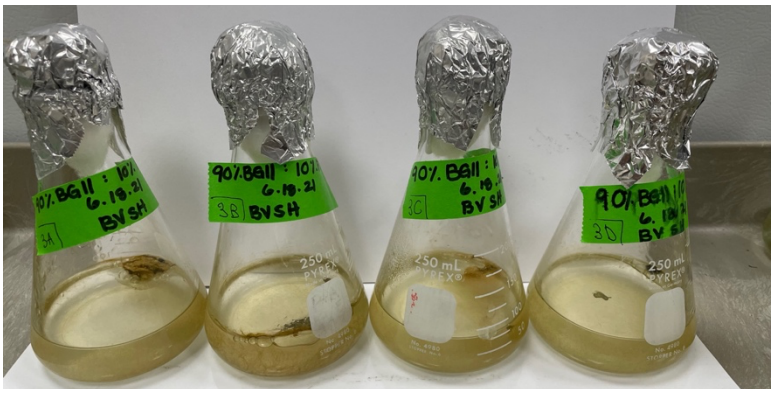


**Figure 21.** Image of T3, 10% eFSW:90% BG11, taken before RNA extraction.

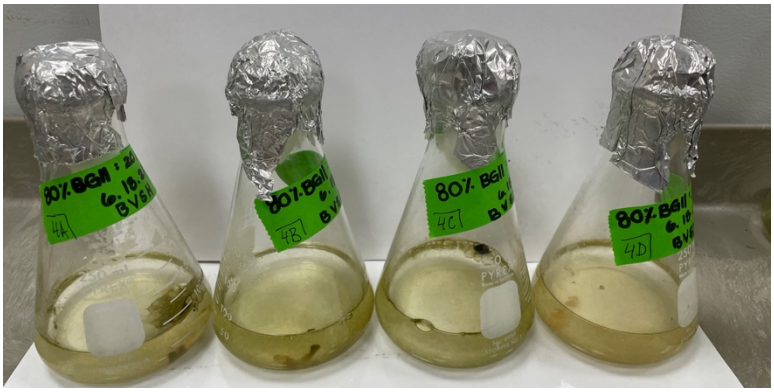


**Figure 22.** Image of T4, 20% eFSW:80% BG11, taken before RNA extraction.

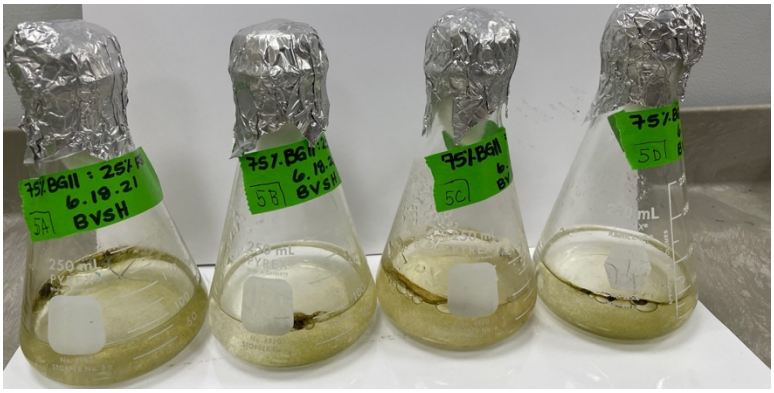


**Figure 23.** Image of T5, 25% eFSW:75% BG11, taken before RNA extraction.


**Figure 24.** Image of T6, BG11 with NaCl, taken before RNA extraction.

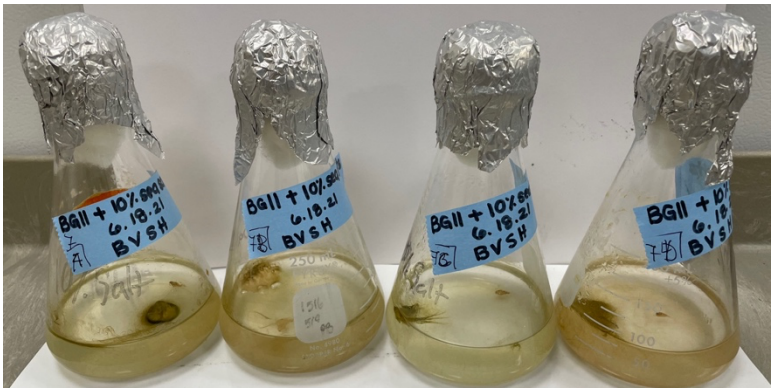


**Figure 25.** Image of T7, 10% SS:90% BG11, taken before RNA extraction.

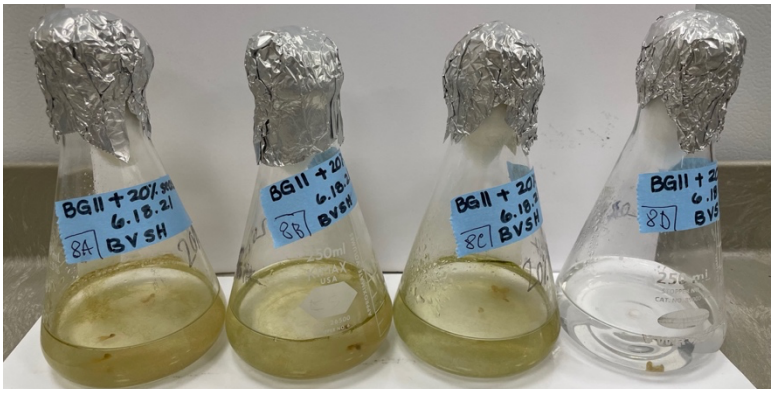


**Figure 26.** Image of T8, 20% SS:80% BG11, taken before RNA extraction.

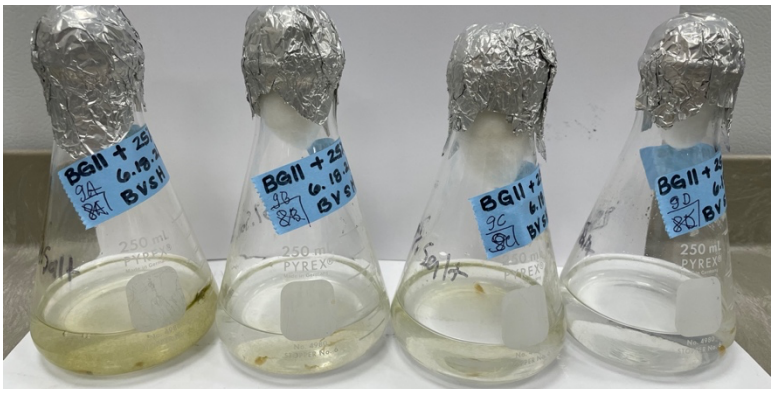

**Figure 27.** Image of T9, 25% SS:75% BG11, taken before RNA extraction.

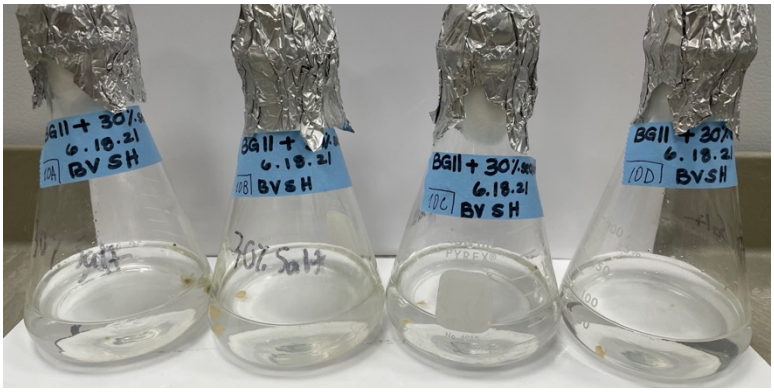

**Figure 28.** Image of T10, 30% SS:70% BG11, taken before RNA extraction.

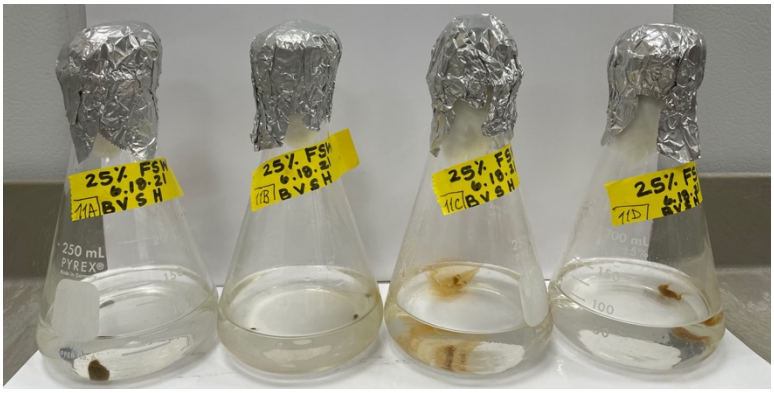

**Figure 29.** Image of T11, 25% pFSW:75% DIW, taken before RNA extraction.

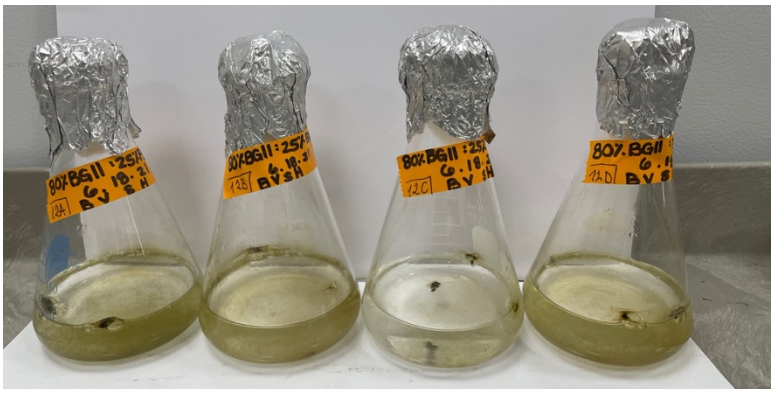

**Figure 30.** I Image of T11, 25% pFSW:75% BG11, taken before RNA extraction.

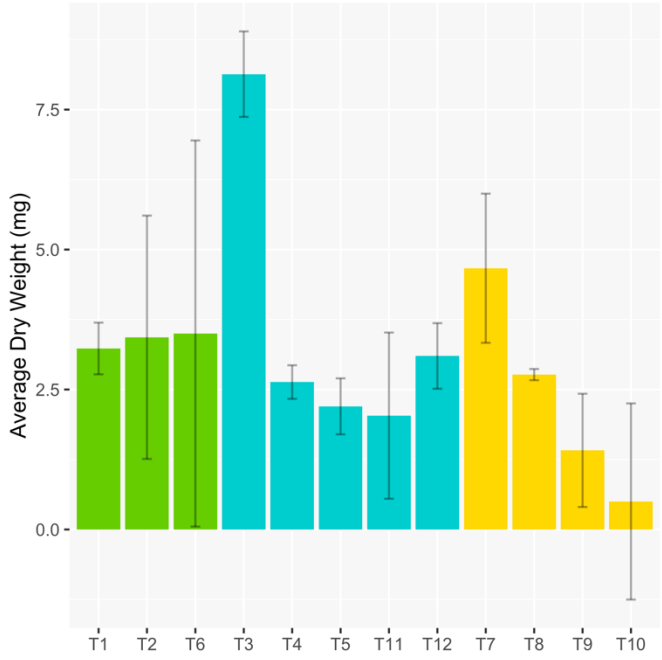


**Figure 31:** *M. anatoxicus* average dry weight mass and standard error (n=3 per treatment) in all culturing treatments (T1 – T12). Bar color corresponds to the grouping for statistical analysis (BG11 group = green, FSW group = cyan, SS group = yellow).

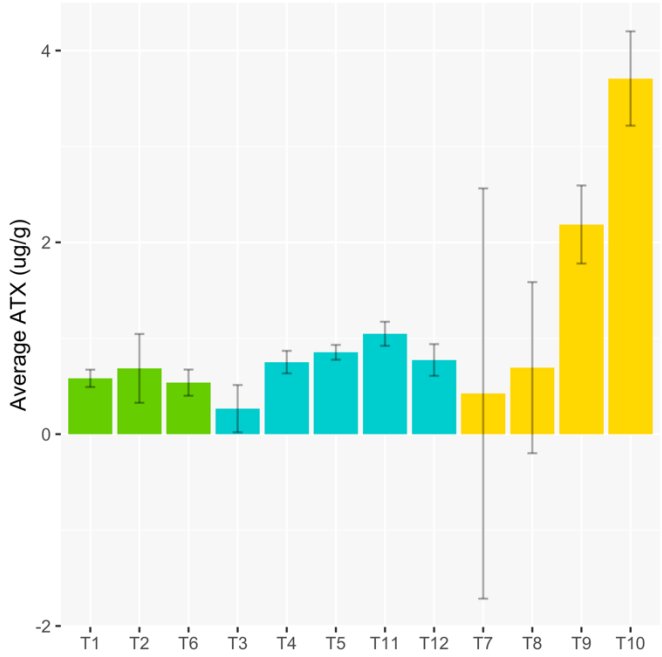


**Figure 32:** *M. anatoxicus* average intracellular ATX (µg/g) and standard error (n=3 per treatment) in all culturing treatments (T1 – T12). Bar color corresponds to the grouping for statistical analysis (BG11 group = green, FSW group = cyan, SS group = yellow).

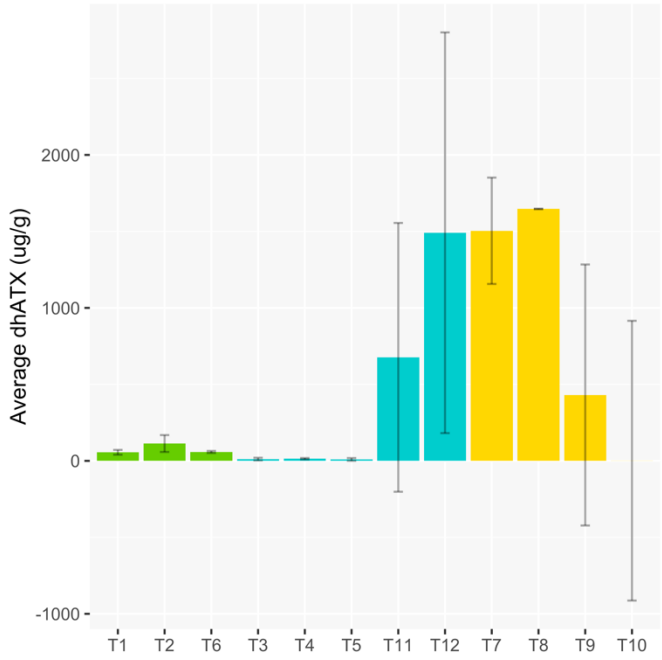


**Figure 33:** *M. anatoxicus* average intracellular dhATX (µg/g) and standard error (n=3 per treatment) in all culturing treatments (T1 – T12). Bar color corresponds to the grouping

for statistical analysis (BG11 group = green, FSW group = cyan, SS group = yellow).

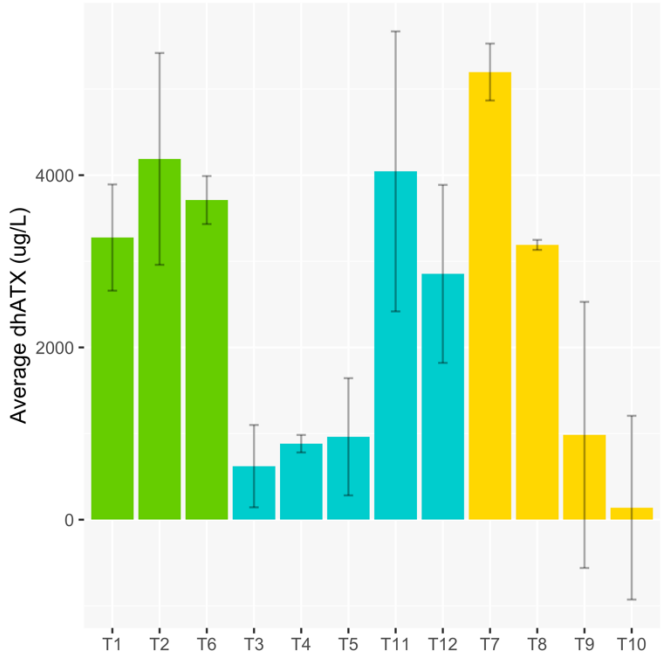


**Figure 34:** *M. anatoxicus* average extracellular dhATX (µg/L) and standard error (n=3 per treatment) in all culturing treatments (T1 – T12). Bar color corresponds to the grouping for statistical analysis (BG11 group = green, FSW group = cyan, SS group = yellow).

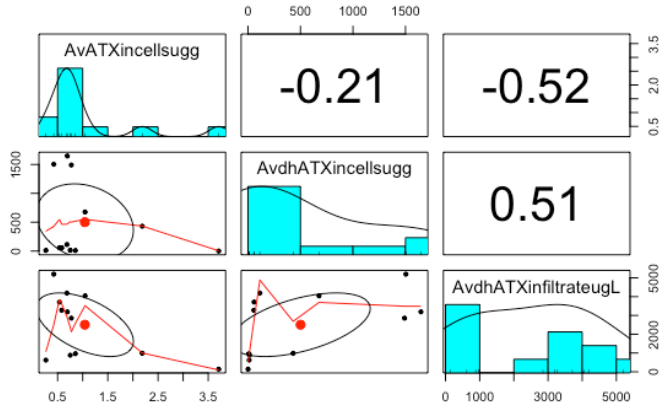


**Figure 35:** Covariance of intracellular ATX, dhATX, and extracellular dhATX across all treatments (T1 – T12).

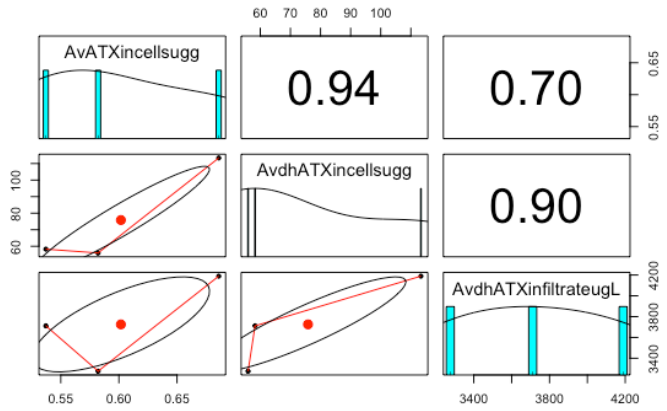


**Figure 36:** Covariance of intracellular ATX, dhATX, and extracellular dhATX across the BG11 treatments (T1, T2, and T6).

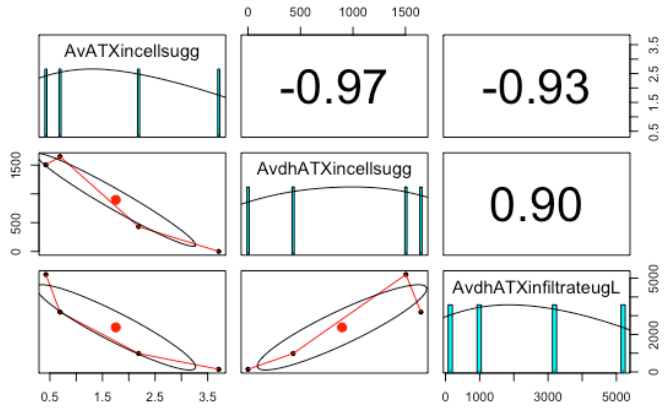


**Figure 37:** Covariance of intracellular ATX, dhATX, and extracellular dhATX across the SS treatments (T6 – T10).

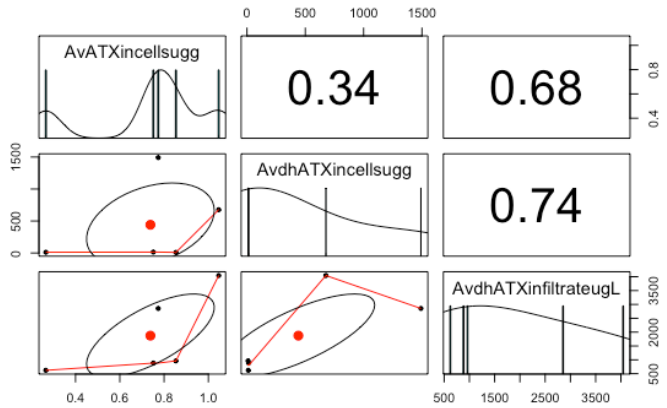

**Figure 38:** Covariance of intracellular ATX, dhATX, and extracellular dhATX across the FSW treatments (T3 - T5, T11, and T12).

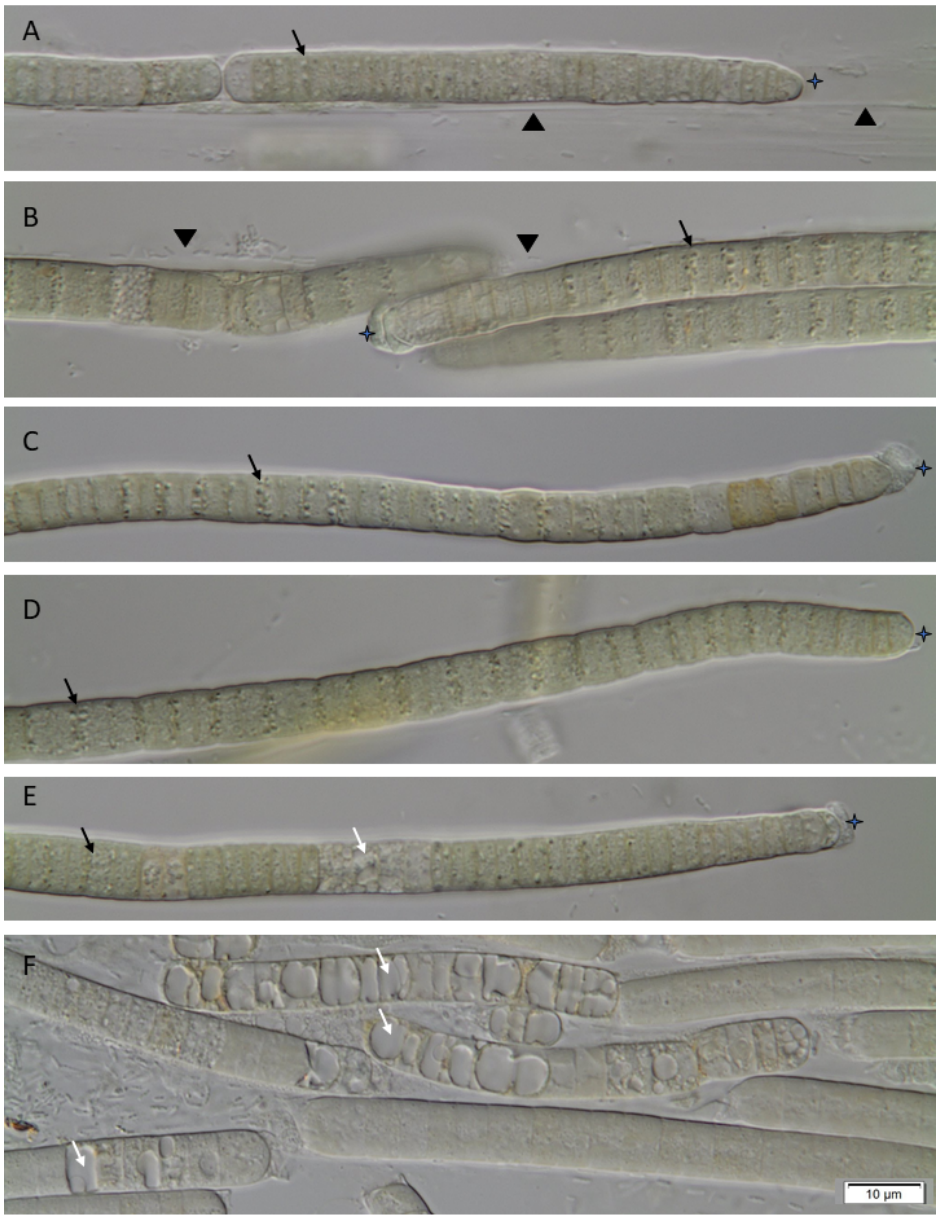


**Figure 39A-F.** *Microcoleus* morphology in different salinity treatments. Figure A. T1 (BG11, control). Figure B. T4 (20% eFSW). Figure C. T5 (25% eFSW). Figures D, E. T9 (25% SS). Figure F. T11 (25% pFSW). Legend: cyanophycin granules (black arrows), kerotomized cells (white arrows), mucilaginous sheath (triangles), kalyptra (stars).

**Table 5.** Regression between the average dry weight (mg) and salinity (ppt) within the BG11 treatment group.

| Simple Linear Regression | | | | | | Spearman | | |
|---|---|---|---|---|---|---|---|---|
| **Equation** | **Adjusted $R^2$** | **F-stat** | **Df1** | **Df2** | **P-value** | **S value** | **P-value** | **rho** |
| y = 0.001469x + 3.387399 | -1 | 2.035e-05 | 1 | 1 | 0.9971 | 2 | 1 | 0.5 |

**Table 6.** Regression between the average dry weight (mg) and salinity (ppt) within the SS treatment group (Figure 40).

| Simple Linear Regression | | | | | | Spearman | | |
|---|---|---|---|---|---|---|---|---|
| **Equation** | **Adjusted $R^2$** | **F-stat** | **Df1** | **Df2** | **P-value** | **S value** | **P-value** | **rho** |
| y = -0.64796x + 7.64507 | 0.9902 | 302.7 | 1 | 2 | **0.003288** | 20 | 0.08333 | -1 |

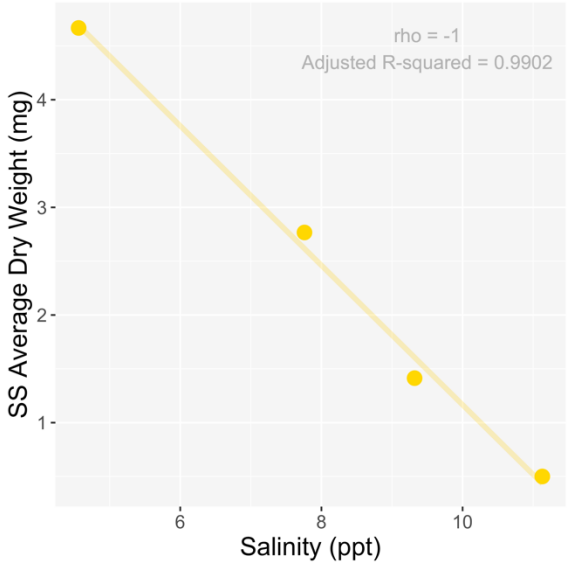


**Figure 40.** Relationship between *M. anatoxicus* average dry weight mass and salinity for the SS treatment group (n=4) (Supplemental Table 6).

**Table 7.** Regression between the average dry weight (mg) and salinity (ppt) within the FSW treatment group (Figure 41).

| Simple Linear Regression | | | | | | Spearman | | |
|---|---|---|---|---|---|---|---|---|
| **Equation** | **Adjusted $R^2$** | **F-stat** | **Df1** | **Df2** | **P-value** | **S value** | **P-value** | **rho** |
| y = -1.0411x + 11.9343 | 0.7901 | 16.06 | 1 | 3 | **0.02788** | 26 | 0.6833 | -0.3 |

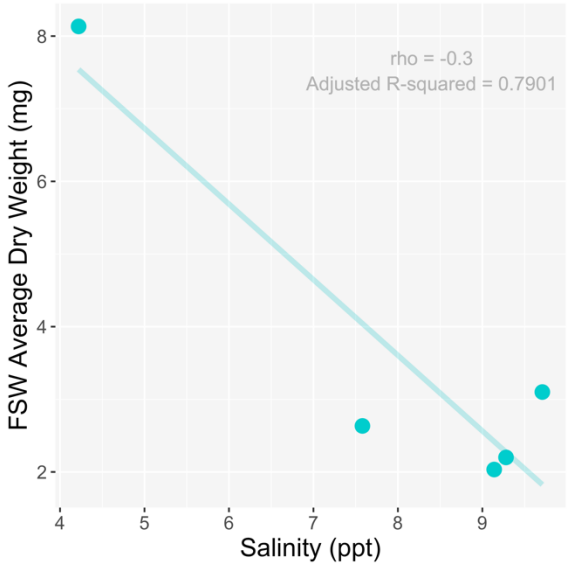


**Figure 40**. Relationship between *M. anatoxicus* average dry weight mass and salinity for the FSW treatment group (n=5) (Supplemental Table 7).

**Table 8.** Regression between the average dry weight (mg) and $NO_3$ (mg/L) within the BG11 treatment group.

| Simple Linear Regression | | | | | | Spearman | | |
|---|---|---|---|---|---|---|---|---|
| **Equation** | **Adjusted $R^2$** | **F-stat** | **Df1** | **Df2** | **P-value** | **S value** | **P-value** | **rho** |
| y = -0.0007444x + 3.5384719 | -0.7359 | 0.1521 | 1 | 1 | 0.7633 | 6 | 0.1 | -0.5 |

**Table 9.** Regression between the average dry weight (mg) and $NO_3$ (mg/L) within the SS treatment group.

| Simple Linear Regression | | | | | | Spearman | | |
|---|---|---|---|---|---|---|---|---|
| **Equation** | **Adjusted $R^2$** | **F-stat** | **Df1** | **Df2** | **P-value** | **S value** | **P-value** | **rho** |
| y = 0.15563x – 36.94211 | 0.4404 | 3.361 | 1 | 2 | 0.2082 | 0 | 0.08333 | 1 |

**Table 10.** Regression between the average dry weight (mg) and $NO_3$ (mg/L) within the FSW treatment group (Figure 41).

| Simple Linear Regression | | | | | | Spearman | | |
|---|---|---|---|---|---|---|---|---|
| **Equation** | **Adjusted $R^2$** | **F-stat** | **Df1** | **Df2** | **P-value** | **S value** | **P-value** | **rho** |

| | | | | | | | | |
|---|---|---|---|---|---|---|---|---|
| y = 0.13347x – 23.46408 | 0.8882 | 32.79 | 1 | 3 | **0.01057** | 10 | 0.45 | 0.5 |

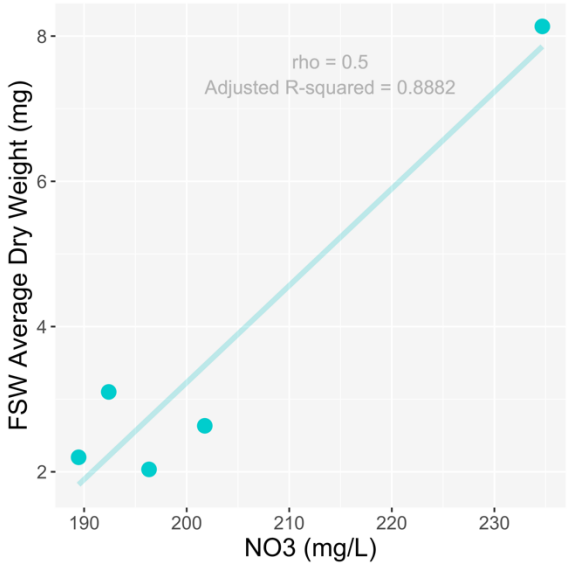


**Figure 41.** Relationship between *M. anatoxicus* average dry weight mass and nitrates for the FSW treatment group (n=5) (Supplemental Table 10).

**Table 11.** Regression between the average dry weight (mg) and $PO_4$ (mg/L) within the BG11 treatment group.

| Simple Linear Regression | | | | | | Spearman | | |
|---|---|---|---|---|---|---|---|---|
| **Equation** | **Adjusted $R^2$** | **F-stat** | **Df1** | **Df2** | **P-value** | **S value** | **P-value** | **rho** |
| y = -0.0374x + 3.54522 | -0.714 | 0.1668 | 1 | 1 | 0.75531 | 6 | 1 | -0.5 |

**Table 12.** Regression between the average dry weight (mg) and $PO_4$ (mg/L) within the SS treatment group.

| Simple Linear Regression | | | | | | Spearman | | |
|---|---|---|---|---|---|---|---|---|
| **Equation** | **Adjusted $R^2$** | **F-stat** | **Df1** | **Df2** | **P-value** | **S value** | **P-value** | **rho** |
| y = 8.907x – 44.547 | 0.3988 | 2.99 | 1 | 2 | 0.2259 | 2 | 0.3333 | 0.8 |

**Table 13.** Regression between the average dry weight (mg) and $PO_4$ (mg/L) within the FSW treatment group.

| Simple Linear Regression | Spearman |
|---|---|

| Equation | Adjusted $R^2$ | F-stat | Df1 | Df2 | P-value | S value | P-value | rho |
|---|---|---|---|---|---|---|---|---|
| y = 1.817x – 3.465 | 0.2196 | 2.126 | 1 | 3 | 0.2409 | 2 | 0.08333 | 0.9 |

**Table 14.** Regression between the average dry weight (mg) and $SO_4$ (mg/L) within the BG11 treatment group.

| Simple Linear Regression | | | | | | Spearman | | |
|---|---|---|---|---|---|---|---|---|
| **Equation** | **Adjusted $R^2$** | **F-stat** | **Df1** | **Df2** | **P-value** | **S value** | **P-value** | **rho** |
| y = 0.001554x + 3.30901 | -0.324 | 0.5106 | 1 | 1 | 0.605 | 2 | 1 | 0.5 |

**Table 15.** Regression between the average dry weight (mg) and $SO_4$ (mg/L) within the SS treatment group.

| Simple Linear Regression | | | | | | Spearman | | |
|---|---|---|---|---|---|---|---|---|
| **Equation** | **Adjusted $R^2$** | **F-stat** | **Df1** | **Df2** | **P-value** | **S value** | **P-value** | **rho** |
| y = -0.039218x + 14.196072 | 0.8381 | 16.53 | 1 | 2 | 0.0555 | 20 | 0.08333 | -1 |

**Table 16.** Regression between the average dry weight (mg) and $SO_4$ (mg/L) within the FSW treatment group (Figure 42).

| Simple Linear Regression | | | | | | Spearman | | |
|---|---|---|---|---|---|---|---|---|
| **Equation** | **Adjusted $R^2$** | **F-stat** | **Df1** | **Df2** | **P-value** | **S value** | **P-value** | **rho** |
| y = -0.012743 + 11.31-847 | 0.8454 | 22.87 | 1 | 3 | **0.01739** | 26 | 0.6833 | -0.3 |

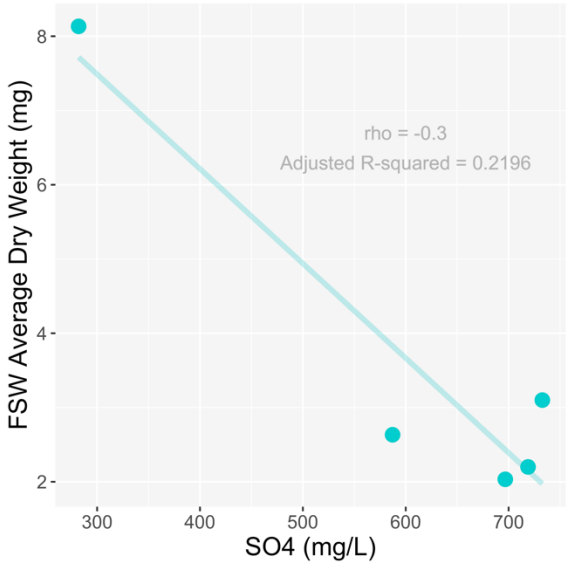


**Figure 42.** Relationship between *M. anatoxicus* average dry weight mass and sulfates for the FSW treatment group (n=5) (Supplemental Table 16).

**Table 17.** Regression between ATX in cells (ug/g) and $PO_4$ (mg/L) within the BG11 treatment group.

| Simple Linear Regression | | | | | | Spearman | | |
|---|---|---|---|---|---|---|---|---|
| **Equation** | **Adjusted $R^2$** | **F-stat** | **Df1** | **Df2** | **P-value** | **S value** | **P-value** | **rho** |
| y = -0.04994x + 0.81045 | 0.6881 | 5.412 | 1 | 1 | 0.2584 | 6 | 1 | -0.5 |

**Table 18.** Regression between ATX in cells (ug/g) and $PO_4$ (mg/L) within the SS treatment group.

| Simple Linear Regression | | | | | | Spearman | | |
|---|---|---|---|---|---|---|---|---|
| **Equation** | **Adjusted $R^2$** | **F-stat** | **Df1** | **Df2** | **P-value** | **S value** | **P-value** | **rho** |
| y = -8.307x + 45.481 | 0.6148 | 5.788 | 1 | 2 | 0.1379 | 18 | 0.3333 | -0.8 |

**Table 19.** Regression between ATX in cells (ug/g) and $PO_4$ (mg/L) within the FSW treatment group (Figure 43).

| Simple Linear Regression | | | | | | Spearman | | |
|---|---|---|---|---|---|---|---|---|
| **Equation** | **Adjusted $R^2$** | **F-stat** | **Df1** | **Df2** | **P-value** | **S value** | **P-value** | **rho** |
| y = -0.2668x + 1.7787 | 0.603 | 7.076 | 1 | 3 | 0.0763 | 40 | **0.01667** | -1 |

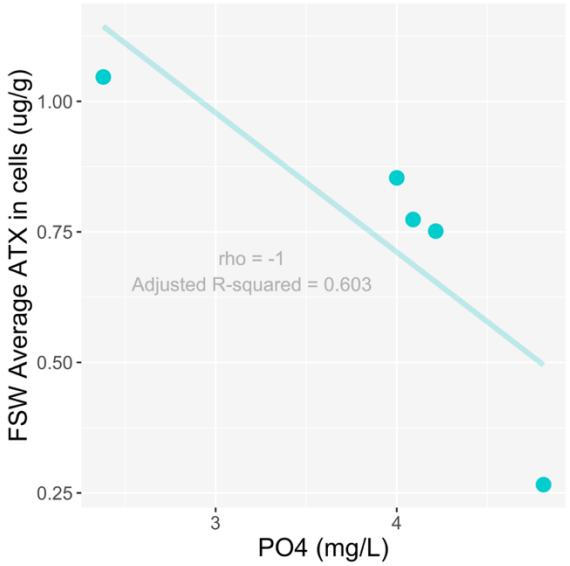


**Figure 43.** Negative relationship between *M. anatoxicus* average intracellular ATX and phosphates in the FSW treatment group (S = 40, $\mathbf{p_S = 0.01667}$, $r_S$ = -1, n=5) (Supplemental Table 19).

**Table 20.** Regression between dhATX in cells (ug/g) and $PO_4$ (mg/L) within the BG11 treatment group (Figure 44).

| **Simple Linear Regression** | | | | | | **Spearman** | | |
|---|---|---|---|---|---|---|---|---|
| **Equation** | **Adjusted $R^2$** | **F-stat** | **Df1** | **Df2** | **P-value** | **S value** | **P-value** | **rho** |
| y = -23.099x + 172.400 | 0.9899 | 197.8 | 1 | 1 | **0.04518** | 8 | 0.3333 | -1 |

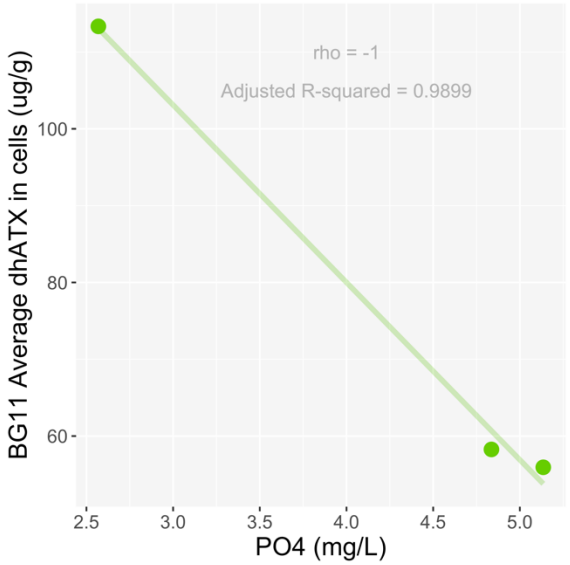


**Figure 44.** Negative relationship between *M. anatoxicus* average intracellular dhATX and phosphates in the BG11 treatment group (Supplemental Table 20).

**Table 21.** Regression between dhATX in cells (ug/g) and $PO_4$ (mg/L) within the SS treatment group.

| Simple Linear Regression | | | | | | Spearman | | |
|---|---|---|---|---|---|---|---|---|
| **Equation** | **Adjusted $R^2$** | **F-stat** | **Df1** | **Df2** | **P-value** | **S value** | **P-value** | **rho** |
| y = 3657x + -18354 | 0.2641 | 2.077 | 1 | 2 | 0.2863 | 6 | 0.75 | 0.4 |

**Table 22.** Regression between dhATX in cells (ug/g) and $PO_4$ (mg/L) within the FSW treatment group (Figure #).

| Simple Linear Regression | | | | | | Spearman | | |
|---|---|---|---|---|---|---|---|---|
| **Equation** | **Adjusted $R^2$** | **F-stat** | **Df1** | **Df2** | **P-value** | **S value** | **P-value** | **rho** |
| y = -221.4x + 1303.8 | -0.2079 | 0.3115 | 1 | 3 | 0.6157 | 24 | 0.7833 | -0.2 |

**Table 23.** Regression between dhATX in filtrate (ug/mL) and $PO_4$ (mg/L) within the BG11 treatment group.

| Simple Linear Regression | | | | | | Spearman | | |
|---|---|---|---|---|---|---|---|---|
| **Equation** | **Adjusted $R^2$** | **F-stat** | **Df1** | **Df2** | **P-value** | **S value** | **P-value** | **rho** |
| y = -0.3011x + 4.9838 | 0.7107 | 5.913 | 1 | 1 | 0.2484 | 8 | 0.3333 | -1 |

**Table 24.** Regression between dhATX in filtrate (ug/mL) and $PO_4$ (mg/L) within the SS treatment group.

| Simple Linear Regression | | | | | | Spearman | | |
|---|---|---|---|---|---|---|---|---|
| **Equation** | **Adjusted $R^2$** | **F-stat** | **Df1** | **Df2** | **P-value** | **S value** | **P-value** | **rho** |
| y = 10.686x – 53.868 | 0.3178 | 2.397 | 1 | 2 | 0.2616 | 2 | 0.3333 | 0.8 |

**Table 25.** Regression between dhATX in filtrate (ug/mL) and $PO_4$ (mg/L) within the FSW treatment group.

| Simple Linear Regression | | | | | | Spearman | | |
|---|---|---|---|---|---|---|---|---|
| **Equation** | **Adjusted $R^2$** | **F-stat** | **Df1** | **Df2** | **P-value** | **S value** | **P-value** | **rho** |
| y = -1.4177x + 7.4002 | 0.6388 | 8.074 | 1 | 3 | 0.06557 | 38 | 0.08333 | -0.9 |

**Table 26.** Regression between ATX in cells (ug/g) and $NO_3$ (mg/L) within the FSW treatment group (Figure 45).

| Simple Linear Regression | | | | | | Spearman | | |
|---|---|---|---|---|---|---|---|---|
| **Equation** | **Adjusted $R^2$** | **F-stat** | **Df1** | **Df2** | **P-value** | **S value** | **P-value** | **rho** |
| y = -0.014106x + 3.600715 | 0.7382 | 12.28 | 1 | 3 | **0.03935** | 34 | 0.2333 | -0.7 |

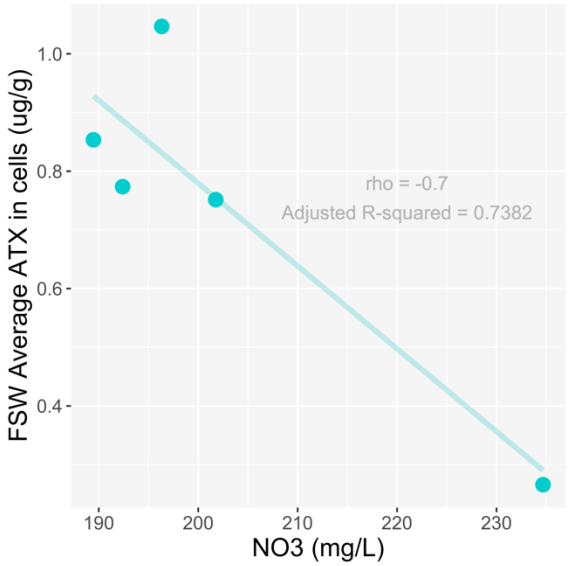

**Figure 45.** Relationship between *M. anatoxicus* average intracellular ATX and nitrates in the FSW treatment group (n=5) (Supplemental Table 26).

**Table 27.** Regression between dhATX in cells (ug/g) and $NO_3$ (mg/L) within the BG11 treatment group (Figure 46).

| Simple Linear Regression | | | | | | Spearman | | |
|---|---|---|---|---|---|---|---|---|
| **Equation** | **Adjusted $R^2$** | **F-stat** | **Df1** | **Df2** | **P-value** | **S value** | **P-value** | **rho** |
| y = -0.4718x +172.0893 | 0.9939 | 329.2 | 1 | 1 | **0.03505** | 8 | 0.3333 | -1 |

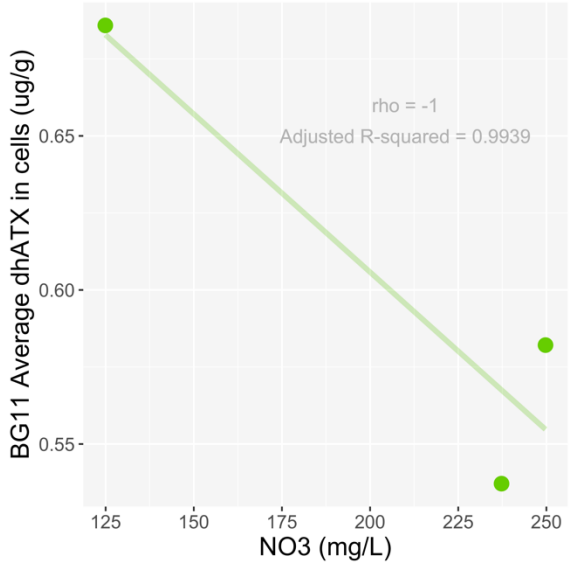


**Figure 46.** Relationship between *M. anatoxicus* average intracellular dhATX and nitrates in the BG11 treatment group (n=3) (Supplemental Table 27).

**Table 28.** Regression between ATX in cell (ug/g) and $NO_3$ (mg/L) within the BG11 treatment group.

| Simple Linear Regression | | | | | | Spearman | | |
|---|---|---|---|---|---|---|---|---|
| **Equation** | **Adjusted $R^2$** | **F-stat** | **Df1** | **Df2** | **P-value** | **S value** | **P-value** | **rho** |
| y = -0.0010259x +0.8109698 | 0.7108 | 5.917 | 1 | 1 | 0.2483 | 6 | 1 | -0.5 |

**Table 29.** Regression between ATX in cell (ug/g) and $NO_3$ (mg/L) within the SS treatment group.

| Simple Linear Regression | Spearman |
|---|---|

| Equation | Adjusted $R^2$ | F-stat | Df1 | Df2 | P-value | S value | P-value | rho |
|---|---|---|---|---|---|---|---|---|
| y = -0.15516x + 40.91425 | 0.8328 | 15.94 | 1 | 2 | 0.0574 | 20 | 0.08333 | -1 |

**Table 30.** Regression between dhATX in cells (ug/g) and $NO_3$ (mg/L) within the SS treatment group.

| Simple Linear Regression | | | | | | Spearman | | |
|---|---|---|---|---|---|---|---|---|
| Equation | Adjusted $R^2$ | F-stat | Df1 | Df2 | P-value | S value | P-value | rho |
| y = 74.55x + -17919.78 | 0.5882 | 5.285 | 1 | 2 | 0.1483 | 2 | 0.3333 | 0.8 |

**Table 31.** Regression between dhATX in cells (ug/g) and $NO_3$ (mg/L) within the FSW treatment group.

| Simple Linear Regression | | | | | | Spearman | | |
|---|---|---|---|---|---|---|---|---|
| Equation | Adjusted $R^2$ | F-stat | Df1 | Df2 | P-value | S value | P-value | rho |
| y = -14.82x + 344853 | -0.1031 | 0.6262 | 1 | 3 | 0.4866 | 20 | 1 | 0 |

**Table 32.** Regression between dhATX in filtrate (ug/mL) and $NO_3$ (mg/L) within the BG11 treatment group.

| Simple Linear Regression | | | | | | Spearman | | |
|---|---|---|---|---|---|---|---|---|
| Equation | Adjusted $R^2$ | F-stat | Df1 | Df2 | P-value | S value | P-value | rho |
| y = -0.006102x + 4.970110 | 0.6879 | 5.409 | 1 | 1 | 0.2585 | 8 | 0.3333 | -0 |

**Table 33.** Regression between dhATX in filtrate (ug/mL) and $NO_3$ (mg/L) within the SS treatment group.

| Simple Linear Regression | | | | | | Spearman | | |
|---|---|---|---|---|---|---|---|---|
| Equation | Adjusted $R^2$ | F-stat | Df1 | Df2 | P-value | S value | P-value | rho |
| y = 0.1932x + -46.3879 | 0.4163 | 3.14 | 1 | 2 | 0.2184 | 0 | 0.083333 | 1 |

**Table 34.** Regression between dhATX in filtrate (ug/mL) and $NO_3$ (mg/L) within the FSW treatment group.

| Simple Linear Regression | | | | | | Spearman | | |
|---|---|---|---|---|---|---|---|---|
| **Equation** | **Adjusted $R^2$** | **F-stat** | **Df1** | **Df2** | **P-value** | **S value** | **P-value** | **rho** |
| y = -0.03790x + 9.56362 | -0.04879 | 0.8139 | 1 | 3 | 0.4335 | 32 | 0.35 | -0.6 |

**Table 35.** Regression between ATX in cells (ug/g) and $SO_4$ (mg/L) within the SS treatment group (Figure 47).

| Simple Linear Regression | | | | | | Spearman | | |
|---|---|---|---|---|---|---|---|---|
| **Equation** | **Adjusted $R^2$** | **F-stat** | **Df1** | **Df2** | **P-value** | **S value** | **P-value** | **rho** |
| y = 0.033137x – 8.267725 | 0.8621 | 19.75 | 1 | 2 | **0.04708** | 0 | 0.08333 | 1 |

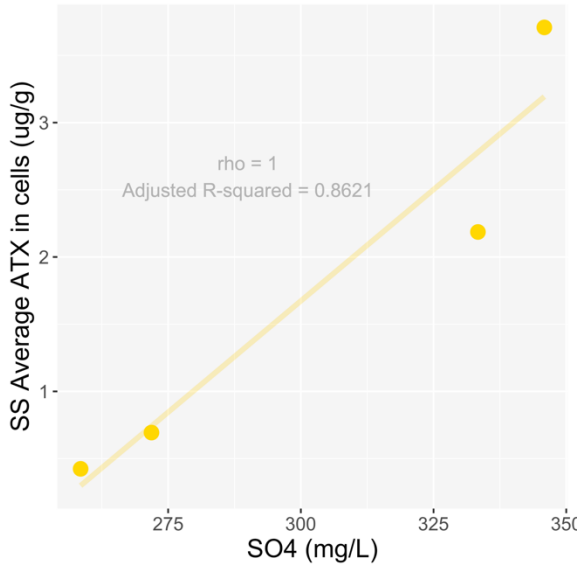


**Figure 47.** Relationship between *M. anatoxicus* average intracellular ATX and sulfates in the SS treatment group (n=4) (Supplemental Table 35).

**Table 36.** Regression between ATX in cells (ug/g) and $SO_4$ (mg/L) within the FSW treatment group (Figure 48).

| Simple Linear Regression | | | | | | Spearman | | |
|---|---|---|---|---|---|---|---|---|
| **Equation** | **Adjusted $R^2$** | **F-stat** | **Df1** | **Df2** | **P-value** | **S value** | **P-value** | **rho** |
| y = 0.0013929x | 0.7727 | 14.59 | 1 | 3 | **0.03157** | 8 | 0.35 | 0.6 |

| | | | | | | | | |
|---|---|---|---|---|---|---|---|---|
| –<br>0.1024462 | | | | | | | | |

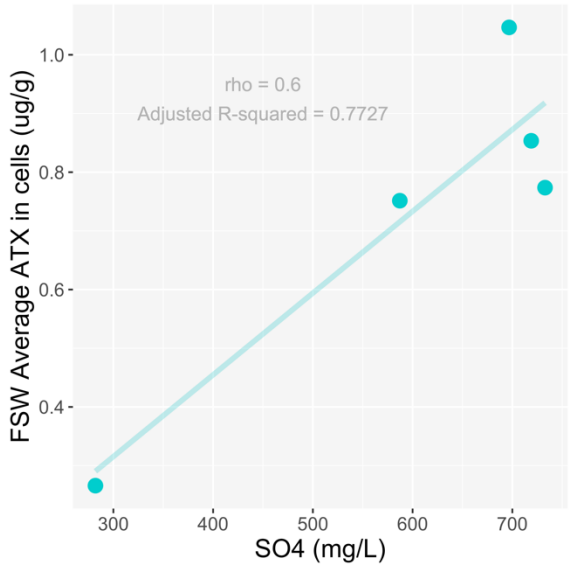


**Figure 48.** Relationship between *M. anatoxicus* average intracellular ATX and sulfates in the FSW treatment group (n=5) (Supplemental Table 36).

**Table 37.** Regression between dhATX in cells (ug/g) and $SO_4$ (mg/L) within the BG11 treatment group.

| **Simple Linear Regression** | | | | | | **Spearman** | | |
|---|---|---|---|---|---|---|---|---|
| **Equation** | **Adjusted $R^2$** | **F-stat** | **Df1** | **Df2** | **P-value** | **S value** | **P-value** | **rho** |
| y = -0.3705x + 94.8705 | -0.2991 | 0.5396 | 1 | 1 | 0.5967 | 6 | 1 | -0.5 |

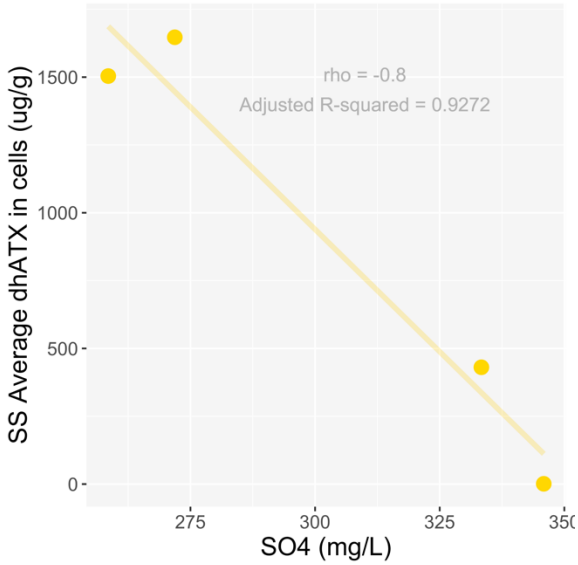


**Figure 49.** Relationship between *M. anatoxicus* average intracellular dhATX and sulfates in the SS treatment group (n=4) (Supplemental Table 38).

**Table 38.** Regression between dhATX in cells (ug/g) and $SO_4$ (mg/L) within the SS treatment group (Figure 49).

| Simple Linear Regression | | | | | | Spearman | | |
|---|---|---|---|---|---|---|---|---|
| **Equation** | **Adjusted $R^2$** | **F-stat** | **Df1** | **Df2** | **P-value** | **S value** | **P-value** | **rho** |
| y = -18.035x + 6349.557 | 0.9272 | 39.2 | 1 | 2 | **0.02457** | 18 | 0.3333 | -0.8 |

**Table 39.** Regression between dhATX in cells (ug/g) and $SO_4$ (mg/L) within the FSW treatment group.

| Simple Linear Regression | | | | | | Spearman | | |
|---|---|---|---|---|---|---|---|---|
| **Equation** | **Adjusted $R^2$** | **F-stat** | **Df1** | **Df2** | **P-value** | **S value** | **P-value** | **rho** |
| y = 1.777x – 631.810 | 0.01684 | 1.069 | 1 | 3 | 0.3773 | 12 | 0.5167 | 0.4 |

**Table 40.** Regression between dhATX in filtrate (ug/mL) and $SO_4$ (mg/L) within the BG11 treatment group.

| Simple Linear Regression | | | | | | Spearman | | |
|---|---|---|---|---|---|---|---|---|
| **Equation** | **Adjusted $R^2$** | **F-stat** | **Df1** | **Df2** | **P-value** | **S value** | **P-value** | **rho** |
| y = -0.001509x | -0.9411 | 0.03032 | 1 | 1 | 0.8902 | 6 | 1 | -0.5 |

| | | | | | | | | |
|---|---|---|---|---|---|---|---|---|
| + 3.802877 | | | | | | | | |

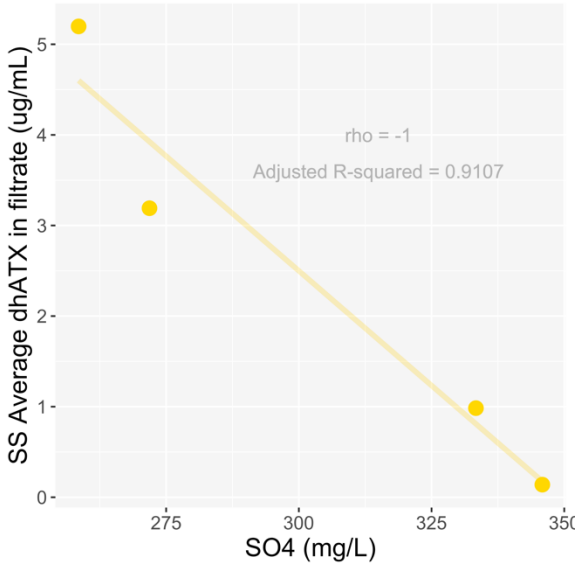


**Figure 50.** Relationship between *M. anatoxicus* average extracellular dhATX and sulfates in the SS treatment group (n=4) (Supplemental Table 41).

**Table 41.** Regression between dhATX in filtrate (ug/mL) and $SO_4$ (mg/L) within the SS treatment group (Figure 50).

| Simple Linear Regression | | | | | | Spearman | | |
|---|---|---|---|---|---|---|---|---|
| **Equation** | **Adjusted $R^2$** | **F-stat** | **Df1** | **Df2** | **P-value** | **S value** | **P-value** | **rho** |
| y = -0.050646x + 17.69324 | 0.9107 | 31.6 | 1 | 2 | **0.03022** | 20 | 0.08333 | -1 |

**Table 42.** Regression between dhATX in filtrate (ug/mL) and $SO_4$ (mg/L) within the FSW treatment group.

| Simple Linear Regression | | | | | | Spearman | | |
|---|---|---|---|---|---|---|---|---|
| **Equation** | **Adjusted $R^2$** | **F-stat** | **Df1** | **Df2** | **P-value** | **S value** | **P-value** | **rho** |
| y = 0.004515x – 0.851930 | 0.09403 | 1.415 | 1 | 3 | 0.3198 | 6 | 0.2333 | 0.7 |

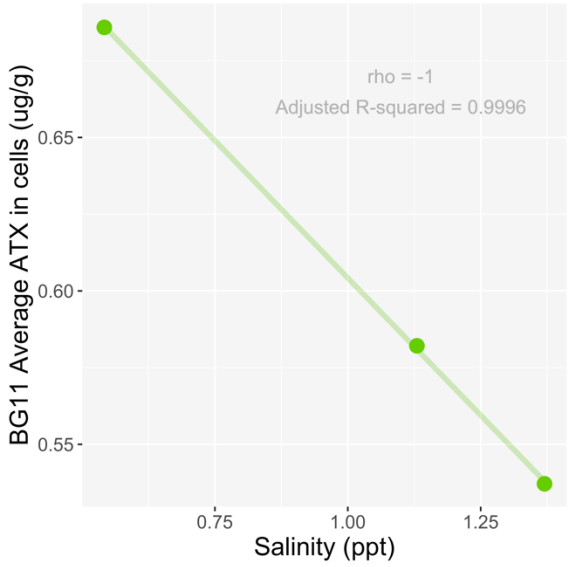


**Figure 51.** Relationship between *M. anatoxicus* average intracellular ATX and salinity in the BG11 treatment group (Supplemental Table 43).

**Table 43.** Regression between ATX in cells (ug/g) and salinity (ppt) within the BG11 treatment group (Figure 51).

| Simple Linear Regression | | | | | | Spearman | | |
|---|---|---|---|---|---|---|---|---|
| **Equation** | **Adjusted $R^2$** | **F-stat** | **Df1** | **Df2** | **P-value** | **S value** | **P-value** | **rho** |
| y = -0.179024x + 0.7383233 | 0.9996 | 5350 | 1 | 1 | **0.008703** | 8 | 0.3333 | -1 |

**Table 44.** Regression between ATX in cells (ug/g) and salinity (ppt) within the SS treatment group.

| Simple Linear Regression | | | | | | Spearman | | |
|---|---|---|---|---|---|---|---|---|
| **Equation** | **Adjusted $R^2$** | **F-stat** | **Df1** | **Df2** | **P-value** | **S value** | **P-value** | **rho** |
| y = 0.4948x – 2.3006 | 0.7389 | 9.488 | 1 | 2 | 0.0912 | 0 | 0.08333 | 1 |

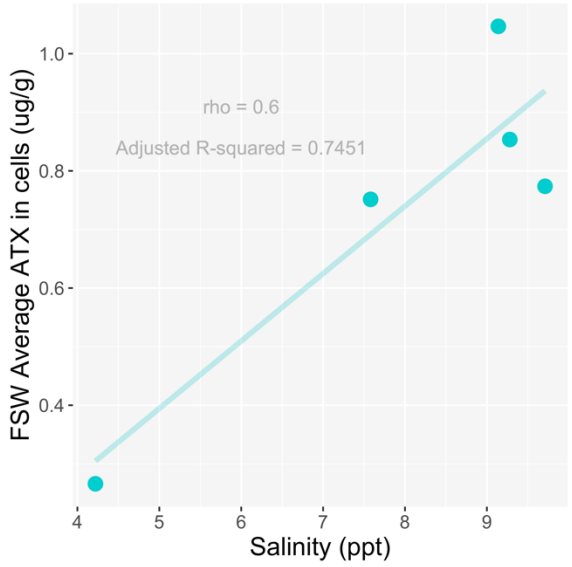


**Figure 52.** Relationship between *M. anatoxicus* average intracellular ATX and salinity in the BG11 treatment group (Supplemental Table 45).

**Table 45.** Regression between ATX in cells (ug/g) and salinity (ppt) within the FSW treatment group (Figure 52).

| Simple Linear Regression | | | | | | Spearman | | |
|---|---|---|---|---|---|---|---|---|
| **Equation** | **Adjusted $R^2$** | **F-stat** | **Df1** | **Df2** | **P-value** | **S value** | **P-value** | **rho** |
| y = 0.11511x – 0.18101 | 0.7451 | 12.69 | 1 | 3 | **0.03775** | 8 | 0.35 | 0.6 |

**Table 46.** Regression between dhATX in cells (ug/g) and salinity (ppt) within the BG11 treatment group.

| Simple Linear Regression | | | | | | Spearman | | |
|---|---|---|---|---|---|---|---|---|
| **Equation** | **Adjusted $R^2$** | **F-stat** | **Df1** | **Df2** | **P-value** | **S value** | **P-value** | **rho** |
| y = -72.37x + 149.23 | 0.8005 | 9.026 | 1 | 1 | 0.2046 | 6 | 1 | -0.5 |

**Table 47.** Regression between dhATX in cells (ug/g) and salinity (ppt) within the SS treatment group.

| Simple Linear Regression | | | | | | Spearman | | |
|---|---|---|---|---|---|---|---|---|
| **Equation** | **Adjusted $R^2$** | **F-stat** | **Df1** | **Df2** | **P-value** | **S value** | **P-value** | **rho** |
| y = -244.3x + 2896.7 | 0.5679 | 4.943 | 1 | 2 | 0.1562 | 18 | 0.3333 | -0.8 |

**Table 48.** Regression between dhATX in cells (ug/g) and salinity (ppt) within the FSW treatment group.

| Simple Linear Regression | | | | | | Spearman | | |
|---|---|---|---|---|---|---|---|---|
| **Equation** | **Adjusted $R^2$** | **F-stat** | **Df1** | **Df2** | **P-value** | **S value** | **P-value** | **rho** |
| y = -861.6x +163.1 | 0.08773 | 1.385 | 1 | 3 | 0.3242 | 12 | 0.5167 | 0.4 |

**Table 49.** Regression between dhATX in filtrate (ug/mL) and salinity (ppt) within the BG11 treatment group.

| Simple Linear Regression | | | | | | Spearman | | |
|---|---|---|---|---|---|---|---|---|
| **Equation** | **Adjusted $R^2$** | **F-stat** | **Df1** | **Df2** | **P-value** | **S value** | **P-value** | **rho** |
| y = -0.7604x + 4.4964 | 0.005886 | 1.012 | 1 | 1 | 0.4981 | 6 | 1 | -0.5 |

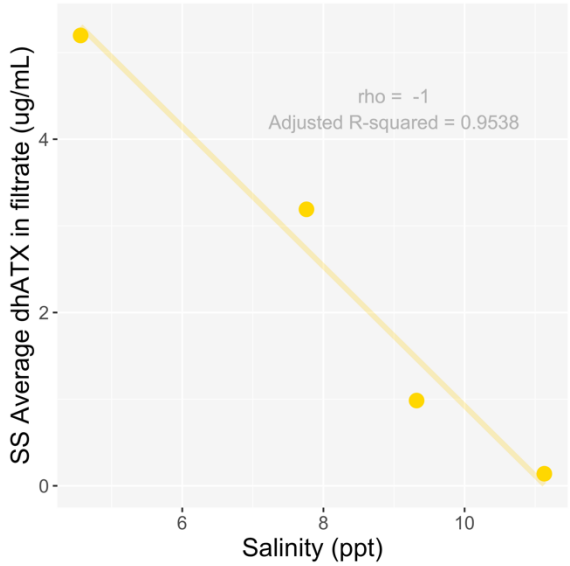


**Figure 53.** Relationship between *M. anatoxicus* average extracellular dhATX and salinity in the SS treatment group (Supplemental Table #).

**Table 50.** Regression between dhATX in filtrate (ug/mL) and salinity (ppt) within the SS treatment group (Figure 53).

| Simple Linear Regression | | | | | | Spearman | | |
|---|---|---|---|---|---|---|---|---|
| **Equation** | **Adjusted $R^2$** | **F-stat** | **Df1** | **Df2** | **P-value** | **S value** | **P-value** | **rho** |

| | | | | | | | | |
|---|---|---|---|---|---|---|---|---|
| y = -0.8050x + 8.9726 | 0.9538 | 62.96 | 1 | 2 | **0.01551** | 20 | 0.08333 | -1 |

**Table 51.** Regression between dhATX in filtrate (ug/mL) and salinity (ppt) within the FSW treatment group.

| Simple Linear Regression | | | | | | Spearman | | |
|---|---|---|---|---|---|---|---|---|
| **Equation** | **Adjusted $R^2$** | **F-stat** | **Df1** | **Df2** | **P-value** | **S value** | **P-value** | **rho** |
| y = 0.4001x – 1.3227 | 0.146 | 1.684 | 1 | 3 | 0.2852 | 34 | 0.2333 | -0.7 |

**Table 52.** Regression between ATX in cell (ug/g) and dry weight (mg) within the BG11 treatment group.

| Simple Linear Regression | | | | | | Spearman | | |
|---|---|---|---|---|---|---|---|---|
| **Equation** | **Adjusted $R^2$** | **F-stat** | **Df1** | **Df2** | **P-value** | **S value** | **P-value** | **rho** |
| y = -0.009992x + 0.635566 | -0.9993 | 0.0003306 | 1 | 1 | 0.9884 | 6 | 1 | -0.5 |

**Table 53.** Regression between ATX in cell (ug/g) and dry weight (mg) within the SS treatment group.

| Simple Linear Regression | | | | | | Spearman | | |
|---|---|---|---|---|---|---|---|---|
| **Equation** | **Adjusted $R^2$** | **F-stat** | **Df1** | **Df2** | **P-value** | **S value** | **P-value** | **rho** |
| y = -0.7668x + 3.5446 | 0.7573 | 10.36 | 1 | 2 | 0.08446 | 20 | 0.08333 | -1 |

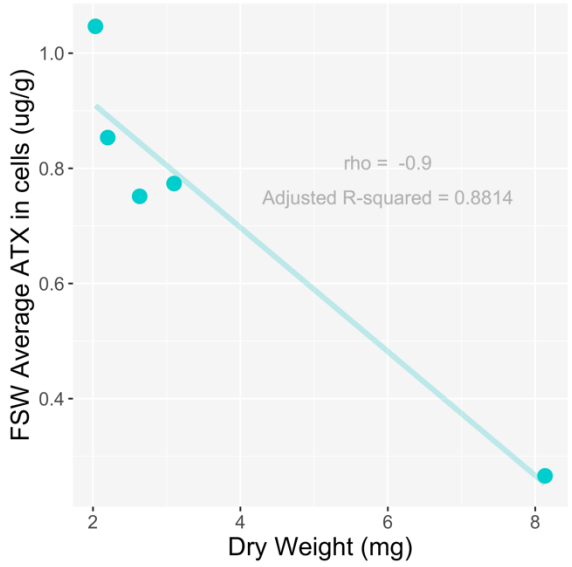


**Figure 54.** Relationship between *M. anatoxicus* average dry weight and average intracellular ATX in the FSW treatment group (n=5) (Supplemental Table 54).

**Table 54.** Regression between ATX in cell (ug/g) and dry weight (mg) within the FSW treatment group (Figure 54).

| Simple Linear Regression | | | | | | Spearman | | |
|---|---|---|---|---|---|---|---|---|
| **Equation** | **Adjusted $R^2$** | **F-stat** | **Df1** | **Df2** | **P-value** | **S value** | **P-value** | **rho** |
| y = -0.10771x + 1.12813 | 0.8814 | 30.72 | 1 | 3 | **0.01158** | 38 | 0.08333 | -0.9 |

**Table 55.** Regression between the dhATX in cell (ug/g) and dry weight (mg) within the BG11 treatment group.

| Simple Linear Regression | | | | | | Spearman | | |
|---|---|---|---|---|---|---|---|---|
| **Equation** | **Adjusted $R^2$** | **F-stat** | **Df1** | **Df2** | **P-value** | **S value** | **P-value** | **rho** |
| y = 72.94x – 171.35 | -0.8059 | 0.1075 | 1 | 1 | 0.7983 | 2 | 1 | 0.5 |

**Table 56.** Regression between the dhATX in cell (ug/g) and dry weight (mg) within the SS treatment group.

| Simple Linear Regression | | | | | | Spearman | | |
|---|---|---|---|---|---|---|---|---|
| **Equation** | **Adjusted $R^2$** | **F-stat** | **Df1** | **Df2** | **P-value** | **S value** | **P-value** | **rho** |
| y = 387.510x – 9.843 | 0.6359 | 6.24 | 1 | 2 | 0.1298 | 2 | 0.3333 | 0.8 |

**Table 57.** Regression between the dhATX in cell (ug/g) and dry weight (mg) within the FSW treatment group.

| Simple Linear Regression | | | | | | Spearman | | |
|---|---|---|---|---|---|---|---|---|
| **Equation** | **Adjusted $R^2$** | **F-stat** | **Df1** | **Df2** | **P-value** | **S value** | **P-value** | **rho** |
| y = -69.75x + 693.06 | -0.2342 | 0.2409 | 1 | 3 | 0.6572 | 20 | 1 | 0 |

**Table 58.** Regression between the dhATX in filtrate (ug/mL) and dry weight (mg) within the BG11 treatment group.

| Simple Linear Regression | | | | | | Spearman | | |
|---|---|---|---|---|---|---|---|---|
| **Equation** | **Adjusted $R^2$** | **F-stat** | **Df1** | **Df2** | **P-value** | **S value** | **P-value** | **rho** |
| y = 2.310x – 4.102 | -0.01491 | 0.9706 | 1 | 1 | 0.5047 | 2 | 1 | 0.5 |

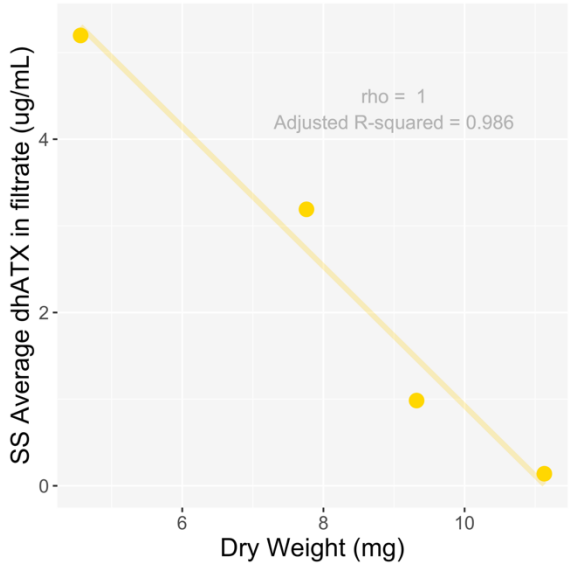


**Figure 55.** Relationship between *M. anatoxicus* average dry weight and average extracellular dhATX in the SS treatment group (n=4) (Supplemental Table 59).

**Table 59.** Regression between the dhATX in filtrate (ug/mL) and dry weight (mg) within the SS treatment group (Figure 55).

| Simple Linear Regression | | | | | | Spearman | | |
|---|---|---|---|---|---|---|---|---|
| **Equation** | **Adjusted $R^2$** | **F-stat** | **Df1** | **Df2** | **P-value** | **S value** | **P-value** | **rho** |

| | | | | | | | | |
|---|---|---|---|---|---|---|---|---|
| y = 1.25186x – 0.54728 | 0.986 | 212.5 | 1 | 2 | **0.004674** | 0 | 0.08333 | 1 |

**Table 60.** Regression between the dhATX in filtrate (ug/mL) and dry weight (mg) within the FSW treatment group.

| **Simple Linear Regression** | | | | | | **Spearman** | | |
|---|---|---|---|---|---|---|---|---|
| **Equation** | **Adjusted $R^2$** | **F-stat** | **Df1** | **Df2** | **P-value** | **S value** | **P-value** | **rho** |
| y = -0.2804X + 2.8879 | -0.03048 | 0.8817 | 1 | 3 | 0.417 | 34 | 0.2333 | -0.7 |

**Table 61.** Summary of Media Chemistry Results.

| **Controlled Variables** | **Response Variables** | | | |
|---|---|---|---|---|
| | **Dry Weight Mass** | **Intracellular ATX** | **Intracellular dhATX** | **Extracellular dhATX** |
| **Salinity** | - FSW / -SS | - BG11 / + FSW | None | - SS |
| **Sulfates** | - FSW | + FSW / + SS | - SS | - SS |
| **Nitrogen** | + FSW | - FSW | - BG11 | None |
| **Phosphates** | None | - FSW | - BG11 | None |
| **Response Variable** | | | | |
| **Dry weight** | N/A | None | - FSW | - SS |

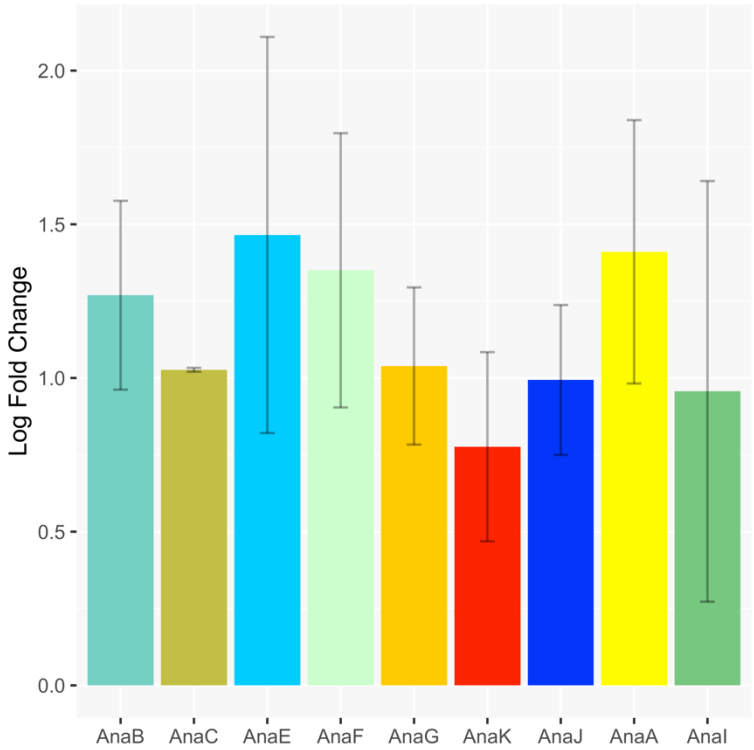


**Figure 56.** Log of the fold change of genes within the Anatoxin-a cassette of T9 (25% SS) compared to T1 (control, 100% BG11) (colors correspond to colors in Figure 9) (Table 62).

**Table 62.** Real-time PCR Gene Amplification Data (Refers to data presented in Figure 56).

| | **Fold Change** | **SD (+/-)** | **BG11 Theoretical Melt Temp** | **BG11 Expected Melt Temp** | **25% SS Theoretical Melt Temp** | **25% SS Expected Melt Temp** |
|---|---|---|---|---|---|---|
| **AnaB** | 3.558 | 1.360 | 82.333 | 82.214 | 79.325 | 78.978 |
| **AnaC** | 2.792 | 0.994 | 84.779 | 84.626 | 82.635 | 81.991 |
| **AnaE** | 4.329 | 1.905 | 84.762 | 84.644 | 77.240 | 74.732 |
| **AnaF** | 3.859 | 1.562 | 85.511 | 85.358 | 77.873 | 78.351 |
| **AnaG** | 2.826 | 1.291 | 84.916 | 84.272 | 78.696 | 77.710 |
| **AnaK** | 2.174 | 0.735 | 82.249 | 82.874 | 78.298 | 75.451 |
| **AnaJ** | 2.701 | 0.784 | 83.776 | 82.539 | 73.367 | 72.250 |
| **AnaA** | 4.098 | 1.535 | 82.227 | 82.844 | 77.495 | 78.316 |
| **AnaI** | 2.603 | 1.982 | 79.292 | 79.458 | 70.513 | 68.622 |

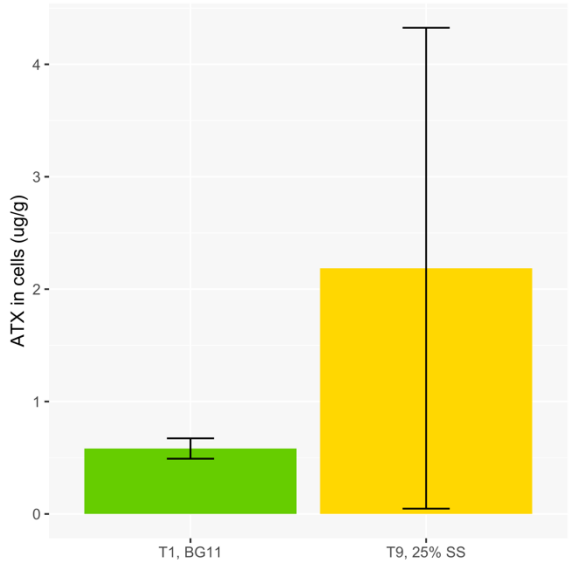


**Figure 57.** Intracellular ATX in *M. anatoxicus* cultures in BG11 compared to 25% SS (Supplemental Table 63) (BG11 = green, 25% SS = yellow).

**Table 63.** ANOVA performed between the ATX in cells (ug/g) in the BG11 and the 25% SS sample (Figure 57).

| ANOVA | | | |
|---|---|---|---|
| **F-stat** | **Df1** | **Df2** | **P-value** |
| 1.68 | 1 | 4 | 0.264651 |

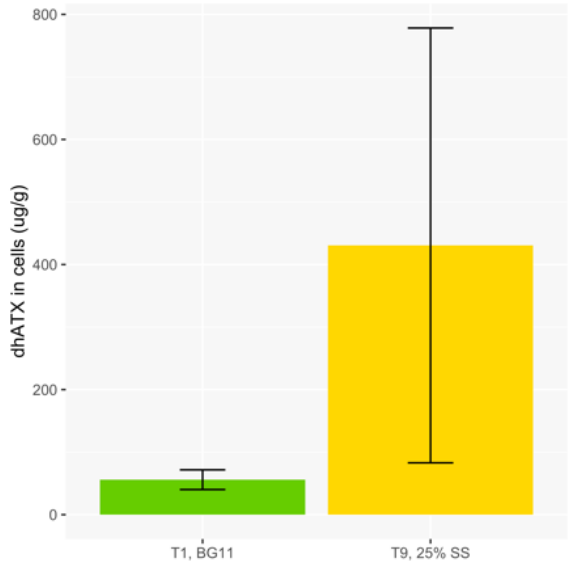


**Figure 58.** Intracellular dhATX in *M. anatoxicus* cultures in BG11 compared to 25% SS (Supplemental Table 64) (BG11 = green, 25% SS = yellow).

**Table 64.** ANOVA performed between the dhATX in cells (ug/g) in the BG11 and the 25% SS sample (Figure 58).

| ANOVA | | | |
|---|---|---|---|
| **F-stat** | **Df1** | **Df2** | **P-value** |
| 3.48 | 1 | 4 | 0.135539 |

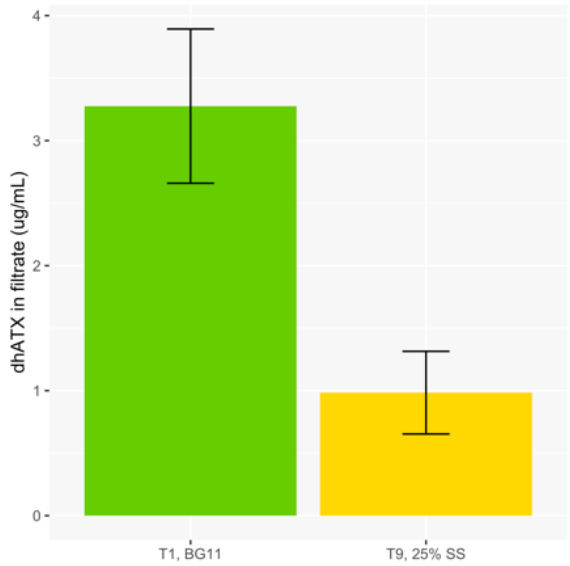


**Figure 59.** Extracellular dhATX in *M. anatoxicus* cultures in BG11 compared to 25% SS ($F_{1,4}$ = 32.18, **p = 0.00477**) (Supplemental Table 65) (BG11 = green, 25% SS = yellow).

**Table 65.** ANOVA performed between the dhATX in filtrate (ug/mL) in the BG11 and the 25% SS sample (Figure 59).

| ANOVA | | | |
|---|---|---|---|
| **F-stat** | **Df1** | **Df2** | **P-value** |
| 32.18 | 1 | 4 | **0.004764** |

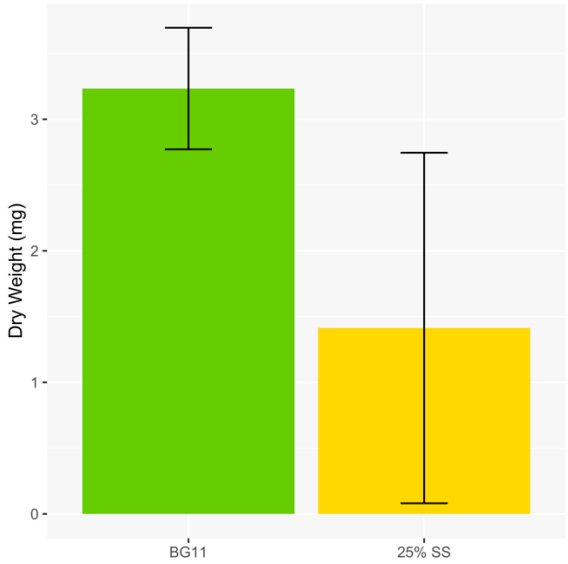


**Figure 60.** Dry weight mass of *M. anatoxicus* in BG11 compared to 25% SS medium (Supplemental Table 66) (BG11 = green, 25% SS = yellow).

| **Table 66.** ANOVA performed between the dry weight (mg) in the BG11 and the 25% SS sample (Figure 60). | | | |
|---|---|---|---|
| **ANOVA** | | | |
| **F-stat** | **Df1** | **Df2** | **P-value** |
| 5 | 1 | 4 | 0.089009 |

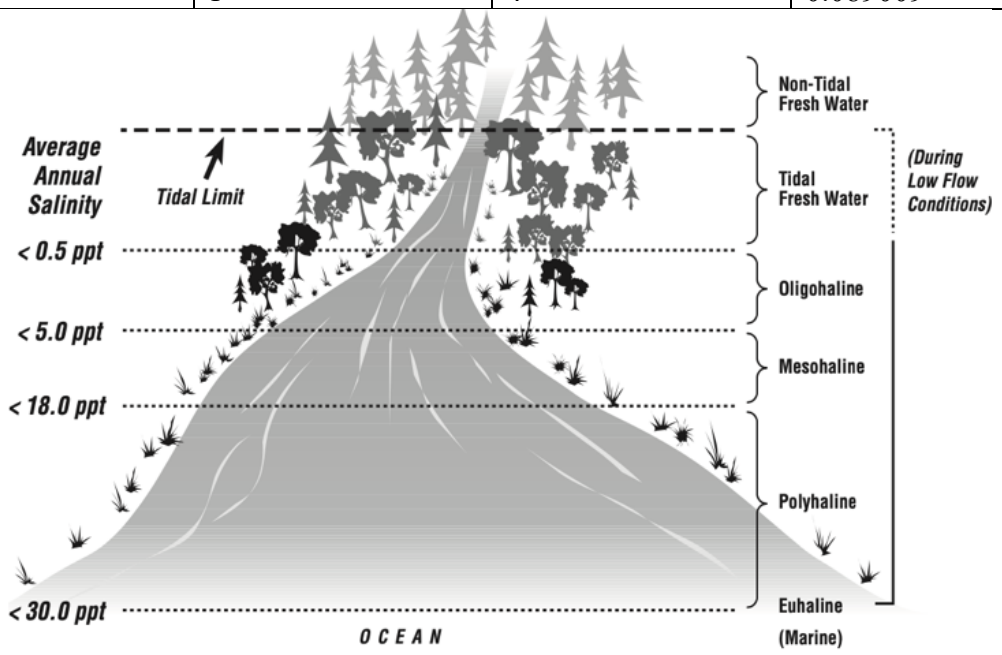


**Figure 61.** Approximate salinity gradient from total freshwater to marine ("Chapter 14: Salinity," 2006)

**Table 67.** Ranges of media chemistry of experimental treatments and of Russian River measurements.

| | **Cl (mg/L)** | **$SO_4$ (mg/L)** | **$NO_3$ (mg/L)** | **$PO_4$ (mg/L)** | **pH** | **Conductivity (mS/cm)** | **TDS (g/L)** | **Salinity (ppt)** |
|---|---|---|---|---|---|---|---|---|
| **T1 – T9** | 20.494 – 5230.17 | 14.152 – 732.780 | 124.905 – 258.510 | 2.38 – 5.390 | 6.67 – 7.42 | 1.102 - 18.87 | 0.765 – 13.3 | 0.542 – 11.13 |
| **Russian River** | N/A | 8.79 – 9.48 | 0.0232 – 0.129 | 0.019 – 0.123 | 7.24 – 8.52 | 0.205 – 0.344 | 67 - 178 | 0.1 – 0.16 |